Coatings and Materials

Michele Magnozzi

Università di Genova

- **P.I., FIS LANCET** – Lowering Optical Absorption in Materials for Cryogenic Mirrors in the Einstein Telescope
- **Chair -** OPTICA Thin Films Technical Group

Mirror coatings in GWD

Università di Genova

Mirror coatings define the Fabry-Pérot cavities of GWDs

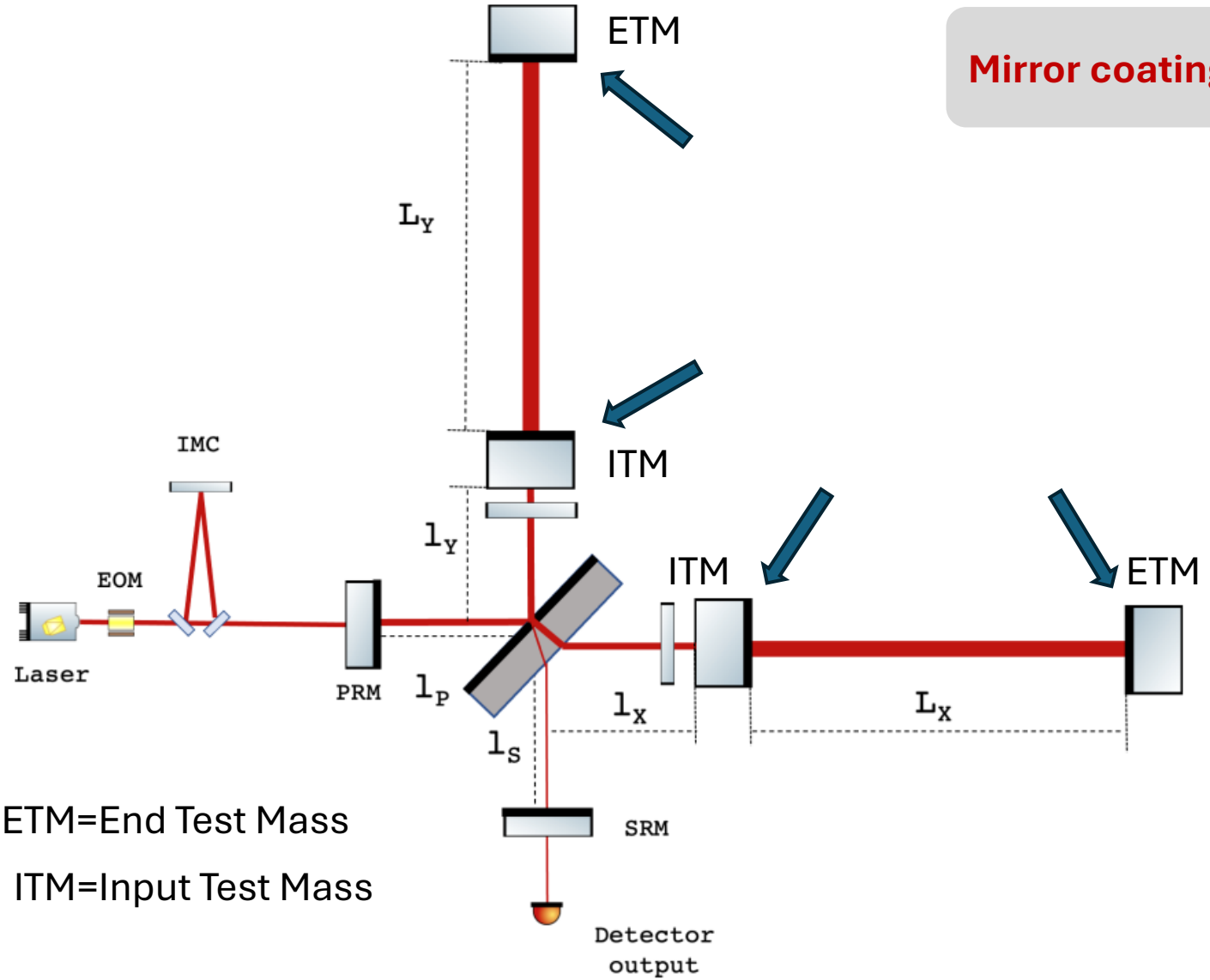

ETM=End Test Mass

ITM=Input Test Mass

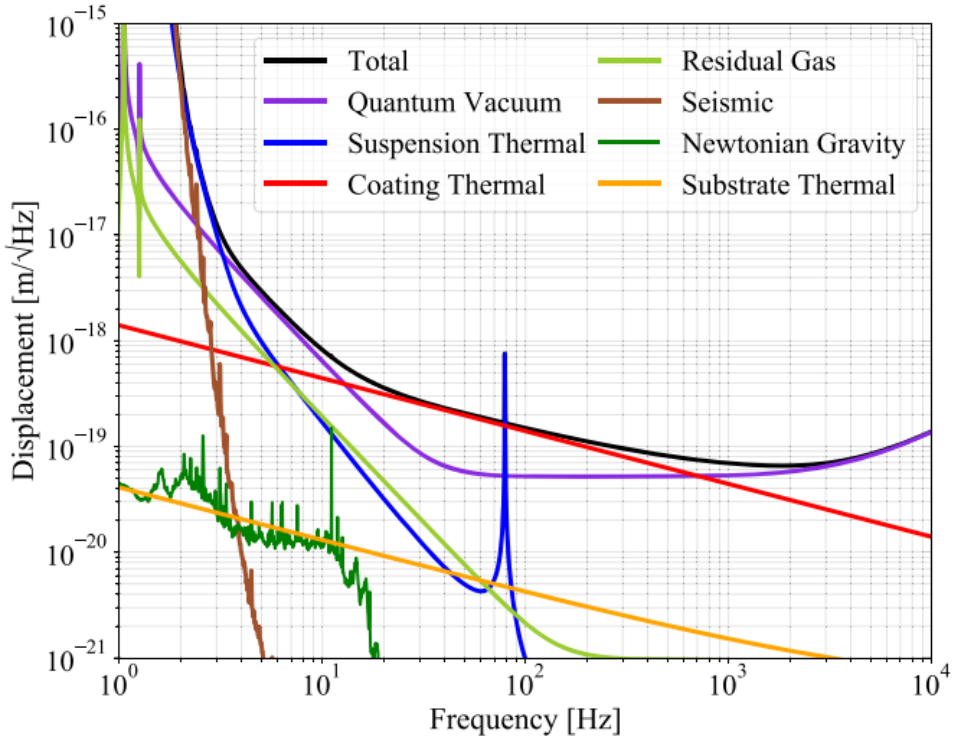

I. Nardecchia, *Galaxies*, *10*, 28, 2022

Utina et al., *Class. Quantum Grav*. 39 (2022) 215008

Outline

Università di Genova

1

Fundamental aspects of coatings

- how dielectric mirrors work
- thermal noise, optical absorption, refractive index, scattering

2

Current coatings for GWD

- history of developments for GWD mirrors
- Ion Beam Sputtering
- Post-deposition annealing
- the low-index and high-index materials

3

Open challenges and metrology

- engineering the deposition
- engineering the annealing
- the importance of metrology
- cryo-operated mirrors for ET-LF

4

New materials and designs

- nitrides
- other oxides
- ternary and quaternary coatings
- crystalline coatings

1

Fundamental aspects of coatings

The fundamental limit of metallic mirrors

Mirrors in everyday life are (mostly) composed of a **metal slab** covered by glass. The mirror is the metal.

Although they seem very shiny when polished, **metals never reflect 100% of the incoming light!**

Moreover, metals absorb a lot of light: **they heat up when illuminated.**

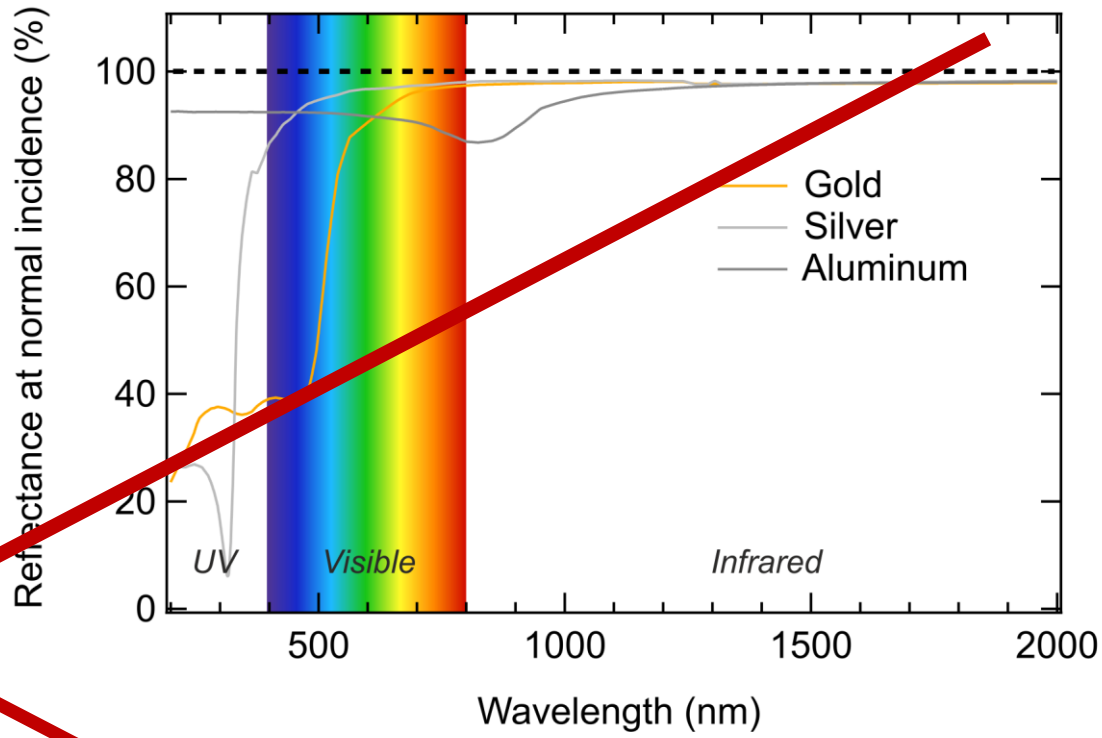

Metal	% Reflectance at 1064 nm
Gold	97.9
Silver	99.7
Aluminum	95.0

Another way of building mirrors

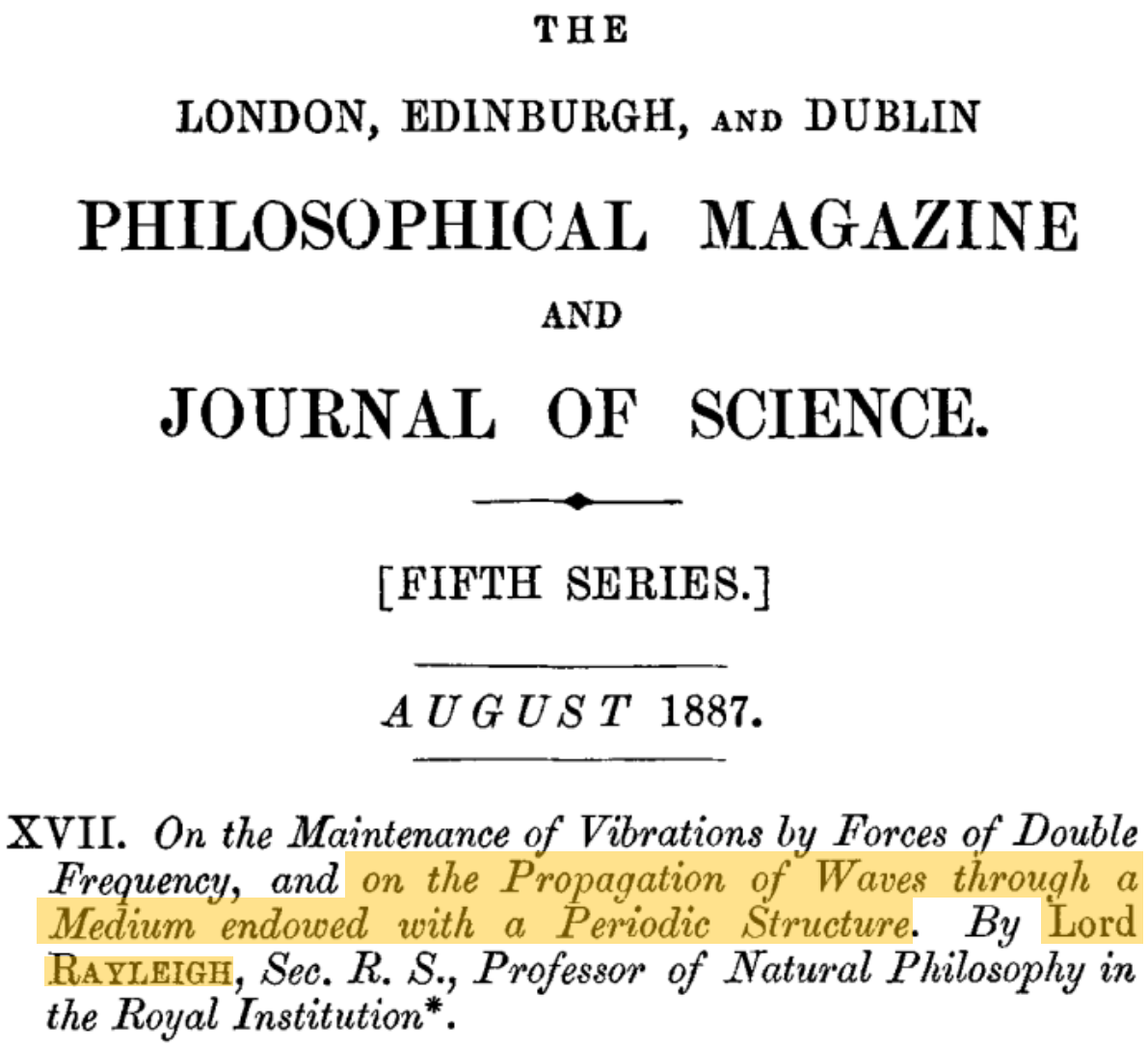

THE

LONDON, EDINBURGH, AND DUBLIN

PHILOSOPHICAL MAGAZINE

AND

JOURNAL OF SCIENCE.

[FIFTH SERIES.]

AUGUST 1887.

XVII. *On the Maintenance of Vibrations by Forces of Double Frequency, and on the Propagation of Waves through a Medium endowed with a Periodic Structure.* By Lord RAYLEIGH, *Sec. R. S., Professor of Natural Philosophy in the Royal Institution*.*

‘A detailed … examination of various cases in which **a laminated structure leads to powerful but highly selected reflection** would be of value’

Lord Rayleigh, 1887

If his [Lord Rayleigh’s] Memoirs of 1912 has passed almost unnoticed among the optical scientists, it is probably because he put the problem in terms of acoustics.

F. Abelès, 1950

Dielectric mirrors: layout

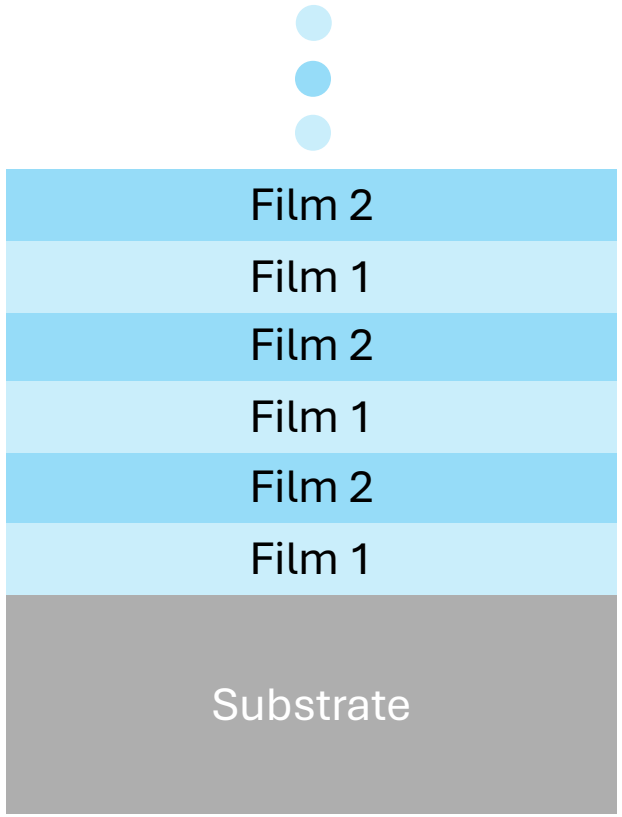

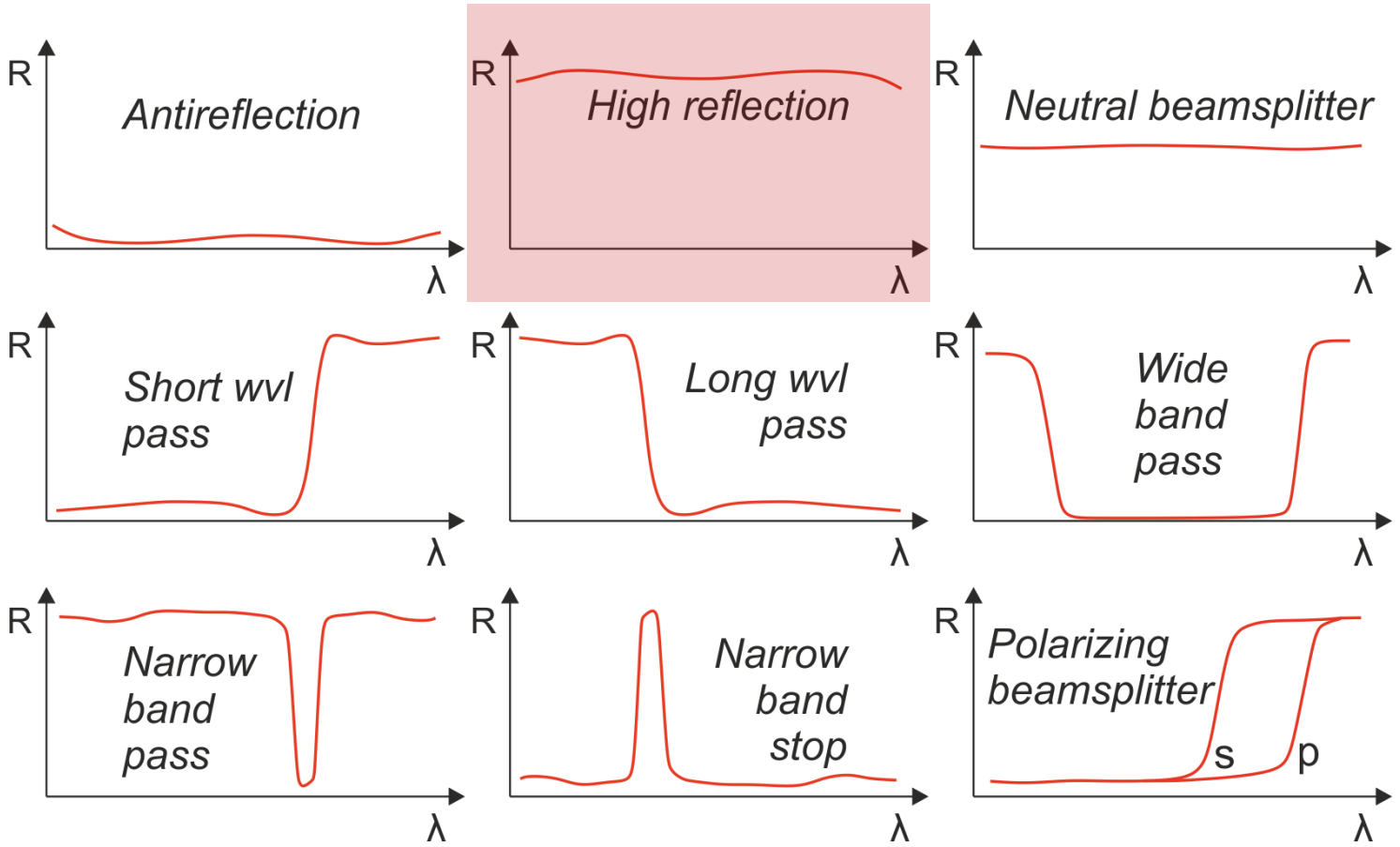

The desired behavior (antireflection, high reflection..) is obtained by selecting **the number, the thickness and the refractive index of each layer**.

Dielectric mirrors: doublets

Each film is transparent! High reflectance is given by the collective behavior of the stack (multiple interference)

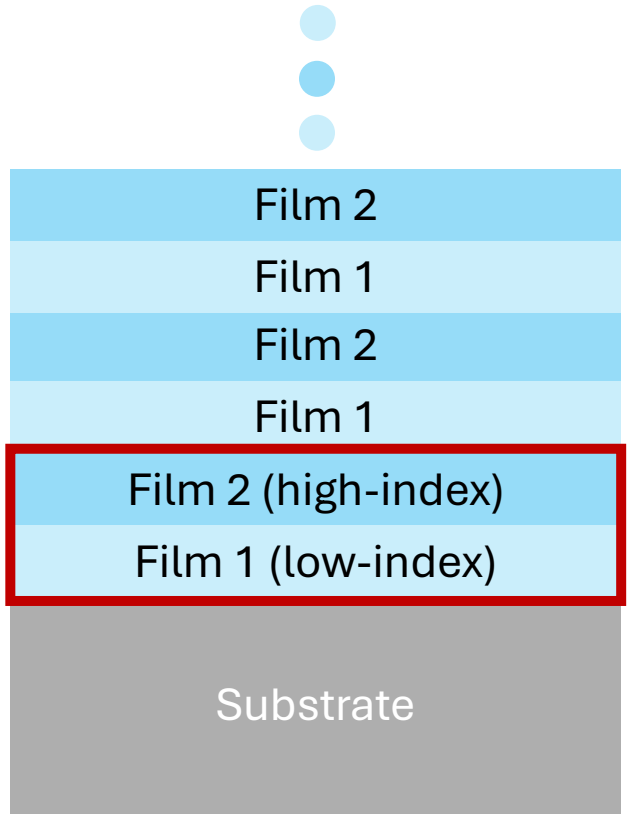

'Doublet'

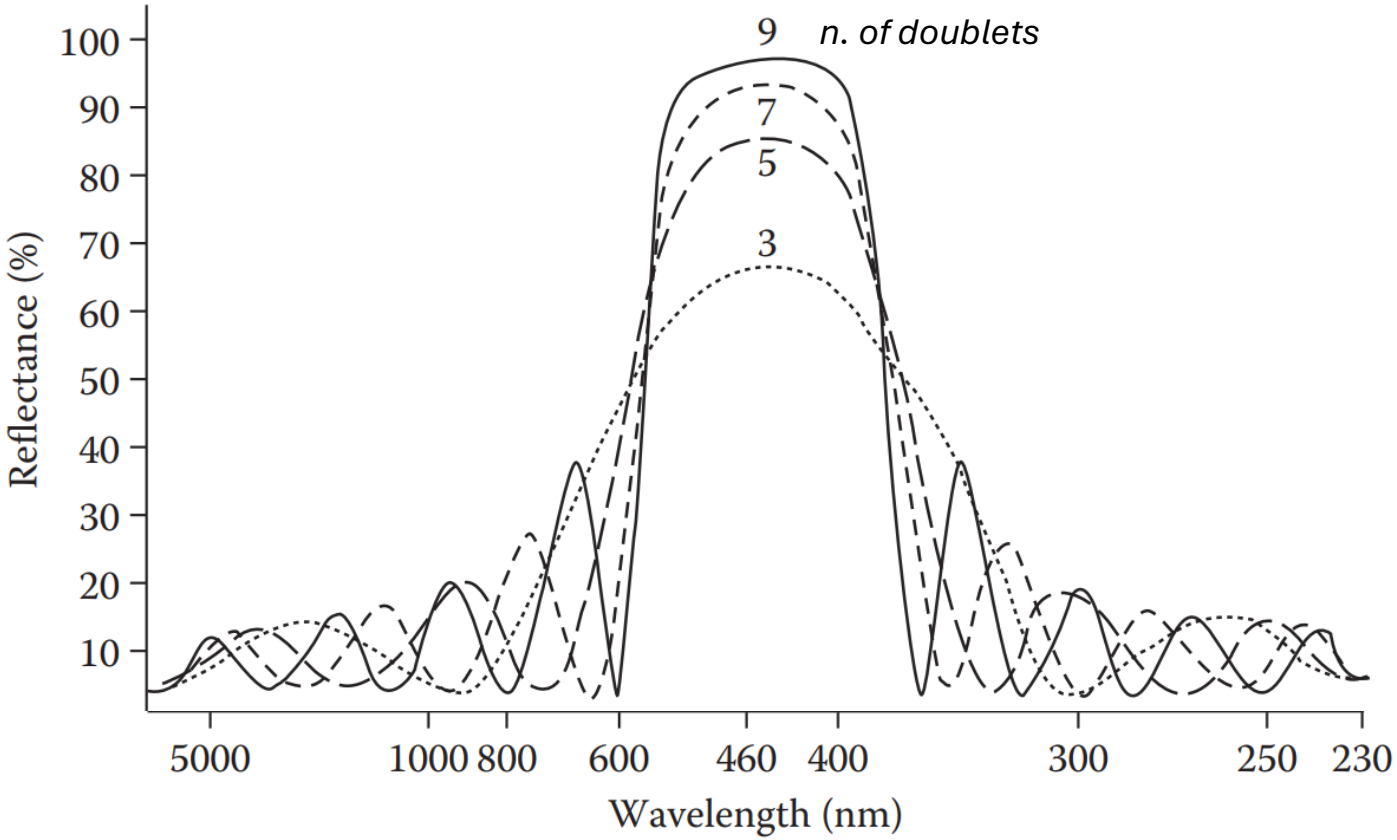

Reflectance approaches 100% for increasing number of doublets

Doublets: refractive index contrast

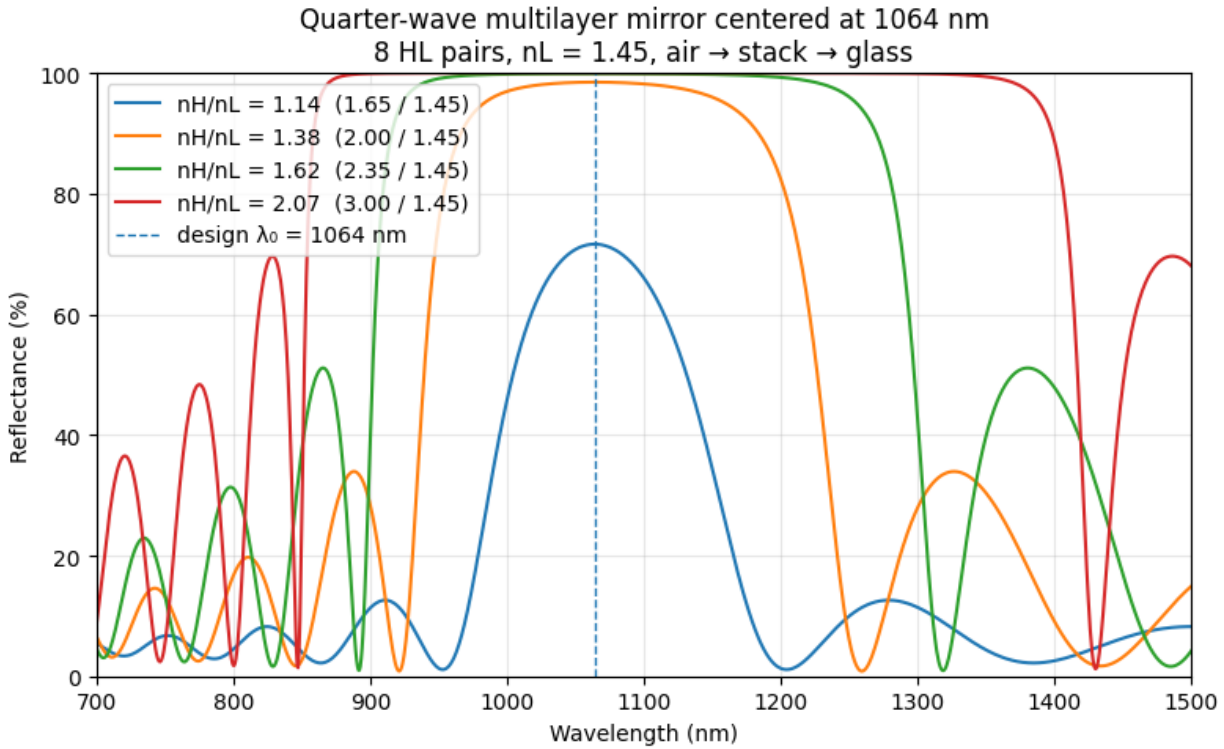

n_H/n_L	R @1064	d_H nm	d_L nm
1.14	71.626%	161.21	183.45
1.38	98.478%	133.00	183.45
1.62	99.884%	113.19	183.45
2.07	99.998%	88.67	183.45

The refractive index contrast within doublets is one of the strongest constraints to the design of optical coatings.

The wider the high-low contrast, the lower the required number of doublets.

GWD mirrors advance the state of the art in optical coatings

Università di Genova

Table 1. Requirements for the Advanced LIGO Coating[a]

Parameter	Advanced LIGO Requirement	Demonstrated Value
Loss angle $\phi_{\parallel}$	5×10^{-5}	1.5×10^{-4}
Optical absorption	0.5 ppm	1 ppm
Scatter	2 ppm	20 ppm
Thickness uniformity	10^{-3}	8×10^{-3}
Transmission	5 ppm	5.5 ppm
Transmission matching	5×10^{-3}	1×10^{-2}

Total Layers	SiO_2 Optical Thickness	Ta_2O_5 Optical Thickness	Loss Angle $\phi_{\parallel}$
2	$\lambda/4$	$\lambda/4$	$2.7 \pm 0.7 \times 10^{-4}$
30	$\lambda/4$	$\lambda/4$	$2.6 \pm 0.7 \times 10^{-4}$
60	$\lambda/8$	$\lambda/8$	$2.7 \pm 0.5 \times 10^{-4}$
30	$\lambda/8$	$3\lambda/8$	$3.7 \pm 0.5 \times 10^{-4}$
30	$3\lambda/8$	$\lambda/8$	$1.9 \pm 0.2 \times 10^{-4}$

"Progress has been made with reducing mechanical loss, but more work remains to be done. **Technical input from all those with knowledge about coatings and optics will be crucial to achieving this goal**"

Table 3. Mechanical Loss of SiO_2/TiO_2-Doped Ta_2O_5 Coatings from LMA/Virgo[a]

Concentration of TiO_2	Loss Angle $\phi_{\parallel}$
None	$2.7 \pm 0.5 \times 10^{-4}$
Low	$1.8 \pm 0.2 \times 10^{-4}$
High	$1.6 \pm 0.2 \times 10^{-4}$

[a]All coatings were composed of 30 layers, with $\lambda/4$ optical thickness for each layer.

Harry et al., *Appl. Opt.* 45, 1569, 2006

Thermal noise in coatings

Università di Genova

Thermal noise in interferometric gravitational wave detectors due to dielectric optical coatings

Harry et al., *Class. Quant. Grav*. 19, 897, 2002

Gregory M Harry[1,2], Andri M Gretarsson[2], Peter R Saulson[2], Scott E Kittelberger[2], Steven D Penn[2], William J Startin[2], Sheila Rowan[3], Martin M Fejer[3], D R M Crooks[4], Gianpietro Cagnoli[4], Jim Hough[4] and Norio Nakagawa[5]

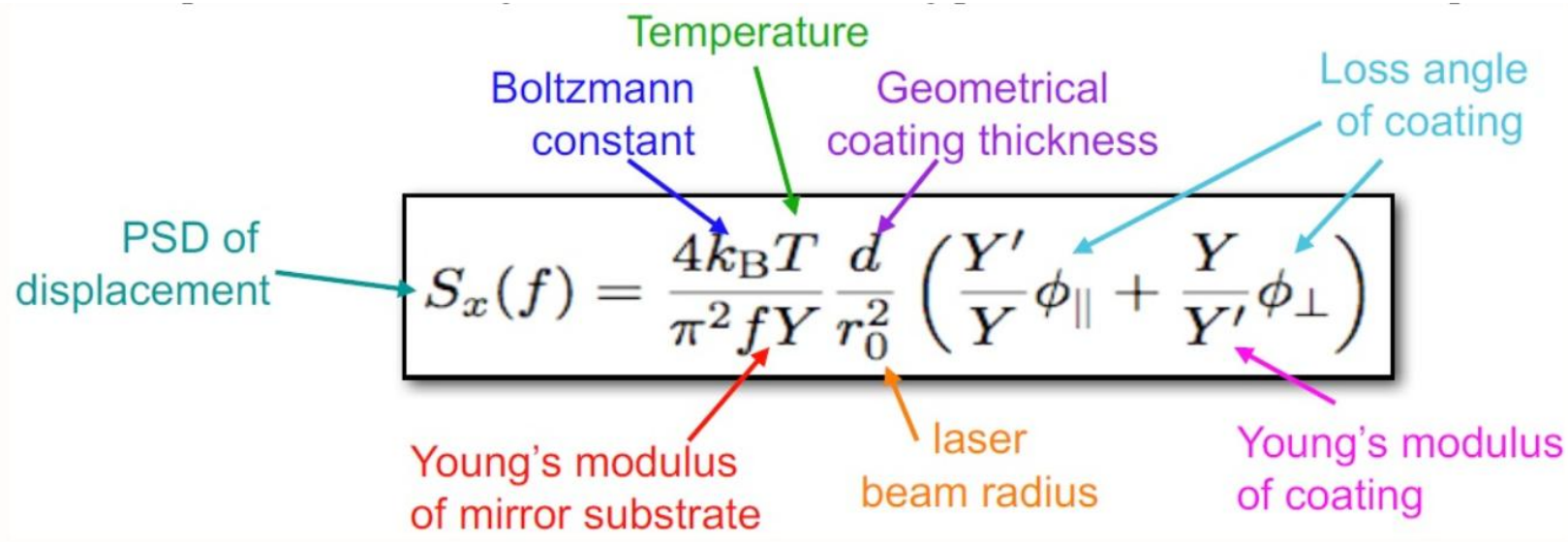

Thermal noise arises from fluctuations of the mirror surface under thermally activated transitions between equilibrium configurations of structure in coatings. Its amplitude is linked to the amount of internal friction within the mirror materials, via the fluctuation-dissipation theorem: **the higher the loss, the higher the thermal noise level**.

Thermal noise in coatings

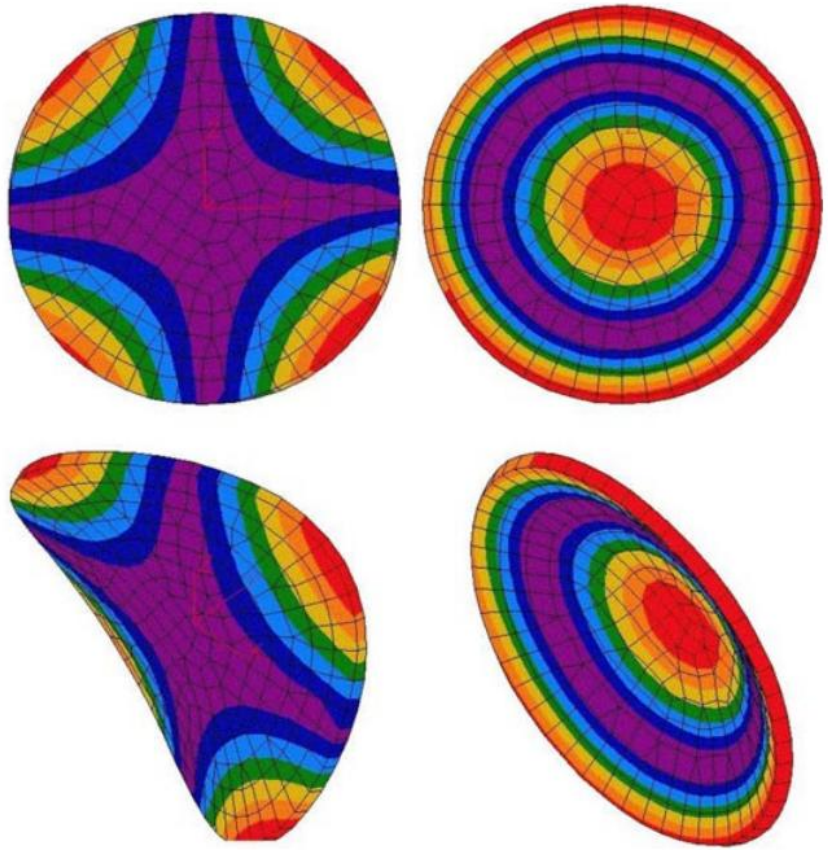

Figure 2. Modes of the thin sample. The first mode (butterfly) on the left and the second mode (drumhead) on the right. The first row is face view and the second row is side view.

Penn et al. 2003 *Class. Quantum Grav*. 20 2917

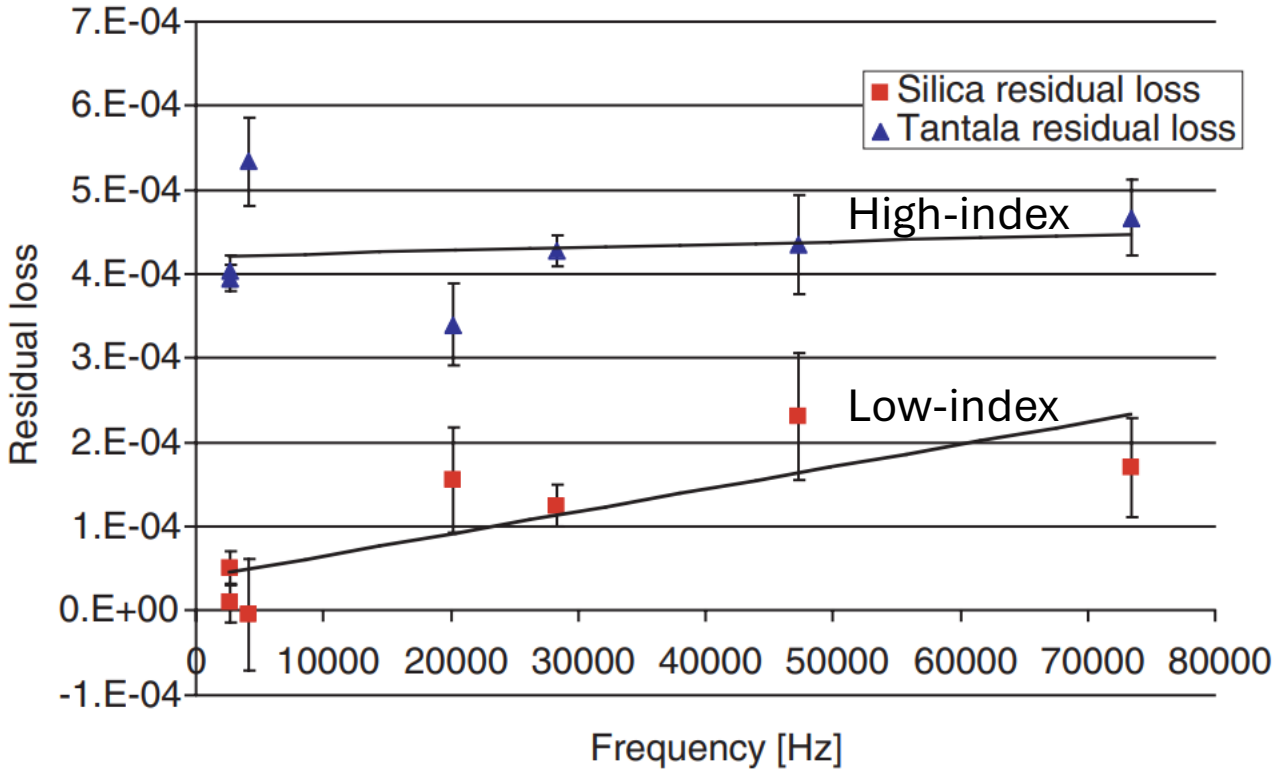

The high-index layers cause the majority of loss in GWD mirrors

Crooks et al. *Class. Quantum Grav*. 21 S1059 2004

Optical absorption

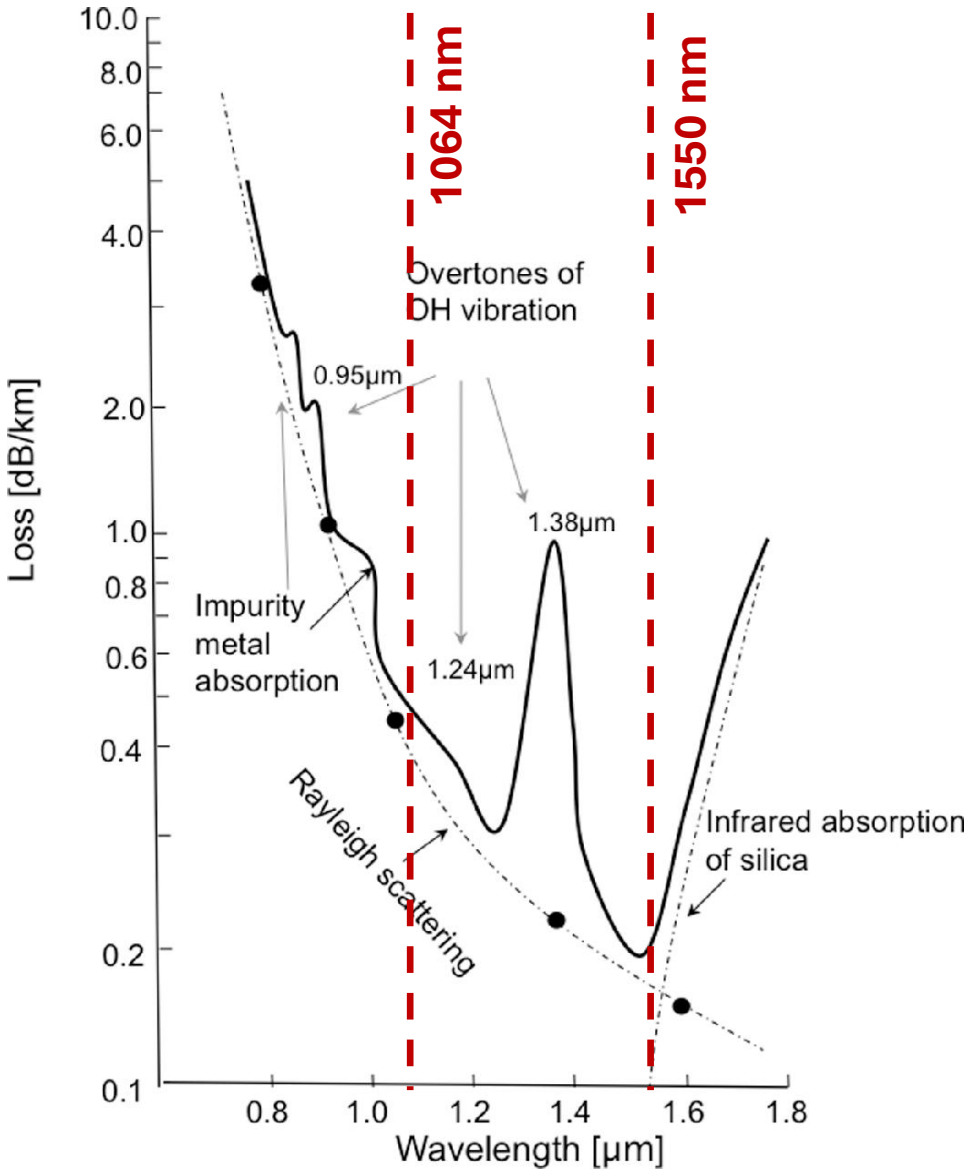

	Peak wavelength (nm)	One part in 10^9 (dB km^{-1})
Cr^{3+}	625	1.6
C^{2+}	685	0.1
Cu^{2+}	850	1.1
Fe^{2+}	1100	0.68
Fe^{3+}	400	0.15
Ni^{2+}	650	0.1
Mn^{3+}	460	0.2
V^{4+}	725	2.7

Metallic impurities can introduce relatively strong optical absorption

The intensity of optical absorption strongly depends on:

- the light wavelength
- the presence of contaminants
  (water is often present, but also other species)

Kitayama, Light Propagation in Optical Fibers, Cambridge 2014

Light scattering

The target for scattering as optical loss is in the order of 10-20 ppm per mirror; **point defects, for their absorption and scatter, must be strictly controlled**

ET-0007B-20

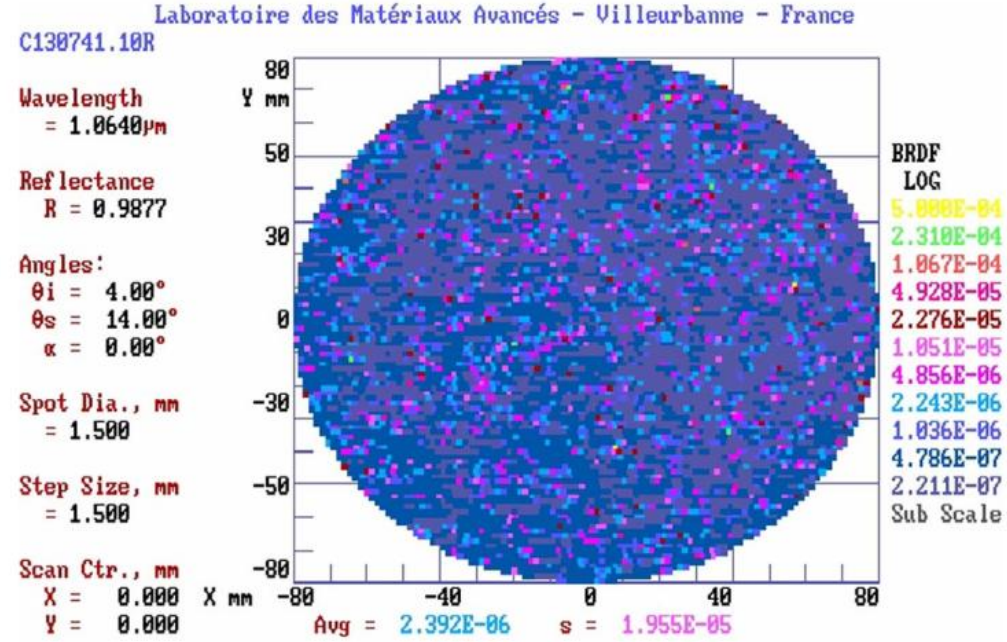

Fig. 6. Average scattering map Ø15 cm on an ITM of Advanced LIGO measured with a CASI scatterometer.

Pinard et al., *Appl. Opt.* 56, C13, 2017

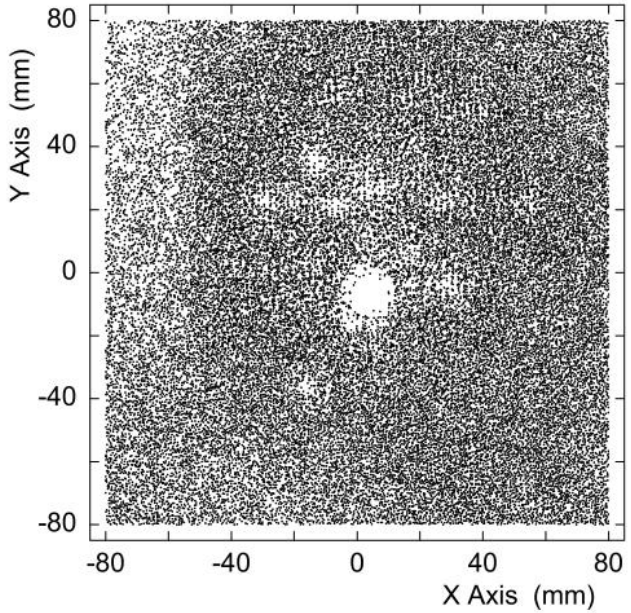

"The sheer number of the observed scatterers implies a fundamental, thermodynamic origin during deposition or processing"

"Theoretical material science considerations indicate that **these scatterers are either nucleation centers, density deficits, or a combination of the two"**

Glover et al., *Physics Letters A* 382 (2018) 2259–2264

Research in optical coatings is multidisciplinary

Università di Genova

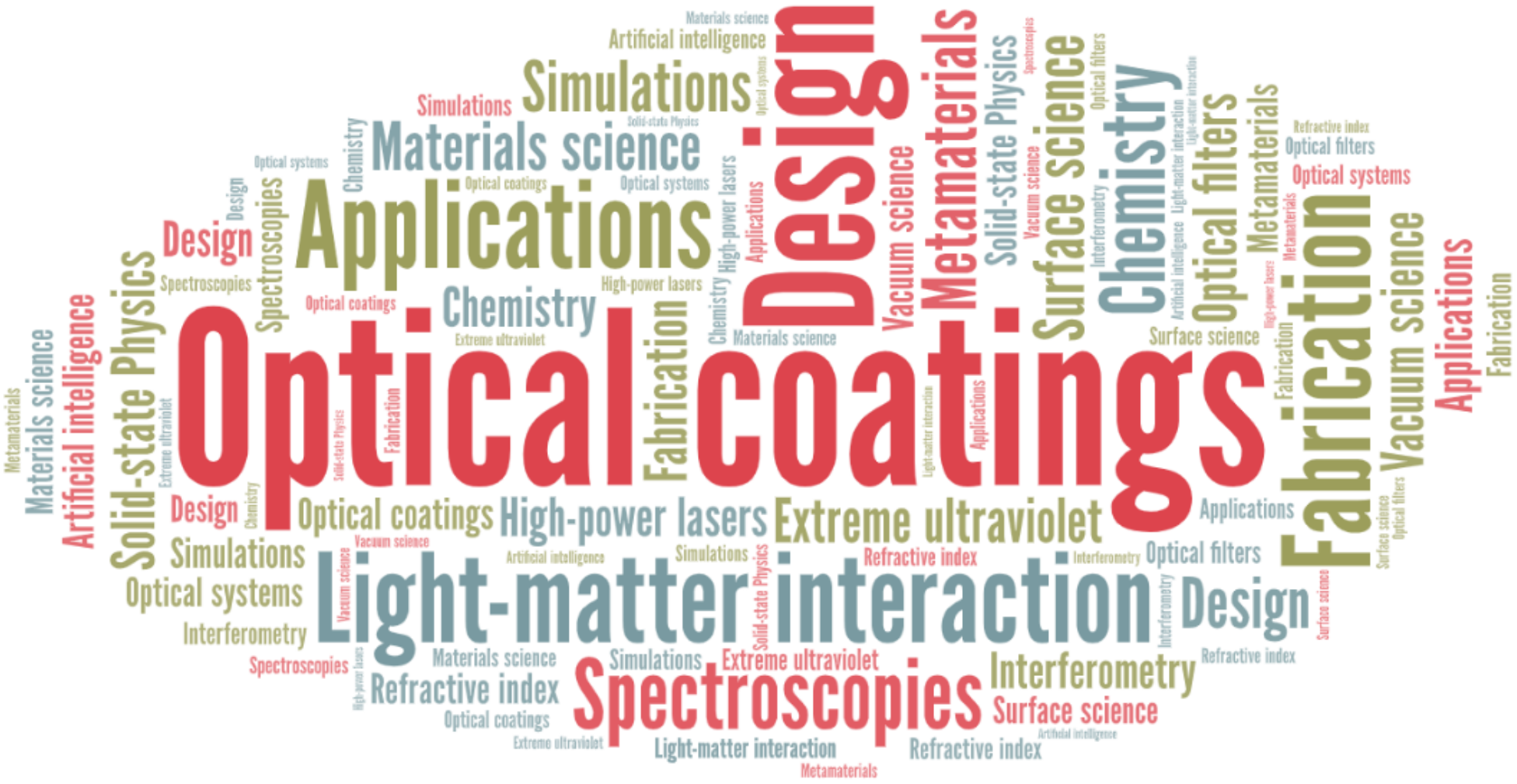

Current status of GWD coatings

(brief) History of developments of GWD mirrors

Università di Genova

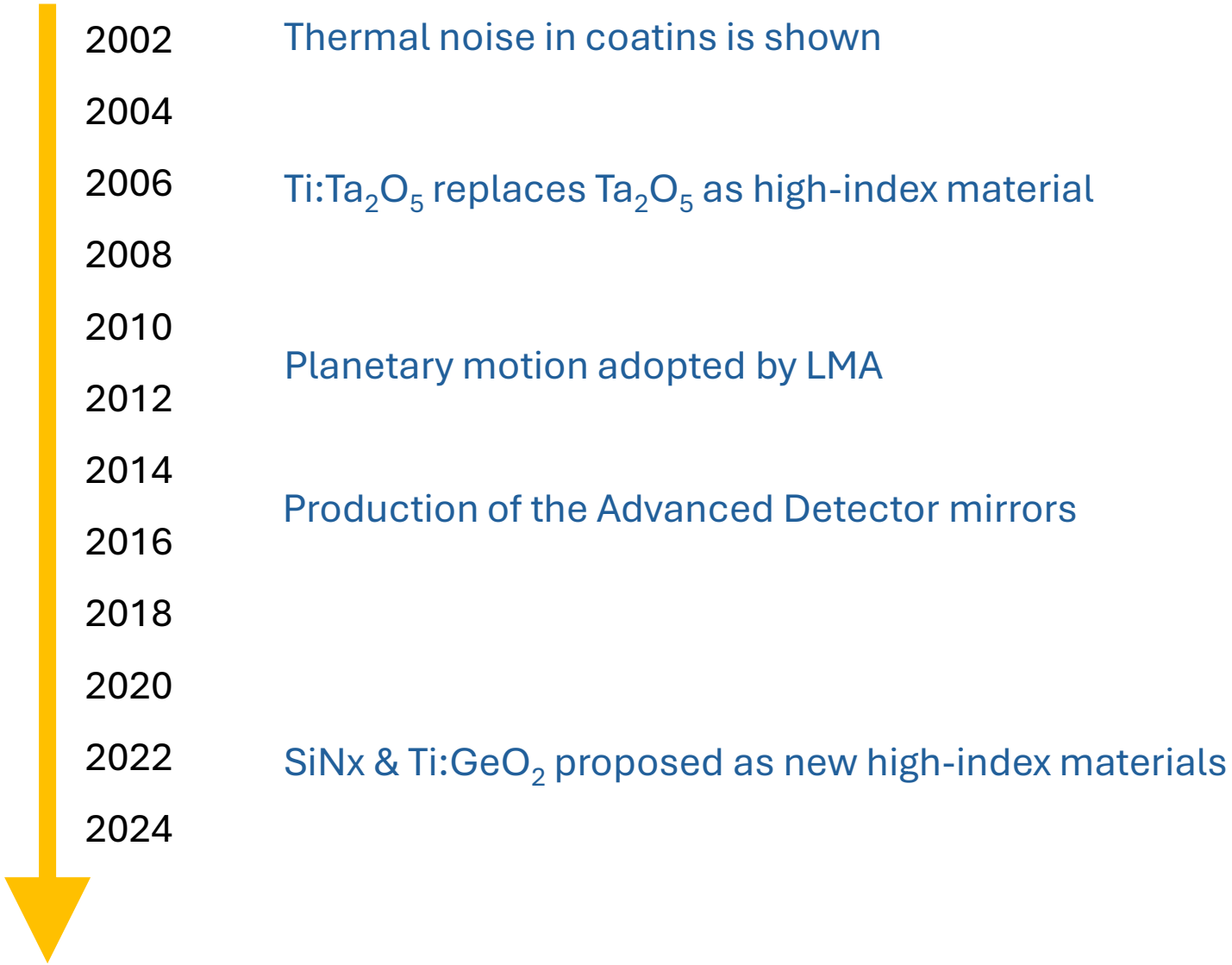

Concept credits: G. Cagnoli

IBS deposition of mirror coatings for GWD

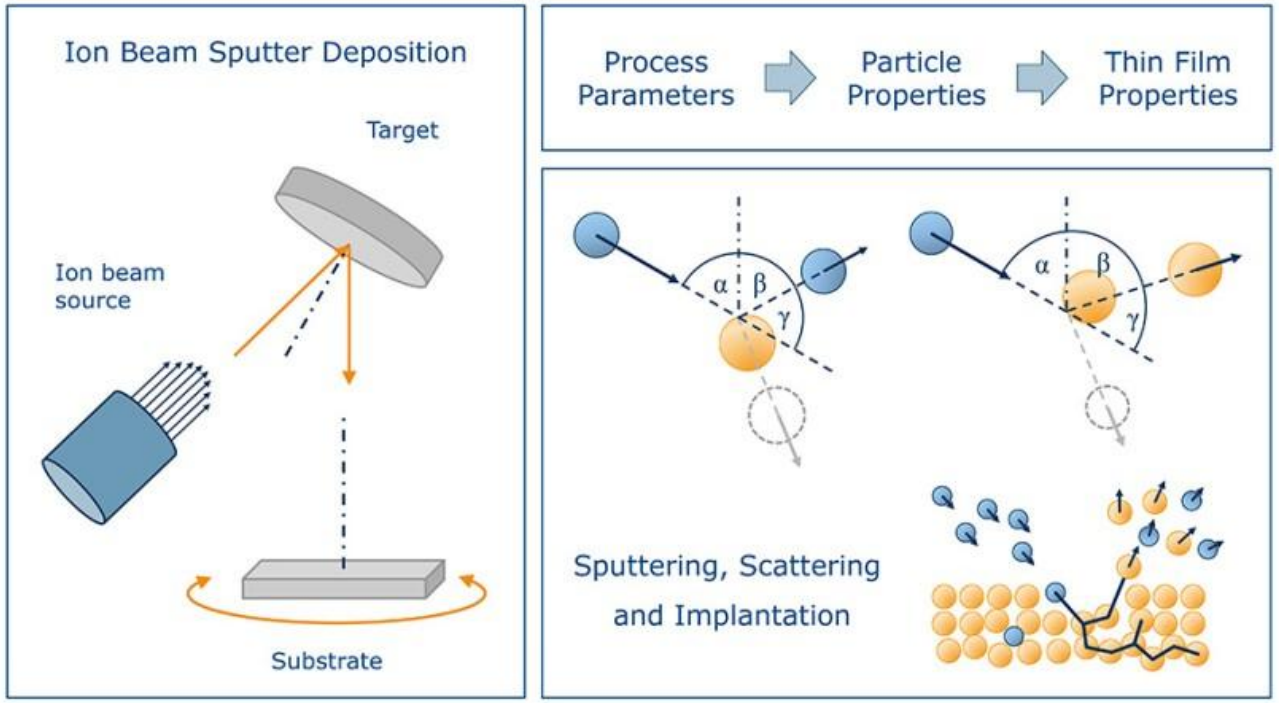

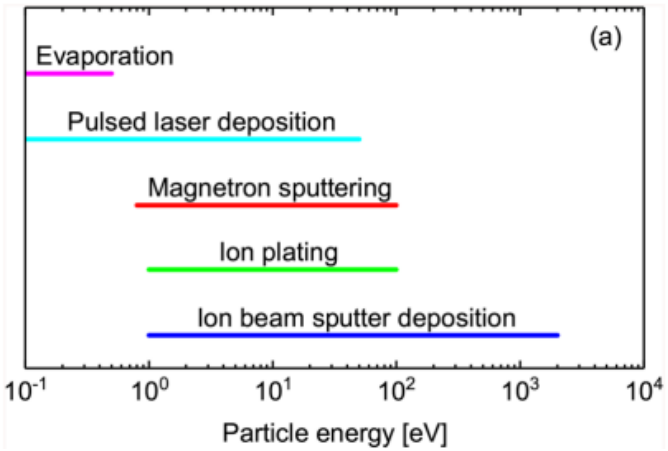

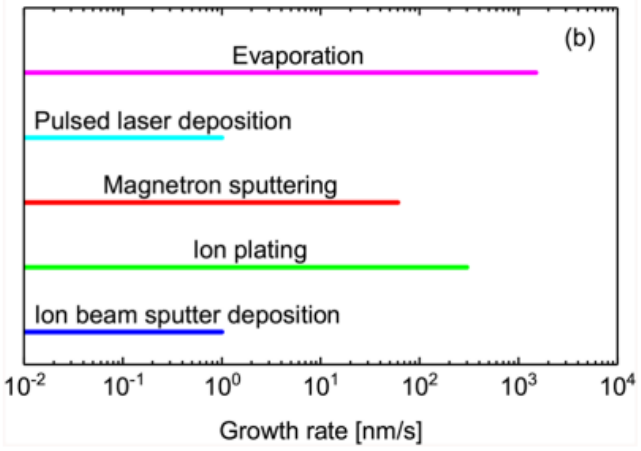

Advantages of films produced with Ion Beam Sputtering (IBS):

- high density
- very low surface roughness
- high purity (but still…)
- widely tunable deposition parameters
- slow film growth
- improved adhesion in many cases

Bundesmann, Neumann, *J. Appl. Phys*. 124, 321102 (2018)

Scaling for GWD

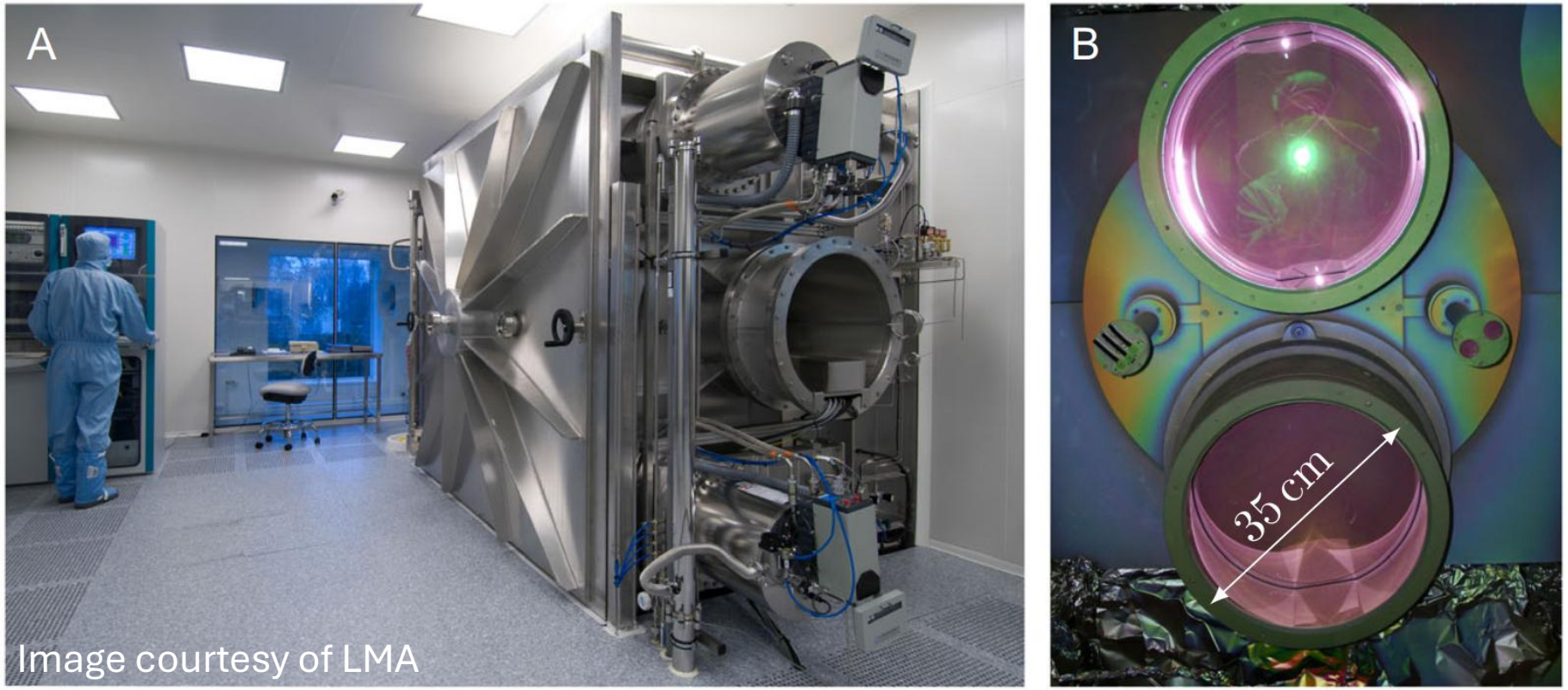

Producing ‘twin’ coatings of the size required by current GWD involves **decades of technical developments and continuous optimization.**

Image from A. Amato, M. Magnozzi, J. Wohler. *Adv. Photon. Res.* 6, 2400117 (2025)

Scaling for GWD

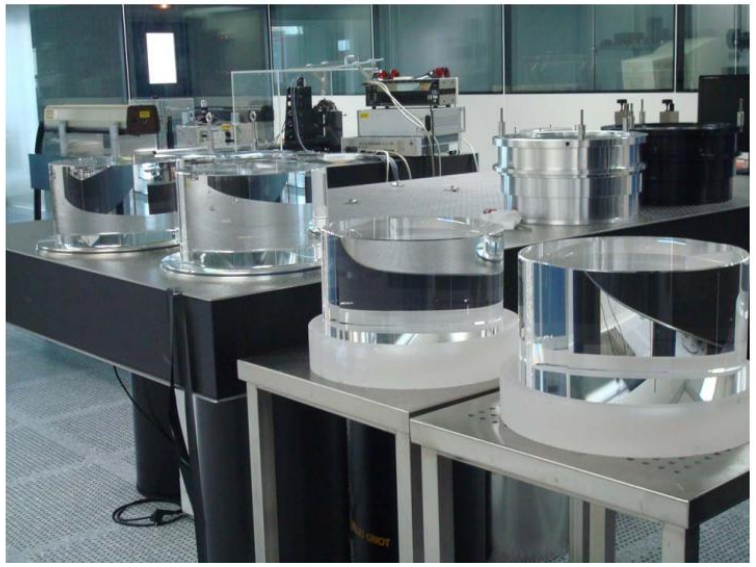

Fig. 2. Four Advanced LIGO ITM substrates before coating.

Pinard et al., *Appl. Opt.* 56, C13, 2017

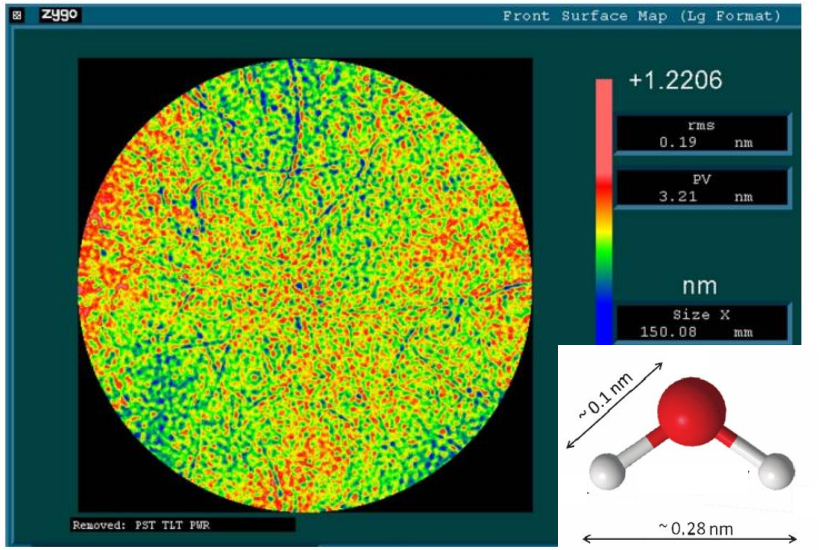

Fig. 4. Surface flatness (0.19 nm RMS Ø15 cm) of an Advanced Virgo EM.

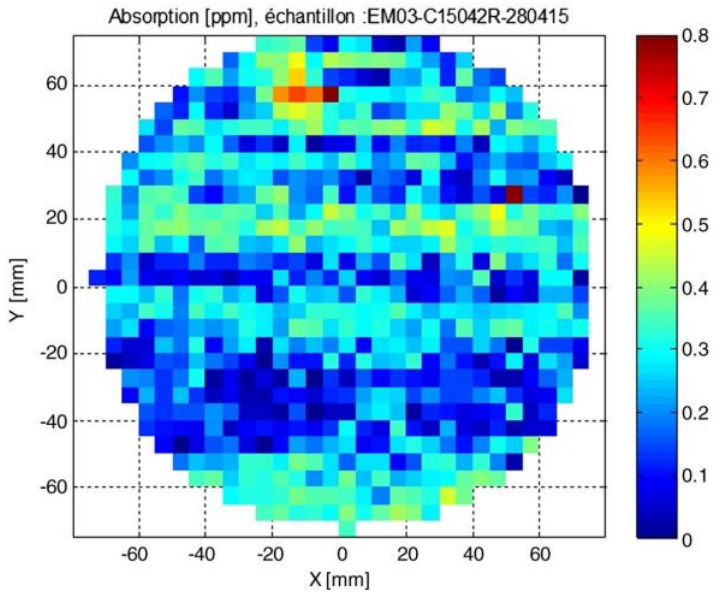

Fig. 5. Absorption map at 1064 nm on Ø15 cm of a high reflectivity coating of an EM of Advanced Virgo.

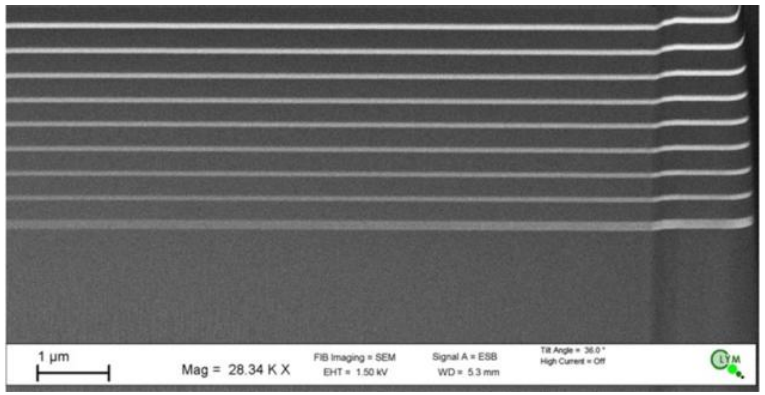

Cagnoli et al., SPIE 2017

Average optical absorption values of test masses for Adv. LIGO:

- Input Test Mass: **0.22 +/- 0.03 ppm**
- End Test Mass: **0.27 +/- 0.07 ppm**

Post-deposition thermal annealing of GWD mirrors

Università di Genova

Coatings produced by IBS are far from equilibrium in the as-deposited state.

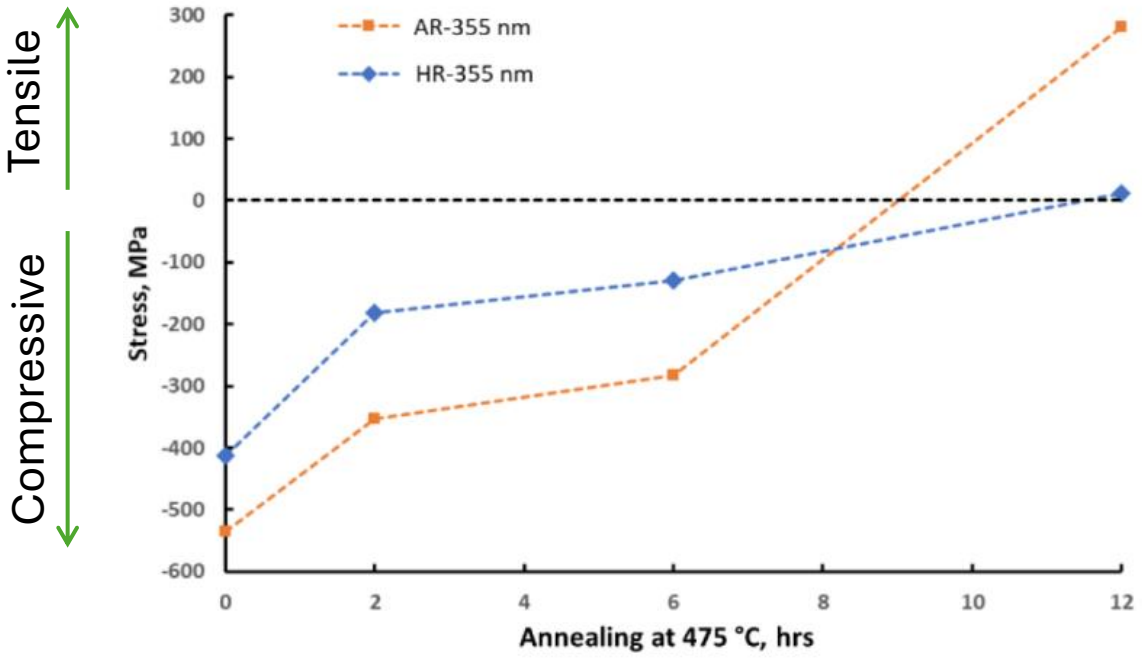

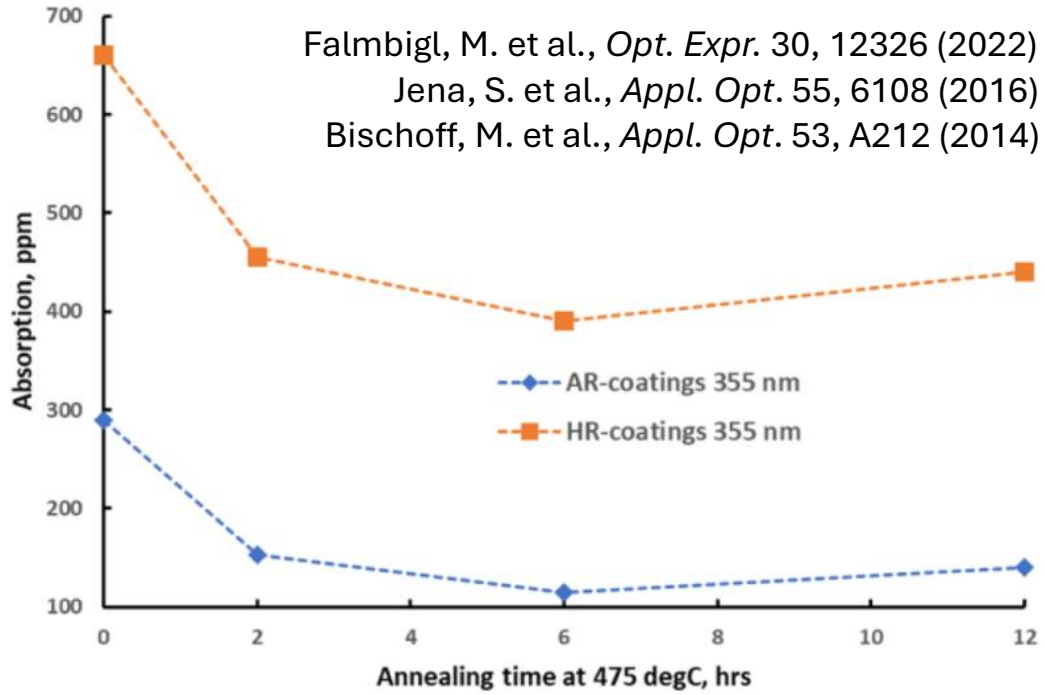

Falmbigl, M. et al., *Opt. Expr.* 30, 12326 (2022)
Jena, S. et al., *Appl. Opt.* 55, 6108 (2016)
Bischoff, M. et al., *Appl. Opt.* 53, A212 (2014)

Post-deposition thermal annealing is mandatory for GWD mirrors because:

- it reduces mechanical stress
- it reduces optical absorption

It’s all about the atomic structure

Università di Genova

Amorphous structure

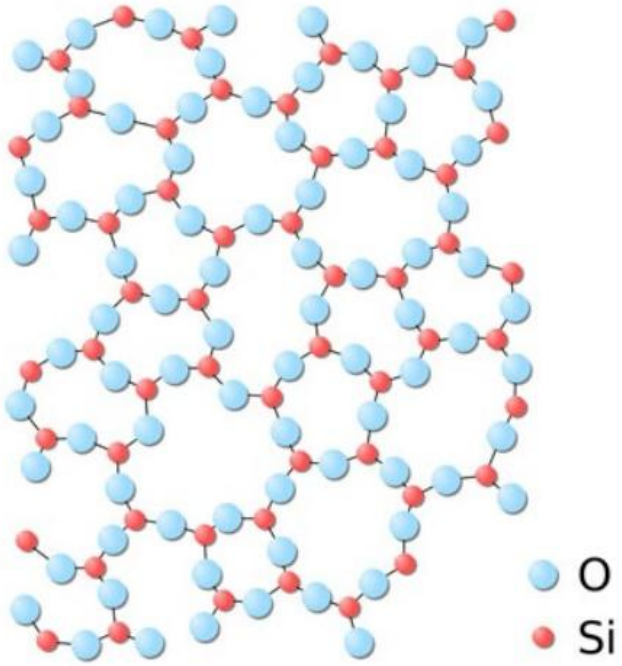

Current GWD mirror coatings have amorphous structure

Crystalline structure

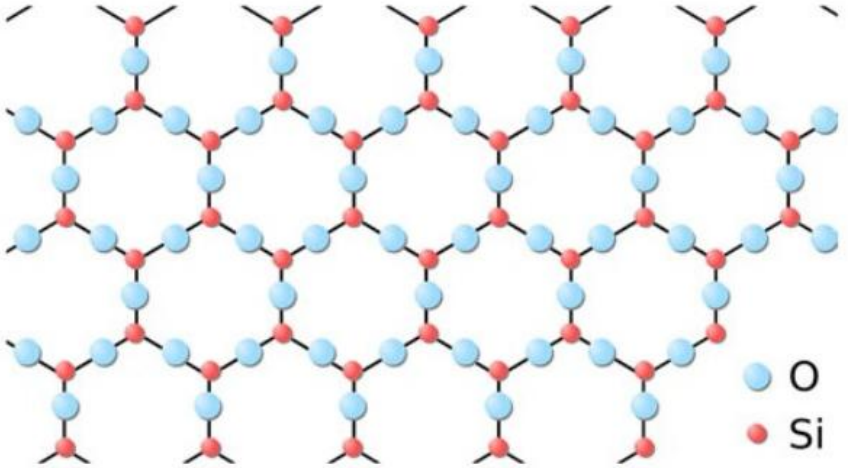

It’s all about the atomic structure

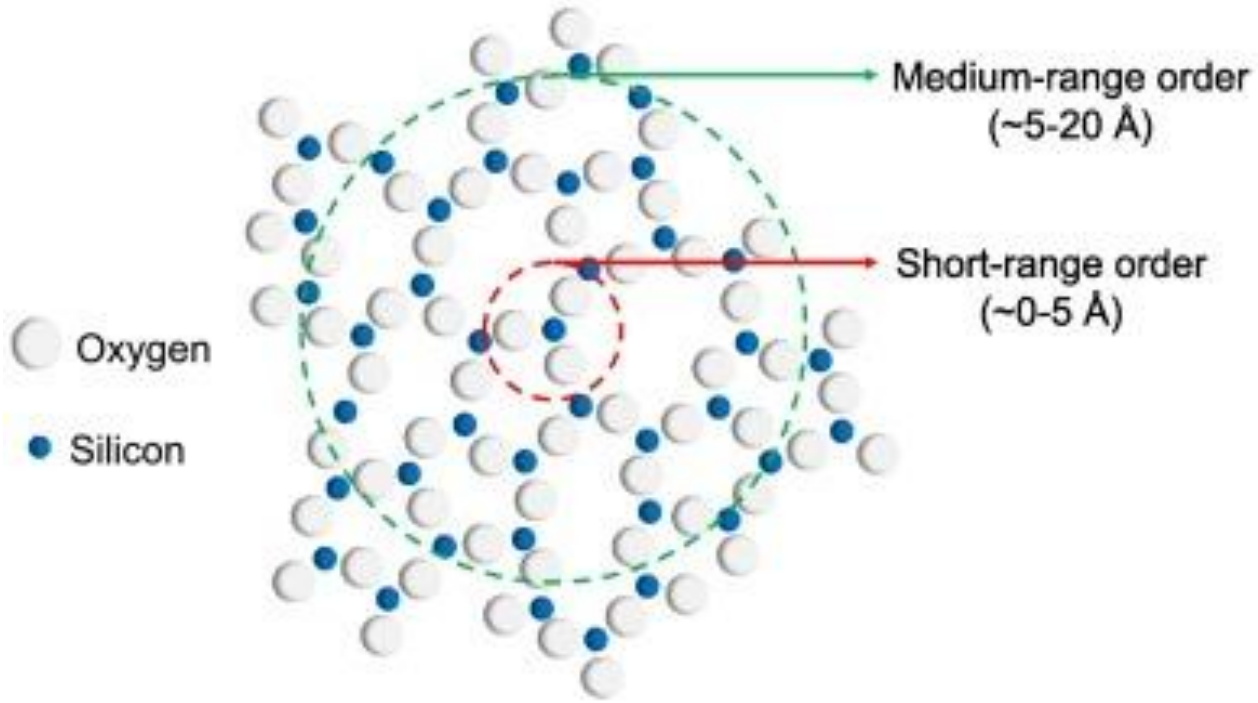

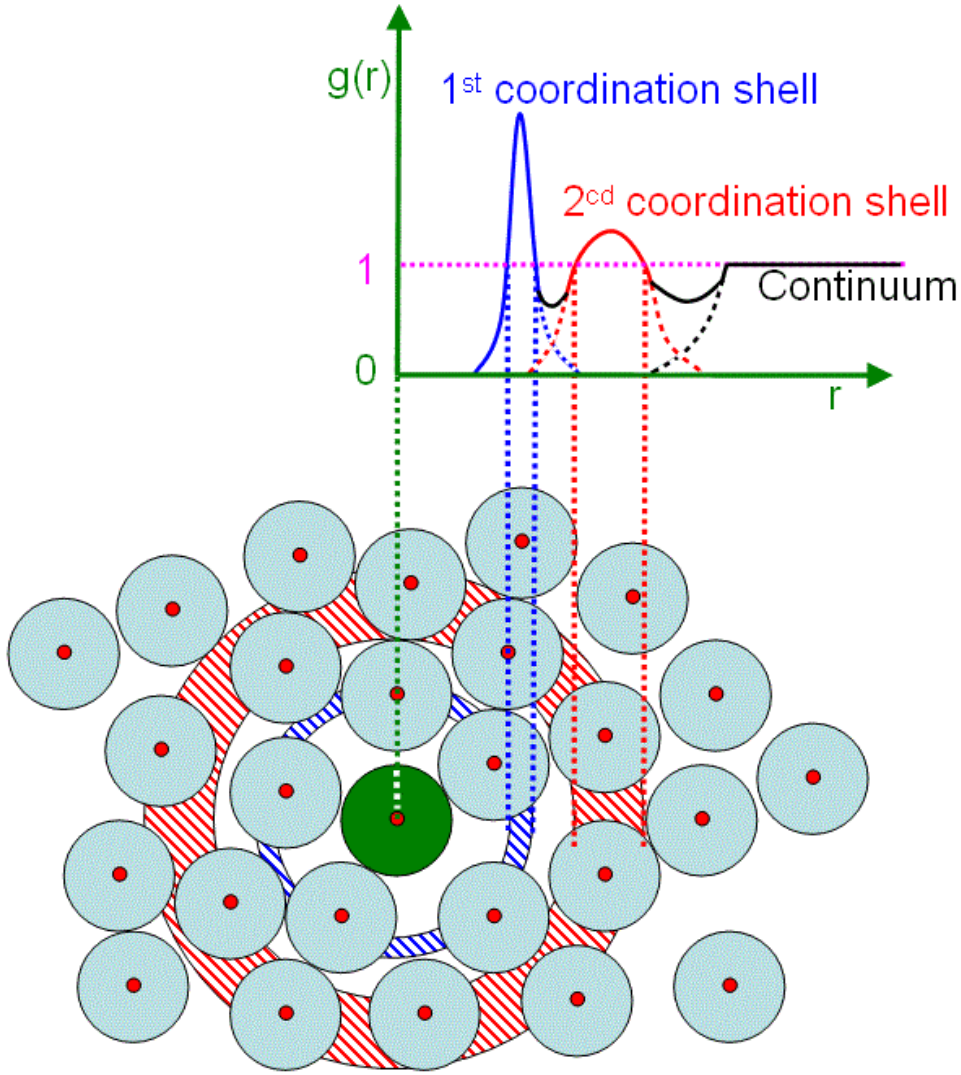

Amorphous materials typically have:

- well-defined *short-range order*
- some degree of *medium-range order*
- complete lack of *long-range order*

Annealing and atomic structure

Raising the annealing temperature improves the amorphous structure. What is the optimal T before crystallization?

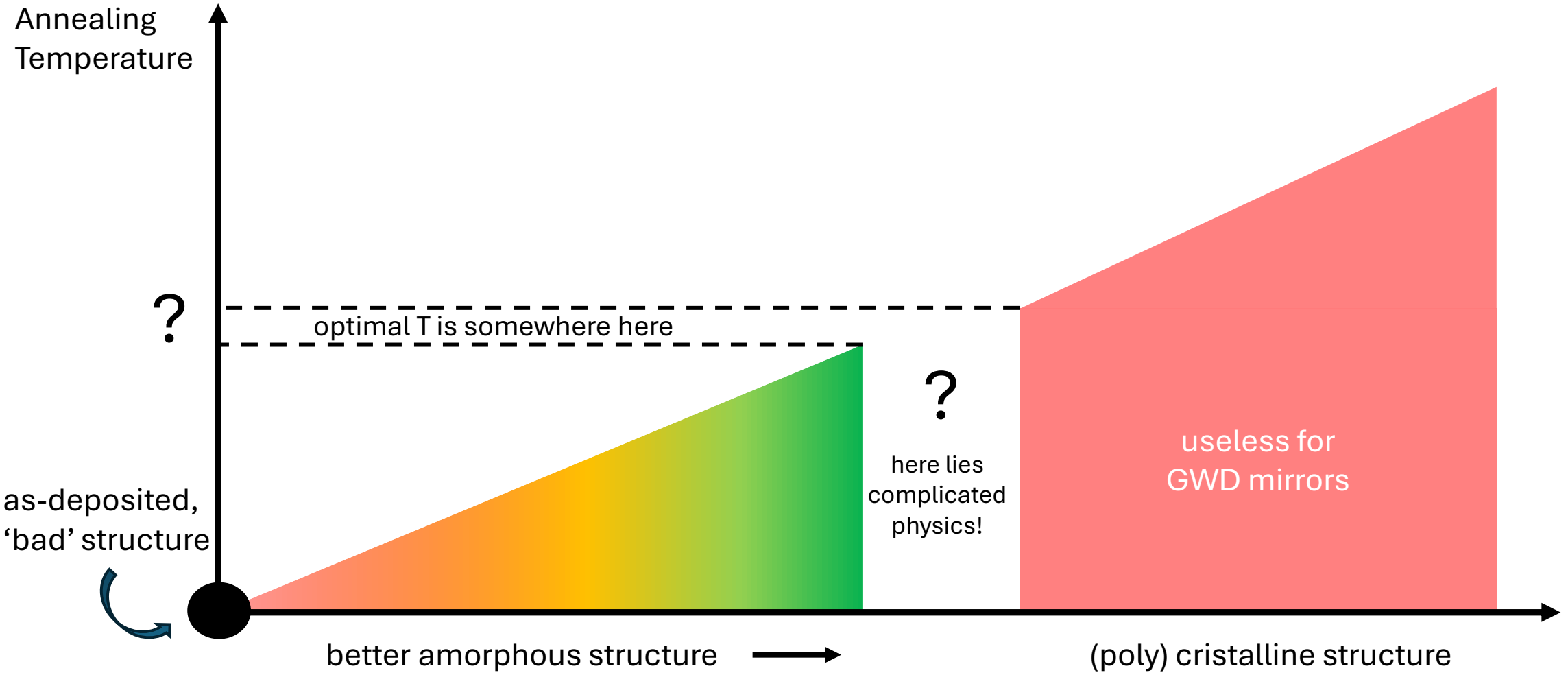

It’s all about the atomic structure

Università di Genova

The **potential energy landscape** is a useful representation to understand which kind of amorphous materials we are looking at.

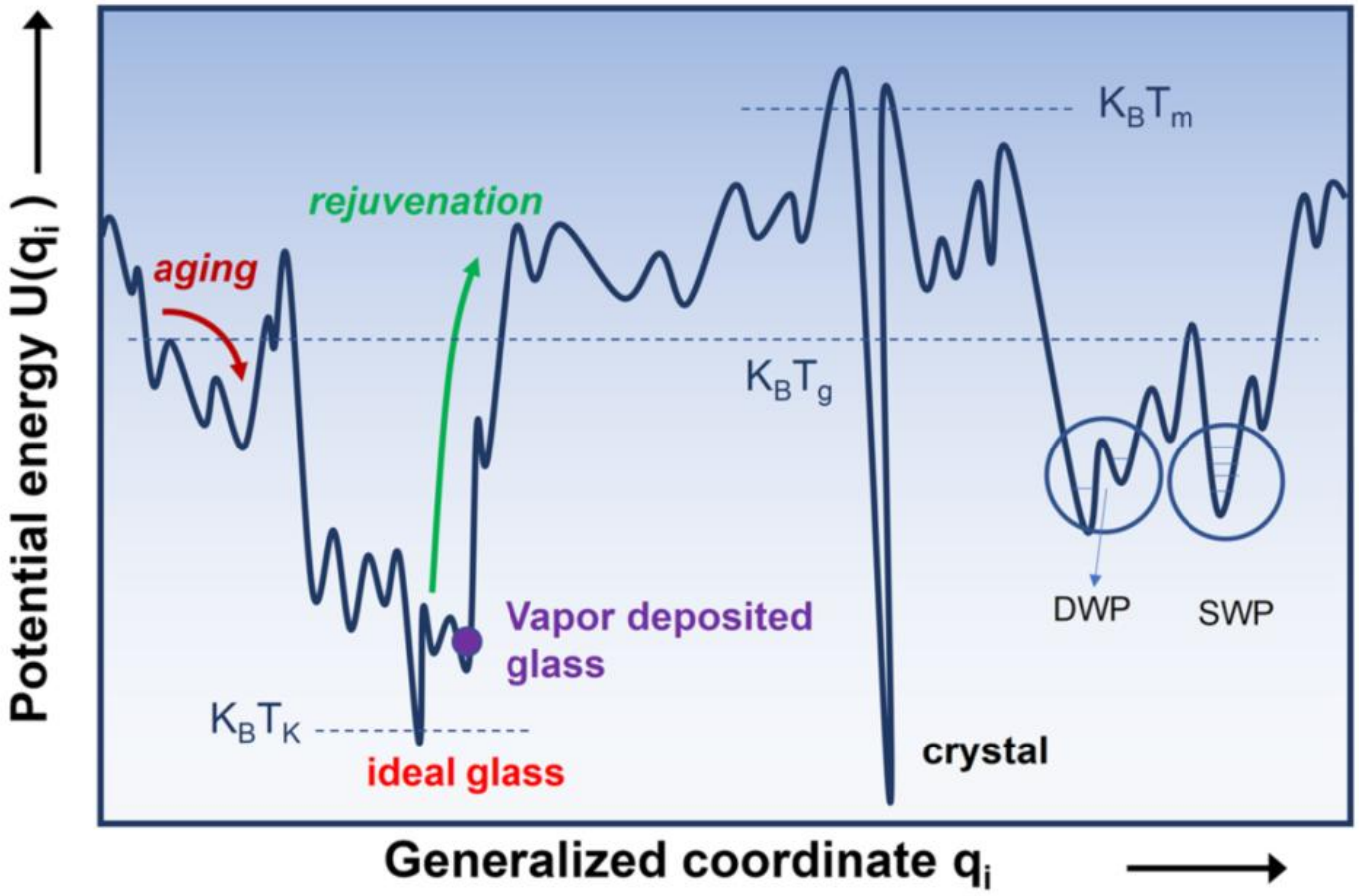

Rodriguez-Tinoco et al., *Rivista Nuovo Cimento* (2022) 45:325–406

Two-level systems: at the heart of thermal noise

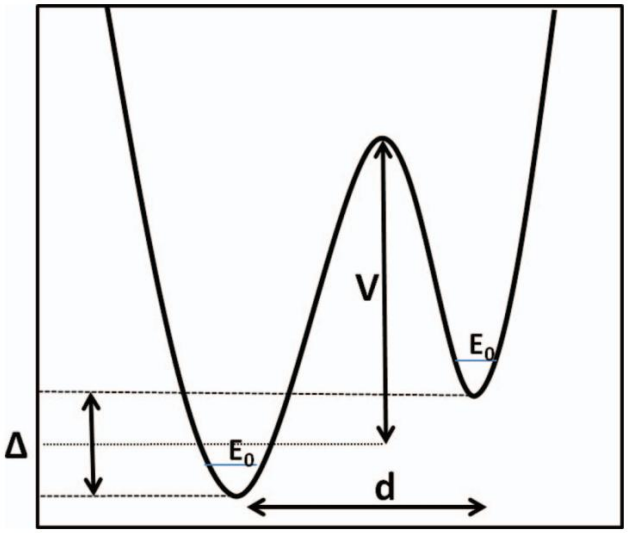

Transitions between different configurations are possible, even at temperatures that are well below the glass transition temperature.

The transitions in amorphous oxides mainly involve **rotations of the oxygen bonds around the tetrahedral structure**

Atoms involved:
20-60 (most transitions)
>100 (few transitions)

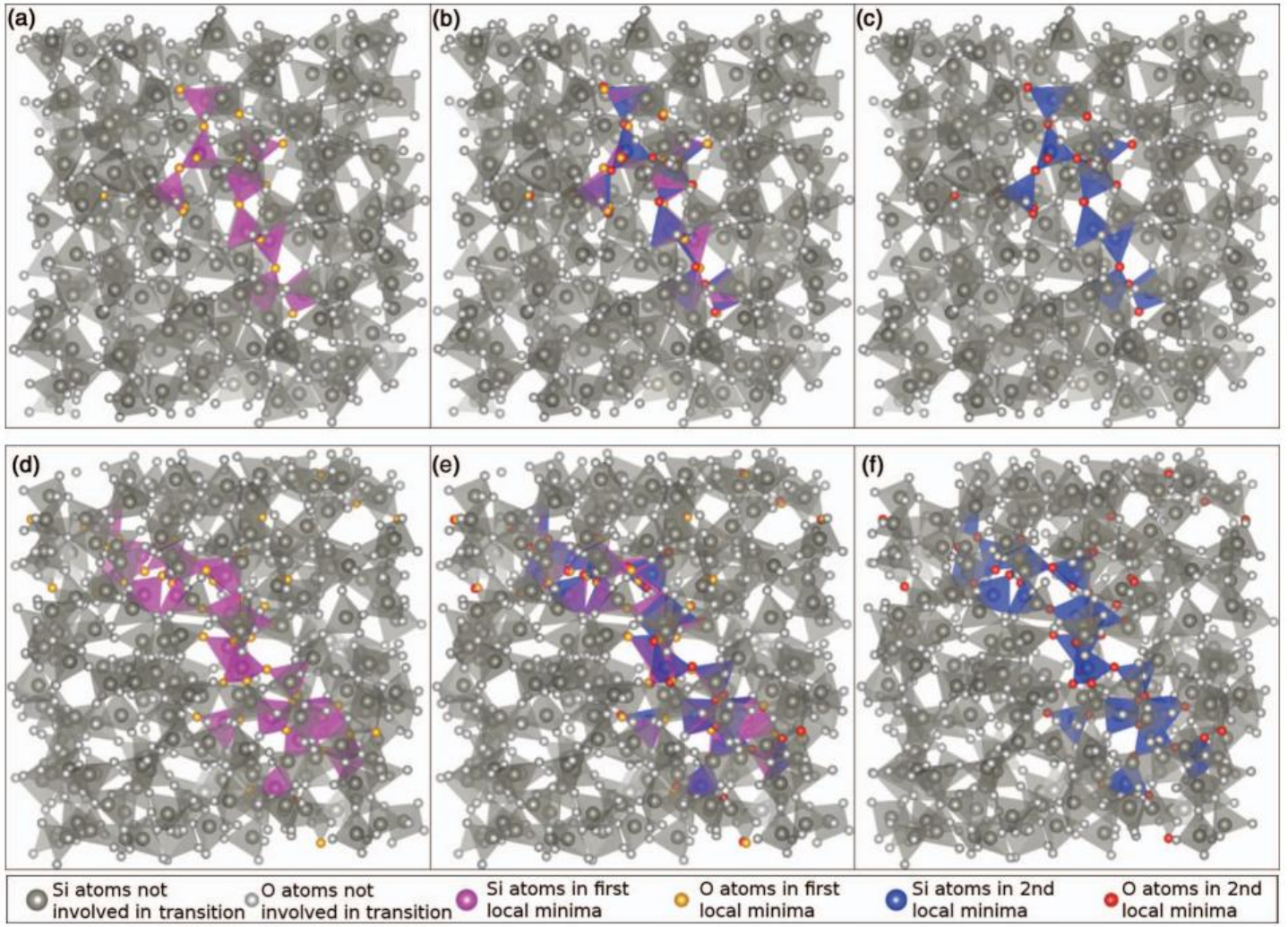

Hamdan et al., *J. Chem. Phys*. 141, 054501 (2014)

The low-index material

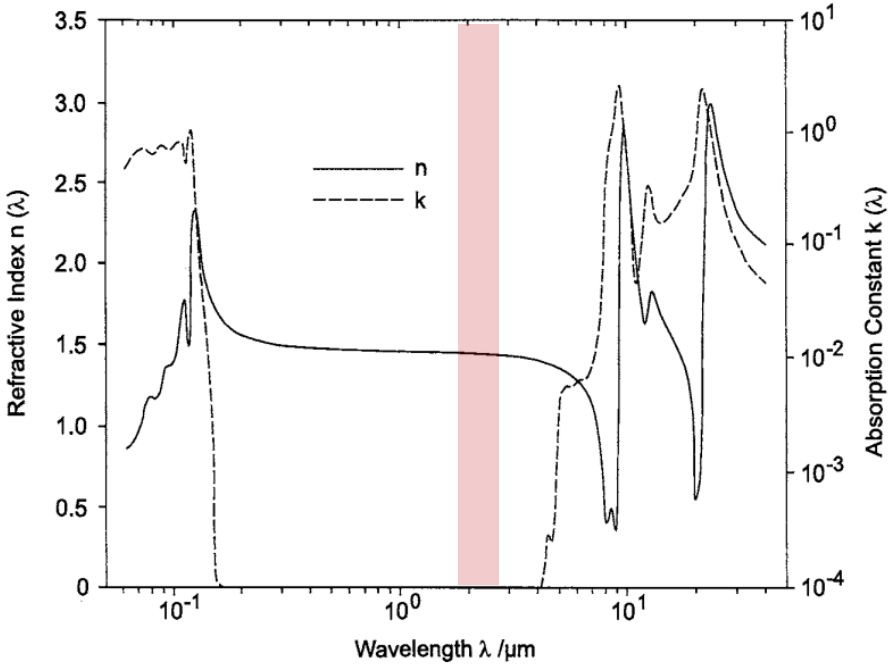

Bach, Neuroth, The Properties of Optical Glass, Springer 1998

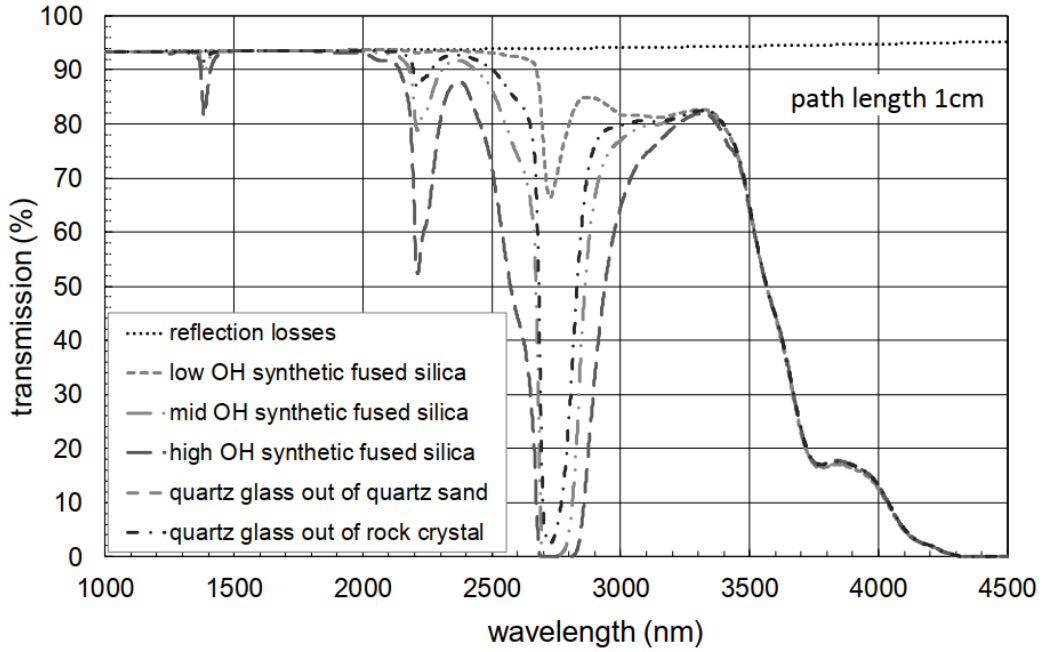

F. Nürnberg, B. Kühn, K. Rollmann, "Metrology of fused silica," Proc. SPIE 10014F, 2016

Fused silica (SiO_2) is the prototypical low-index material for optical coatings:

- easy to produce
- composed of cheap elements
- widely studied
- benchmark for coatings performance at room temperature

The low-index material

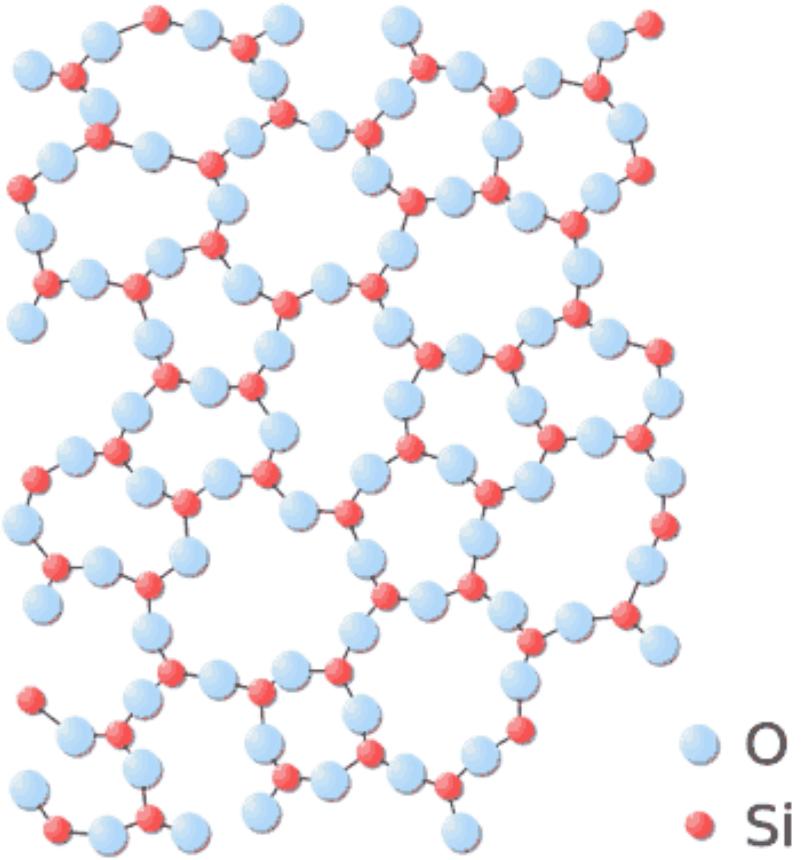

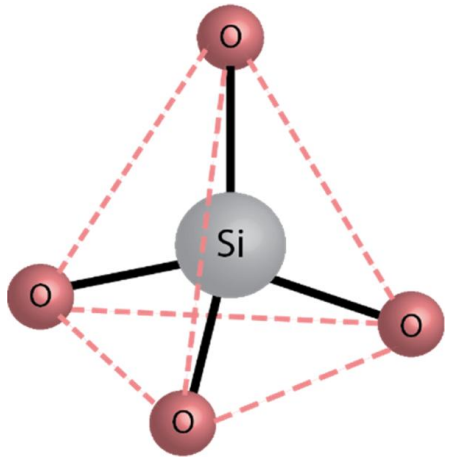

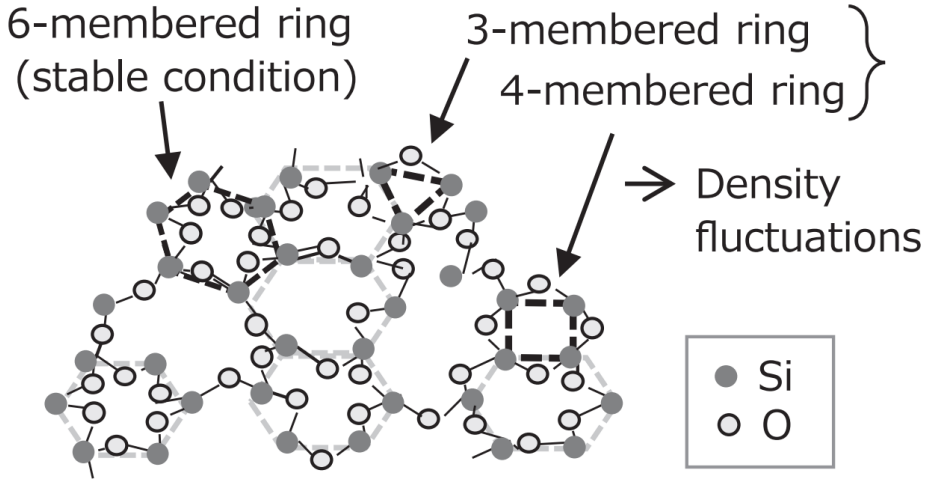

Hasegawa_SeiTechRev_2018

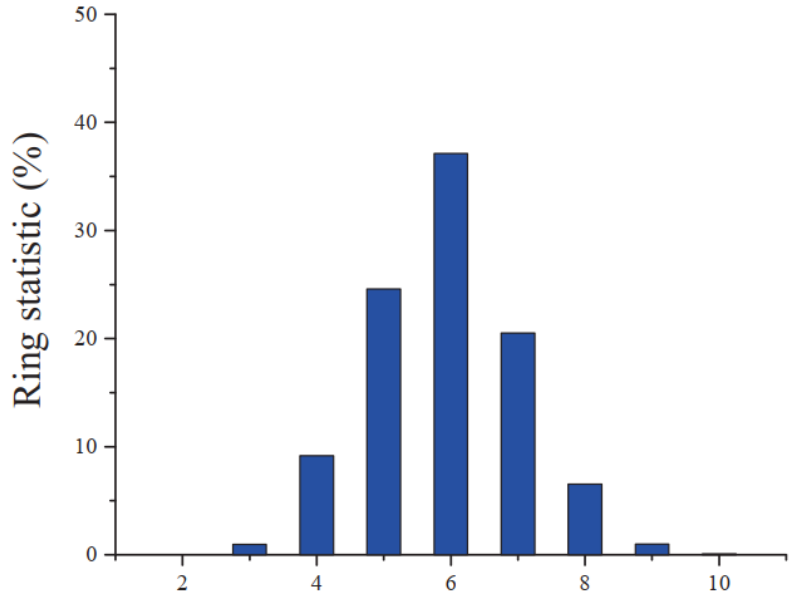

Jin et al., *Phys. Rev. B* 50, 118, 1994

The low-index material

Università di Genova

The thermal noise of mirror coatings for gravitational-wave detectors critically depends on the elastic properties of the constituent materials. Data analyses and theoretical models typically assume each material is homogeneous and isotropic, but isotropy has never been explicitly verified. Using Brillouin light scattering (BLS), we demonstrate that ion-beam-sputtered SiO_2—a material still viable for future mirror coatings—exhibits cylindrical elastic symmetry, with in-plane isotropy but a notable 6% compressive anisotropy along the film normal. This anisotropy remains unchanged after the postdeposition heat treatment currently used in ground-based detectors (500 °C, 10 h) but is nearly eliminated at 900 °C. Infrared reflectivity experiments support these findings by directly revealing heterogeneities in the distribution of bridging and nonbridging oxygen structures along the growth axis. While BLS measures the real part of the elastic constants at gigahertz frequencies, the data reveal negligible contributions from mechanical relaxations in the kilohertz to gigahertz range, making BLS a valid substitute for low-frequency properties obtained from standard anisotropy-insensitive techniques. Our results highlight that restoring isotropy through heat treatment—by softening the material, enabling more than 7% out-of-plane expansion, and smoothing out structural heterogeneities—may play a key role in reducing thermal noise. This proof-of-concept study extends beyond silica, providing critical insights for the design of future coatings.

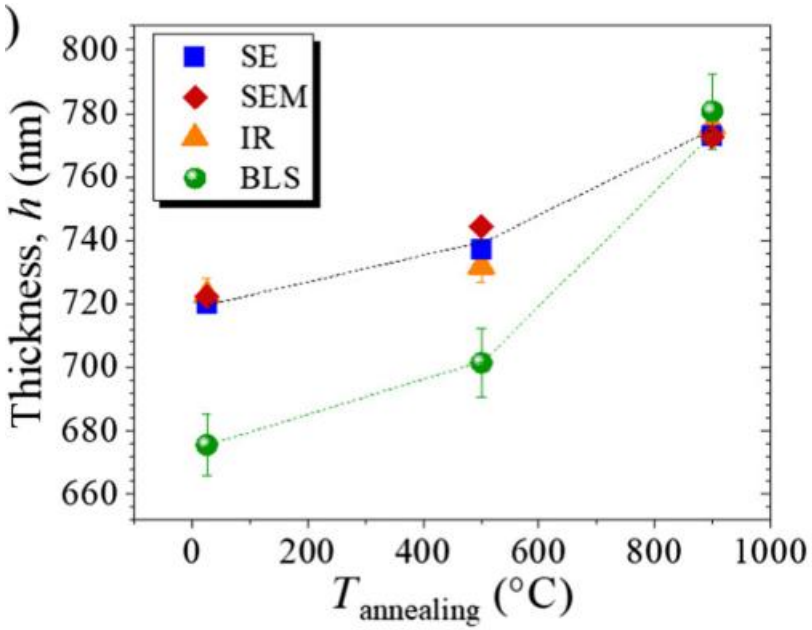

"Our study challenges the **long-standing assumption of elastic and structural isotropy in amorphous materials for GW mirror coatings**, providing quantitative evidence of anisotropy in ion-beam-sputtered SiO_2 and linking it to mechanical dissipation".

Bracco et al., *Phys. Rev. X* 16, 021036 (2026)

The low-index material: a lesson from history

What is the **optical absorption** of silica-based glasses?

Answer:
It depends on how they are produced!

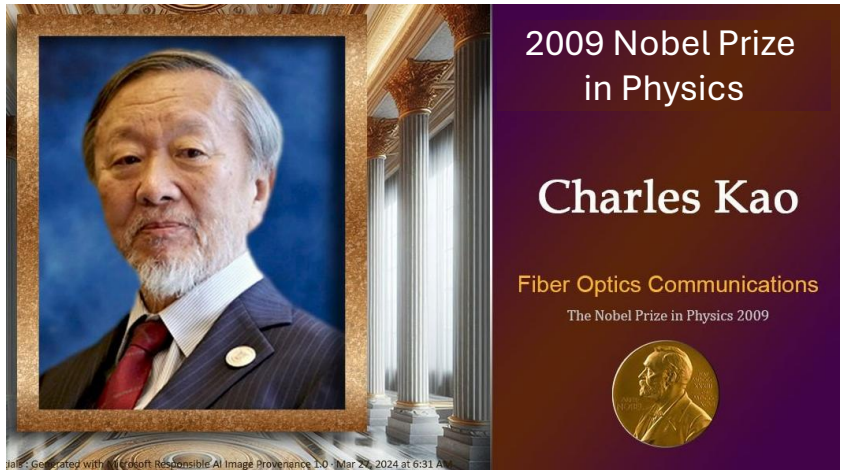

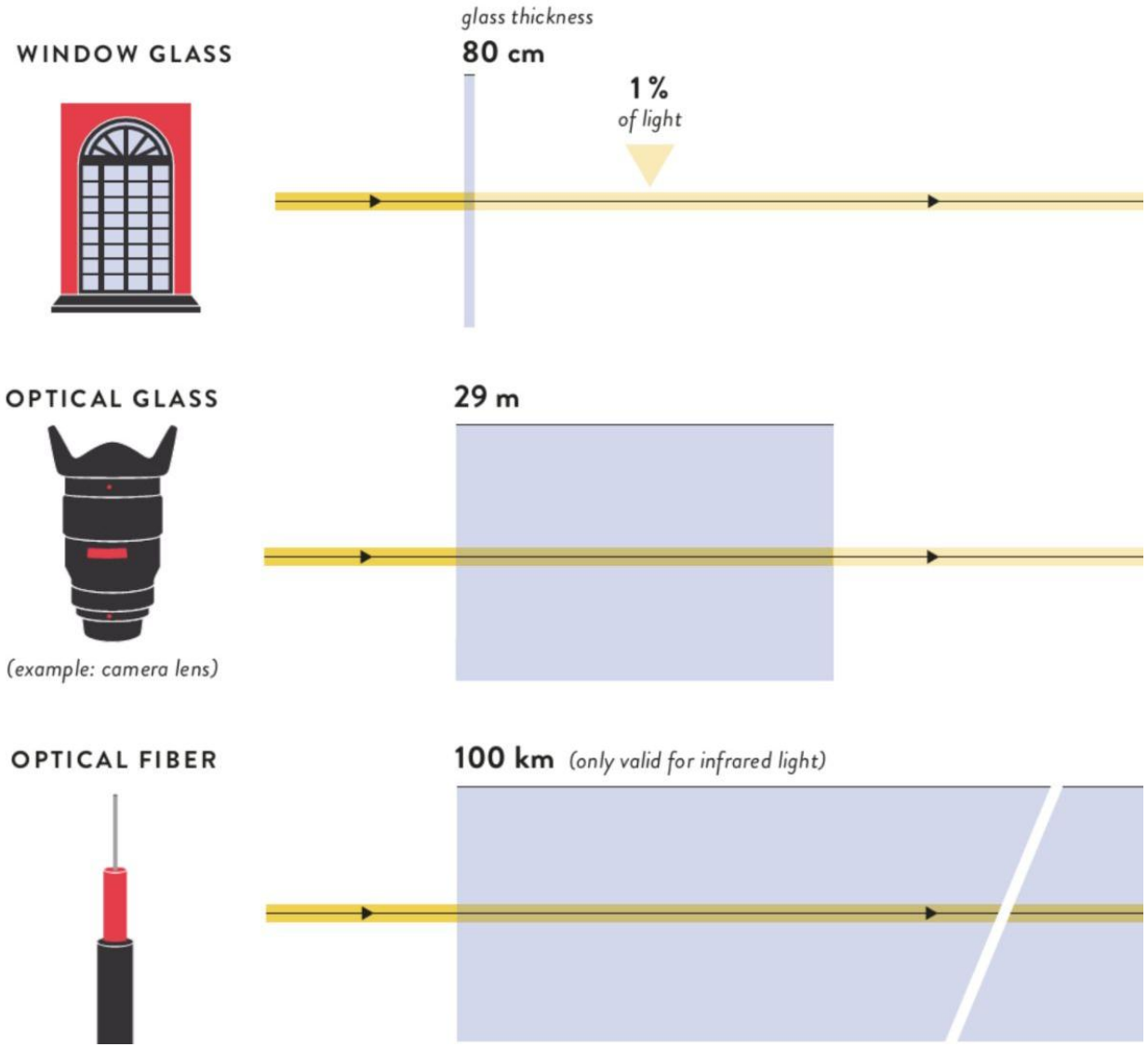

The high-index materials: Ta_2O_5

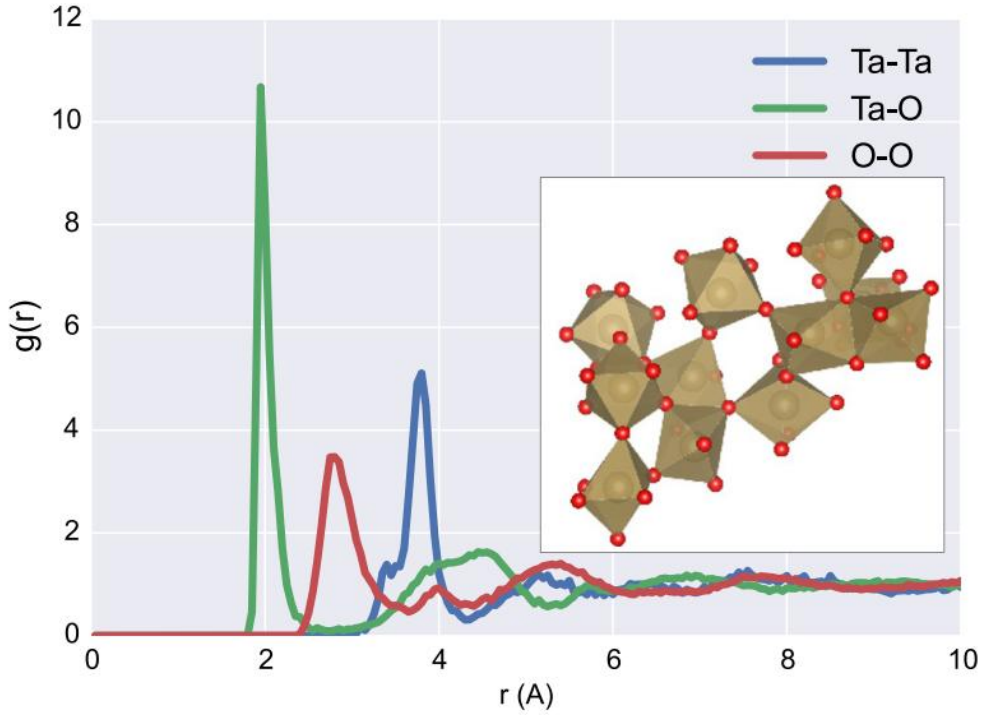

Tantalum	%	Oxygen	%
Coord. 4	0.5	Coord. 2	69.9
Coord. 5	28.5	Coord. 3	30.1
Coord. 6	69.4		
Coord. 7	1.6		

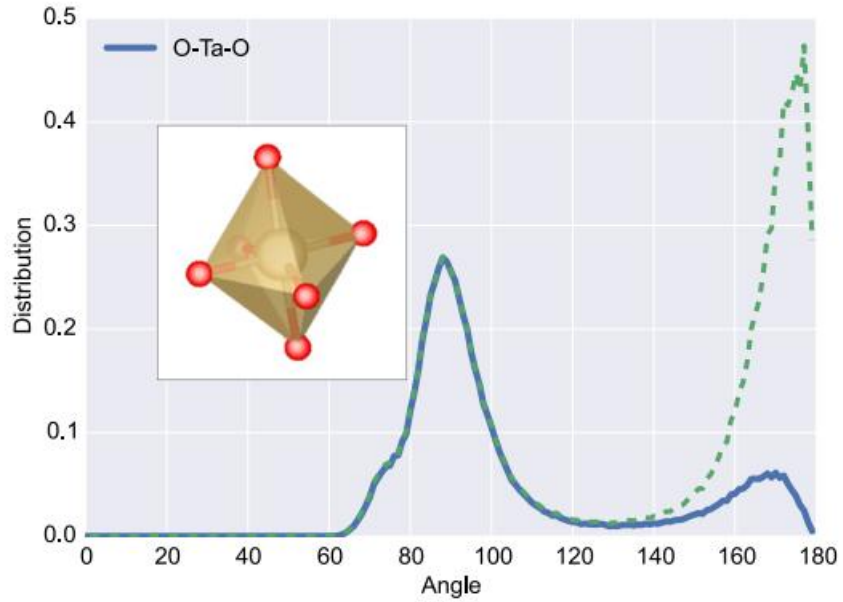

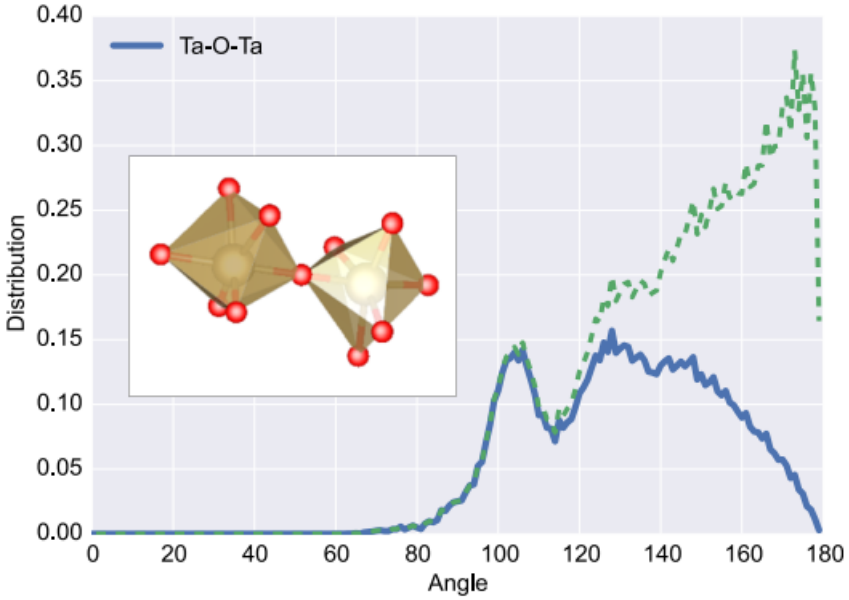

Damart et al., *J. Appl. Phys*. 119, 175106 (2016)

The high-index materials: Ta_2O_5

Simulation of ion-beam-sputtered tantalum oxide with high and low energy

Low energy

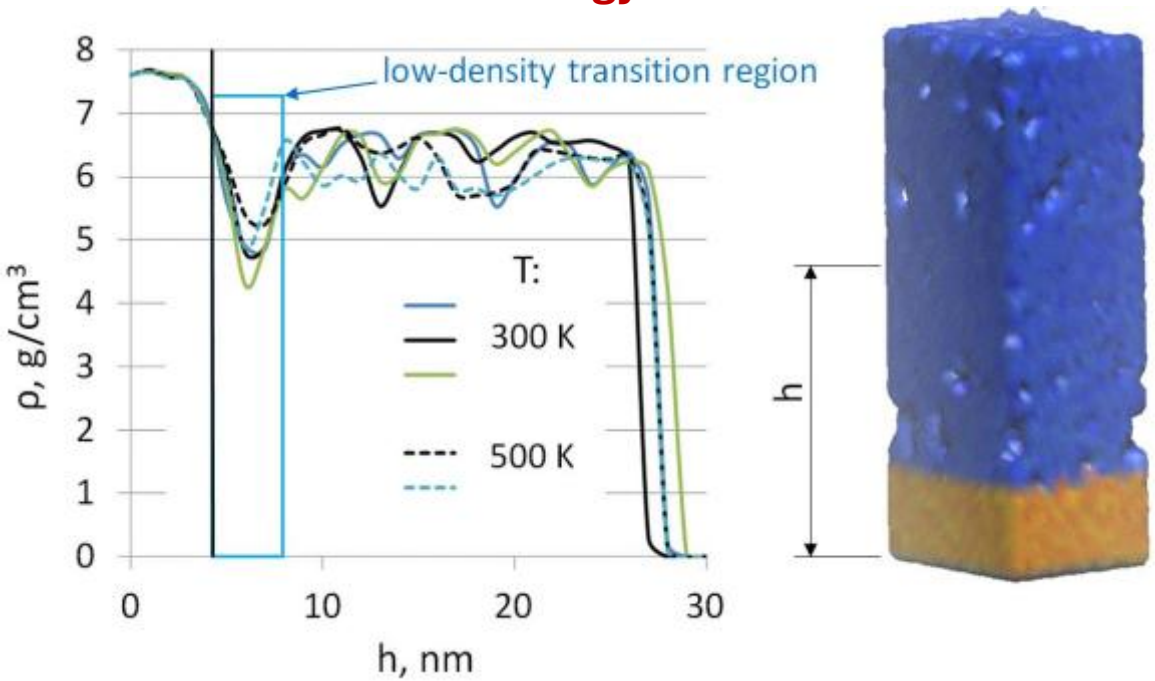

In low-energy deposited films, there are pores which could absorb molecules during deposition.

High energy

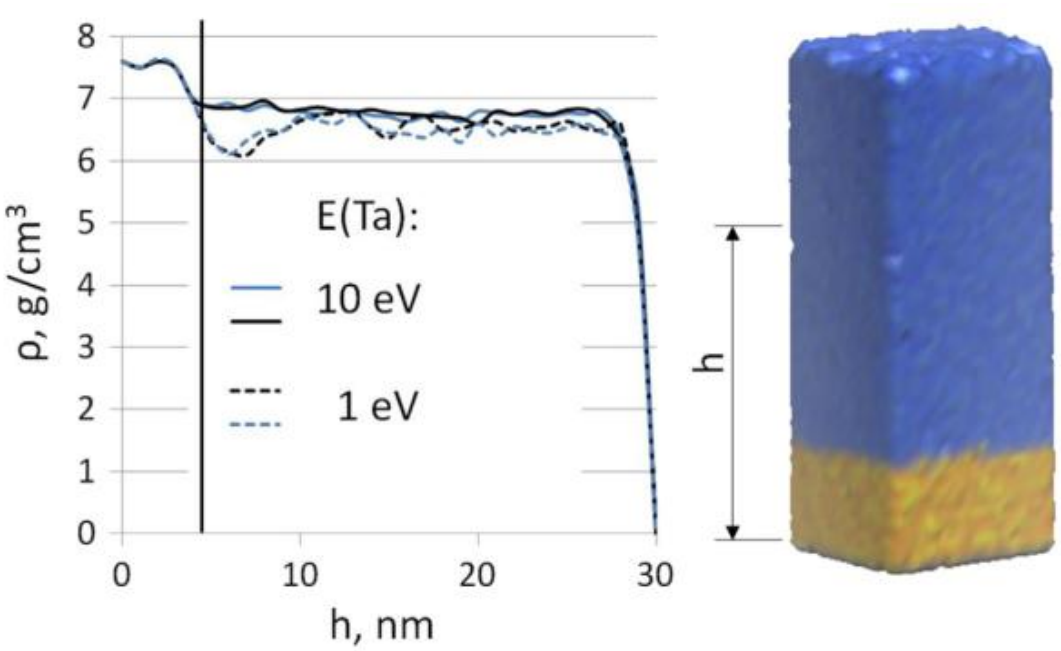

In high-energy deposited films, there are no pores with a characteristic size ofmore than 0.1 nm.

Grigoriev et al., *Appl. Opt*. 64, 369, 2025

Mixed amorphous oxide coatings

Università di Genova

'Pure' amorphous oxide coatings offer a rather limited range of optical constants.

Mixing amorphous oxide coatings can offer possibilities to **tailor the optical and mechanical properties of coatings,** including:

- variable refractive index
- mitigation of deposition-induced stress

Chen et al., *Appl. Opt.* 31, 90 (1996)

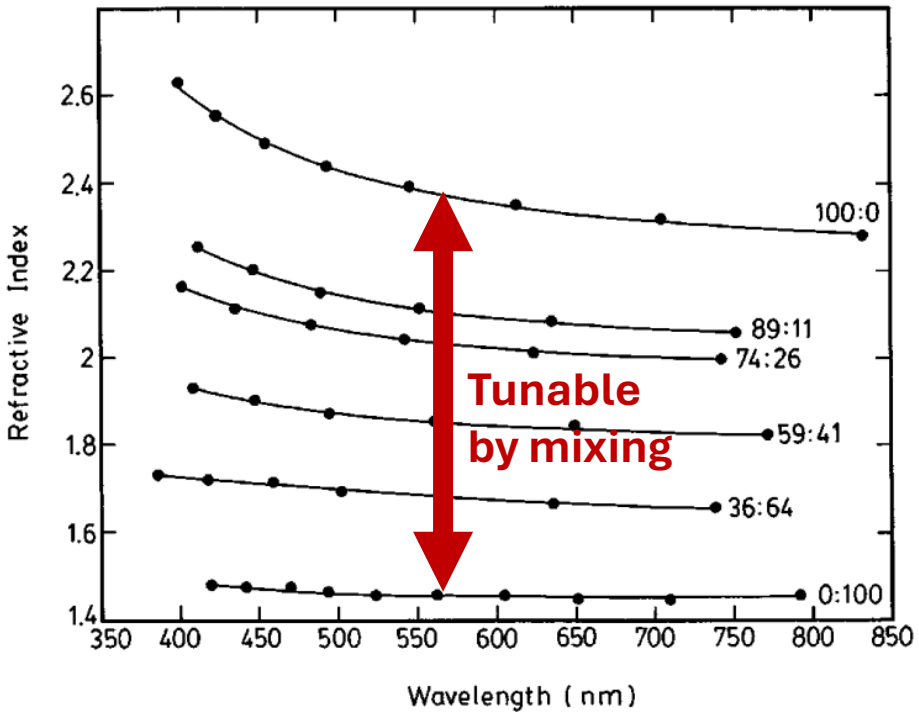

O. Stenzel et al., *Appl. Opt.* C69, 50 (2011)
V.N. Yadava et al., *Thin Sol. Films* 17, 243 (1973)

The high-index materials: Ti:Ta_2O_5

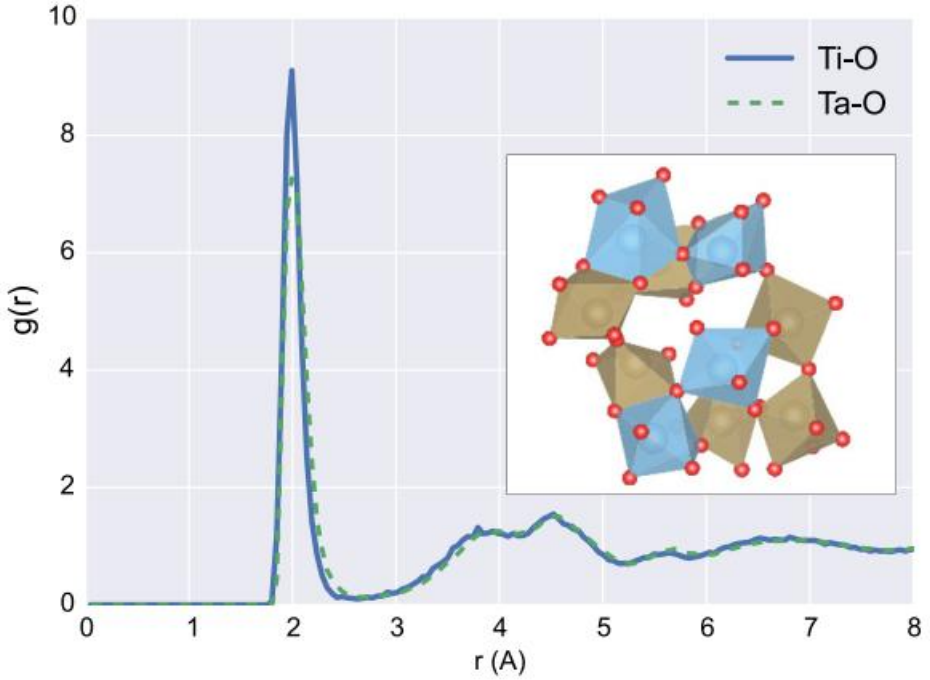

Tantalum	%	Titanium	%	Oxygen	%
Coord. 4	1.1	Coord. 4	4.1	Coord. 2	33.9
Coord. 5	27.6	Coord. 5	45.0	Coord. 3	65.0
Coord. 6	68.7	Coord. 6	50.4	Coord. 4	1.2
Coord. 7	2.6	Coord. 7	0.5		

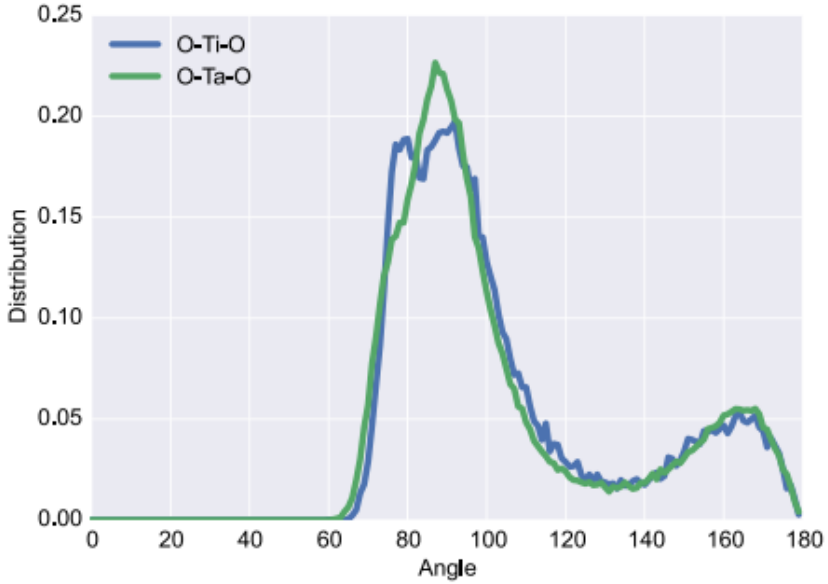

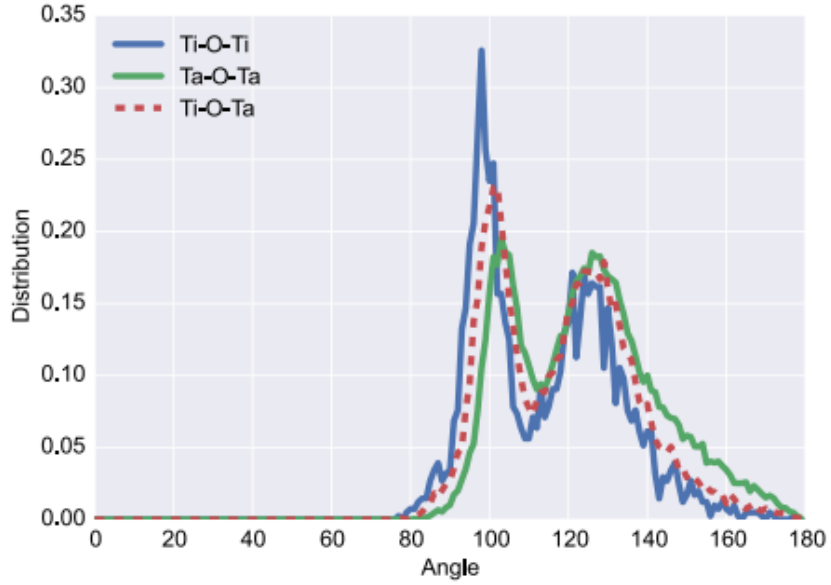

Damart et al., *J. Appl. Phys*. 119, 175106 (2016)

The quest for a better high-index material

Università di Genova

Finding and validating new materials for GWD mirrors requires multiple characterizations:

- mechanical loss
- optical absorption
- surface homogeneity
- refractive index
- scattering
- anisotropy
- …

Material	n_{1064}	n_{1550}	n_{2000}*	Y (GPa)	μ	φ (10^{-4} rad)
Al_2O_3:Ta_2O_5	2.01 ± 0.01	2.00 ± 0.01	1.99 ± 0.01	132 ± 6	0.37 ± 0.08	3.8 ± 1.0
SiO_2:Ta_2O_5	1.93 ± 0.01	1.92 ± 0.01	1.92 ± 0.01	121 ± 2	0.39 ± 0.02	3.16 ± 0.22
Sc_2O_3:Ta_2O_5	2.09 ± 0.01	2.07 ± 0.01	2.06 ± 0.01	133 ± 2	0.39 ± 0.03	3.17 ± 0.20
TiO_2:Ta_2O_5	2.19 ± 0.01	2.18 ± 0.01	2.16 ± 0.01	128 ± 4	0.35 ± 0.02	2.81 ± 0.10
ZnO:Ta_2O_5	2.05 ± 0.01	2.04 ± 0.01	2.04 ± 0.01	103 ± 2	0.49 ± 0.02	2.57 ± 0.22
Y_2O_3:Ta_2O_5	2.03 ± 0.01	2.02 ± 0.01	2.01 ± 0.01	123 ± 5	0.35 ± 0.07	3.74 ± 0.25
ZrO_2:Ta_2O_5	2.07 ± 0.01	2.06 ± 0.01	2.05 ± 0.01	143 ± 5	0.36 ± 0.05	3.12 ± 0.37
Nb_2O_5:Ta_2O_5	2.11 ± 0.01	2.09 ± 0.01	2.09 ± 0.01	118 ± 4	0.3 ± 0.1	4.14 ± 0.29
HfO_2:Ta_2O_5	2.05 ± 0.01	2.04 ± 0.01	2.04 ± 0.01	146 ± 5	0.32 ± 0.06	3.21 ± 0.18

Fazio et al., *Phys. Rev. D*, 105, 102008 (2022)

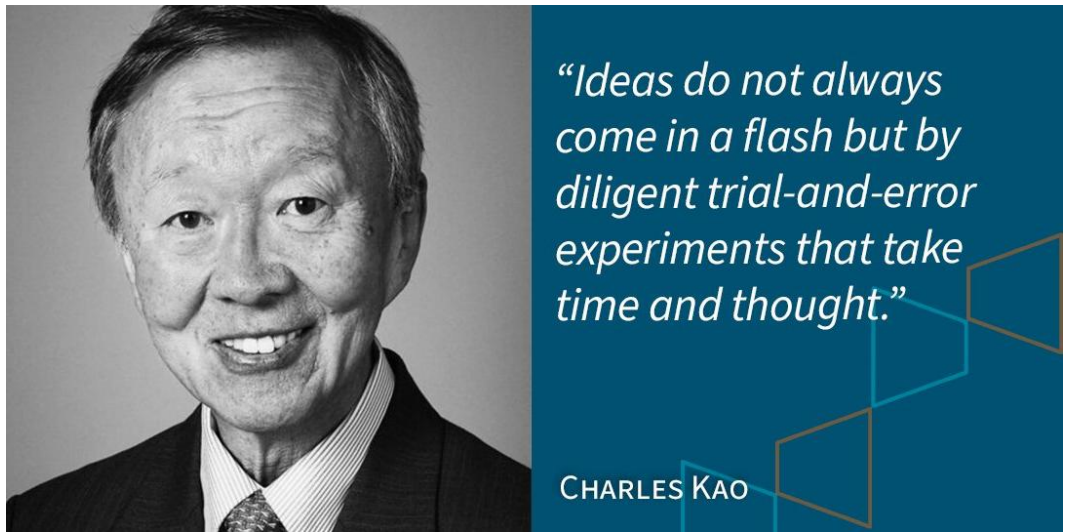

Amato, Magnozzi, Wohler, *Adv. Photon. Res.* 6, 2400117 (2025)

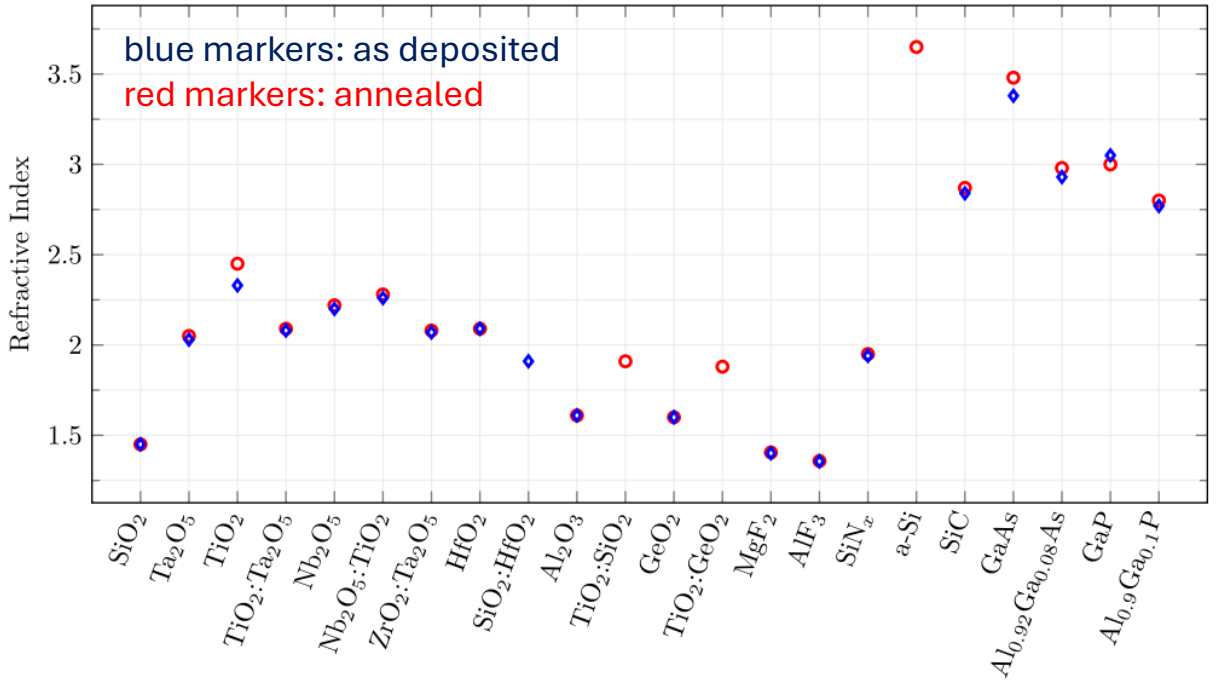

3

Open challenges & metrology

Optimizing coatings performance

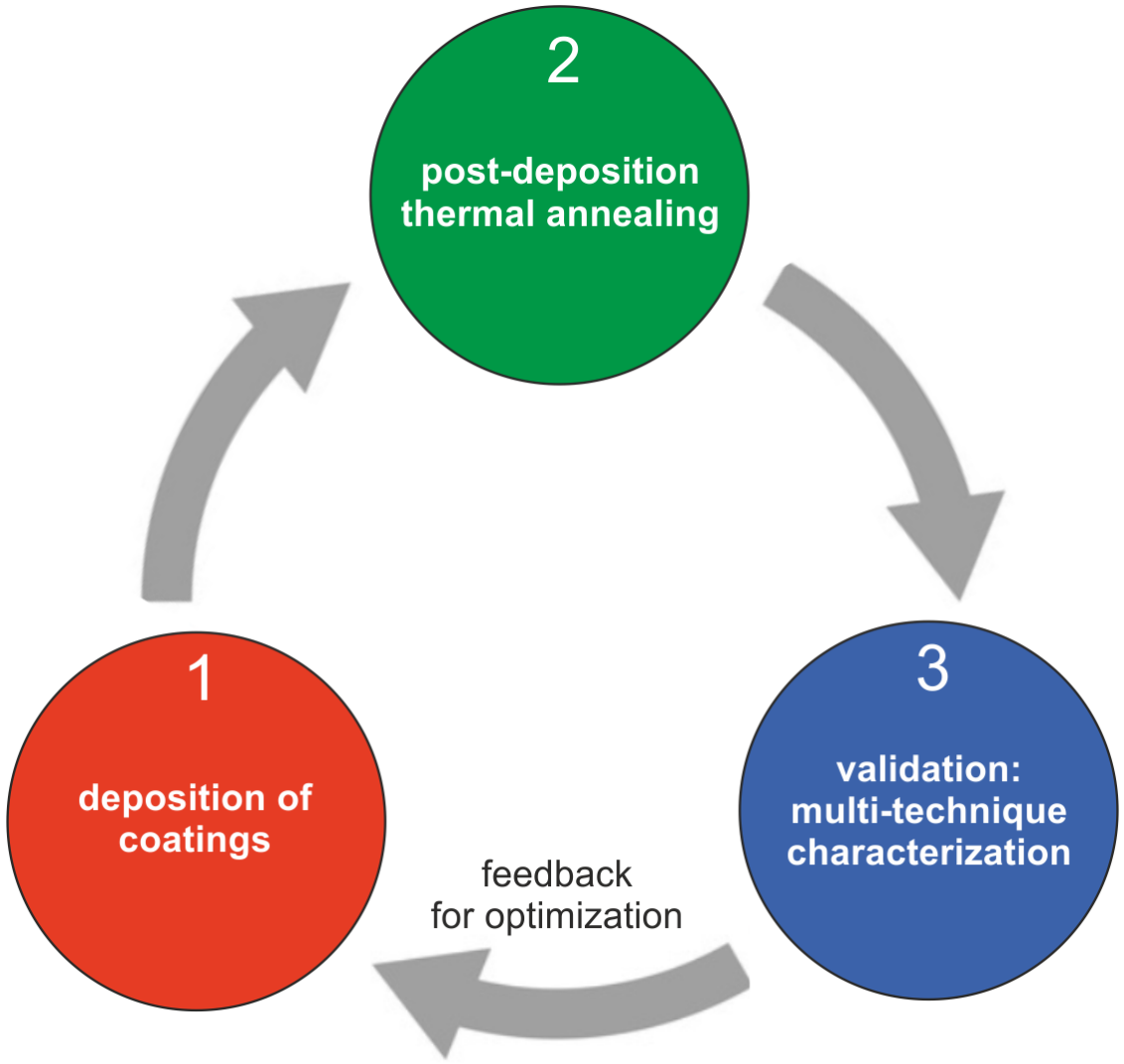

The optimization of coatings performance can be seen as a 3-step cycle composed of:

- Deposition
- Post-deposition annealing
- Characterization / validation

The effort is multidisciplinary and collaborative in nature: no single research group or person possesses the very specialized know-how that is necessary to develop, sustain and improve the cycle.

Over the past two decades and more, several collaborations were built (and, sometimes, financed) to tackle specific aspects of the optimization cycle.

Optimizing deposition

Università di Genova

The optimization of deposition is the first step towards the optimization of coatings performance.

Typically this endeavor is **planned meticolously in advance, with deposition campaigns aimed at exploring the parameters space,** such as (list is not exhaustive):

- deposition rate
- base pressure
- voltage and current of the ion beam
- type of ion gun / materials employed
- geometry of deposition
- type / flow of process gases
- temperature of the substrate

Sample	V (V)	I (mA)	Ar (sccm)	N_2 (sccm)	n	$k \times 10^5$
20043	1000	100	0	10	[a]	15.3
21012	400	100	5	10	2.00 ± 0.01	4.1
21013	500	100	5	10	2.02 ± 0.01	3.2
21014	300	100	5	10	1.97 ± 0.01	5.3
21016	200	75	5	10	1.90 ± 0.01	4.1
21017	400	100	3	12	1.99 ± 0.01	5.1
21018	500	100	3	12	2.01 ± 0.01	4.4
21019	300	100	3	12	1.97 ± 0.01	5.9
21020	700	100	3	12	2.02 ± 0.01	3.4
21021	700	100	5	10	2.03 ± 0.01	2.3
21022	900	100	5	10	2.05 ± 0.01	28.0
21023	700	50	5	10	2.00 ± 0.01	25.2
21025	700	195	5	10	2.04 ± 0.01	1.4
22013	900	195	5	10	2.12 ± 0.01	9.0
22014	500	195	5	10	2.04 ± 0.01	3.5
22015	500	100	0	10	2.03 ± 0.01	7.5

Amato et al., *Phys. Rev. D* 111, 042003 (2025)

Optimizing deposition: substrate temperature

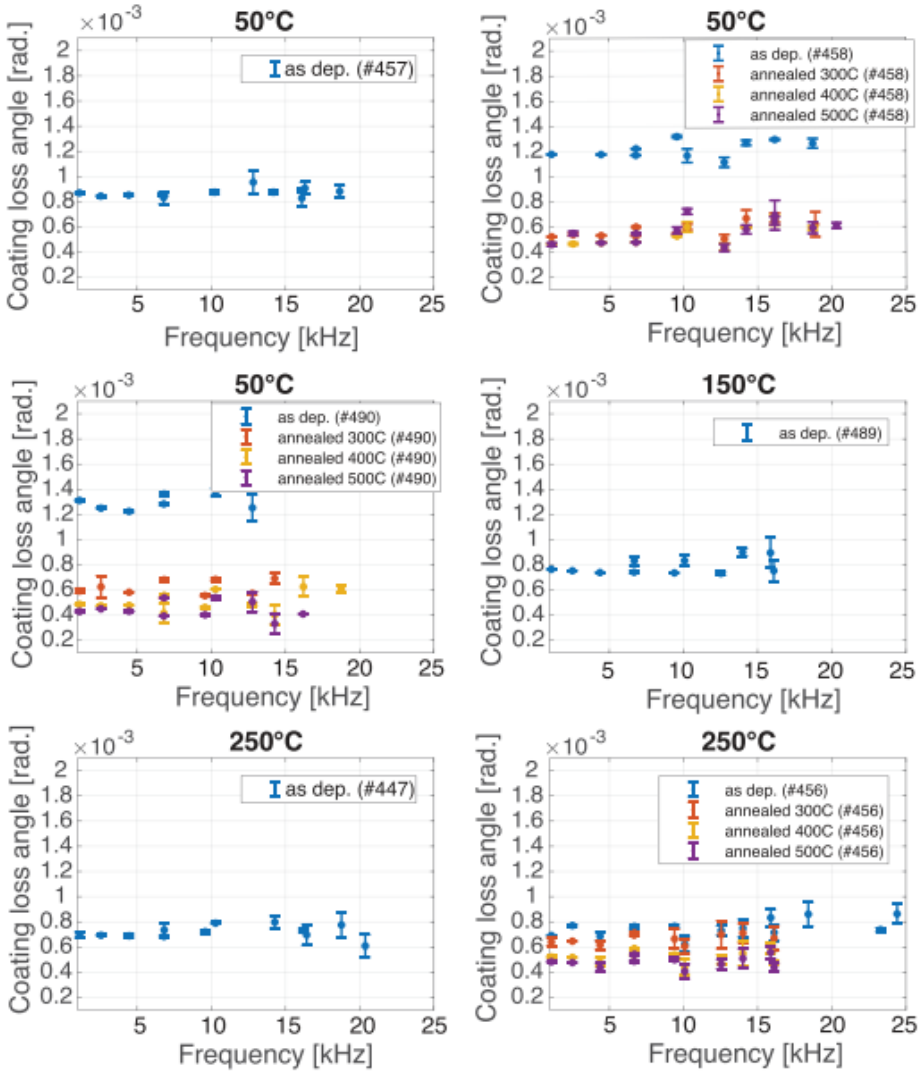

G Vajente et al 2018 *Class. Quantum Grav*. 35 075001

"Depositing tantala on a hot substrate reduced the mechanical losses [..], but subsequent thermal treatments had a larger impact, as they reduced the losses to levels previously reported in the literature"

Yang *et al.*, *Sci. Adv.* 2021; **7** : eabh1117

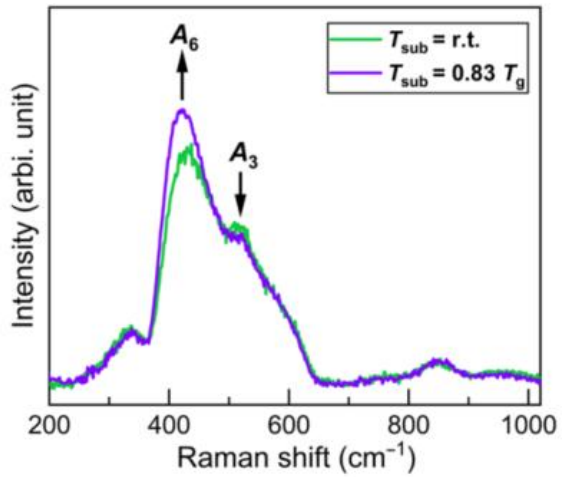

Fig. 1. Raman scattering spectra of a-GeO_2 thin films deposited at different temperatures. T_{sub} = room temperature (r.t.; green) and T_{sub} = 0.83 T_g (purple). The A_6 peak at around 430 cm^{-1} corresponds to the symmetric stretching of bridging oxygen in six-membered rings. The A_3 peak at around 510 cm^{-1} corresponds to the breathing motion of bridging oxygen in three-membered rings. The peak at 337 cm^{-1} is assigned to the Ge "deformation" motion within the network (*33*, *34*).

"Deposition [of germania] near the glass transition temperature is more efficient than postgrowth annealing in modifying atomic structure at medium range"

Optimizing annealing: partial crystallization

Until a few years ago, the upper limit of annealing temperature had to be lower that the onset of crystallization.
Coatings were kept strictly amorphous throughout deposition and annealing.

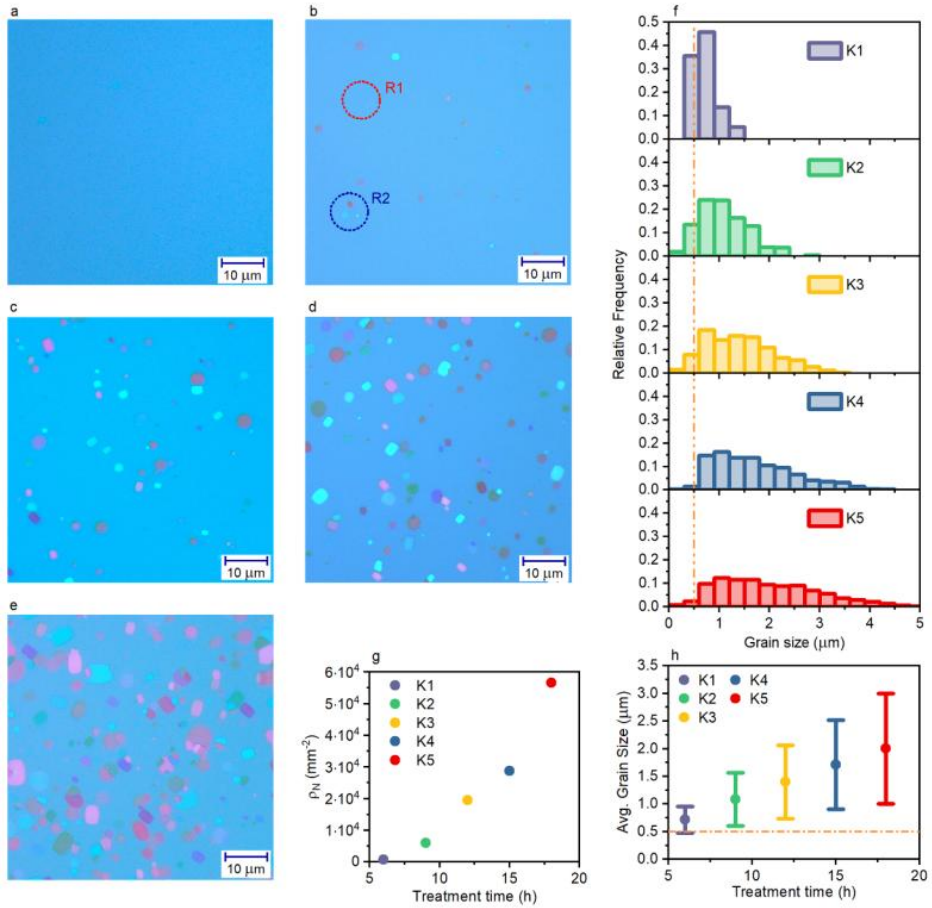

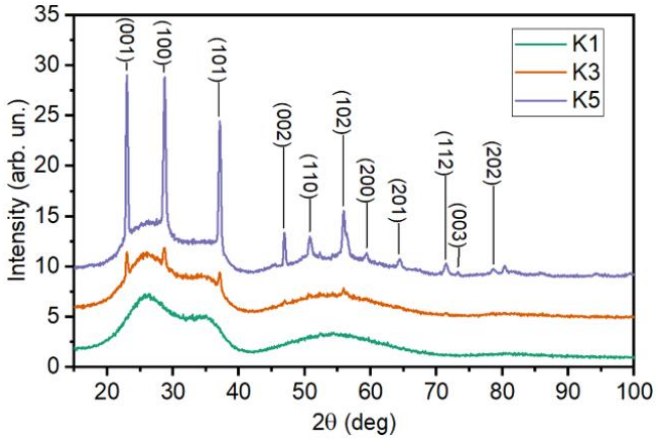

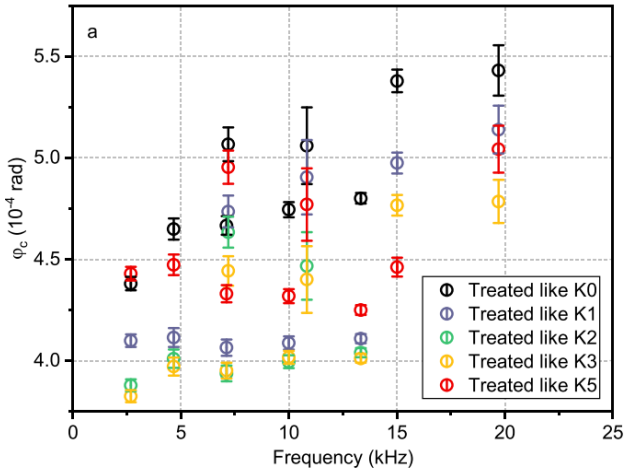

Limited reduction of loss angle for partially-crystallized samples.

Caution! This has to be balanced with scattering!

Favaro et al., *Class. Quant. Grav.* **41** (2024) 105009

Optimizing annealing: structural modifications

Università di Genova

Prasai et al., *Phys. Rev. Lett.* 123, 045501 (2019)

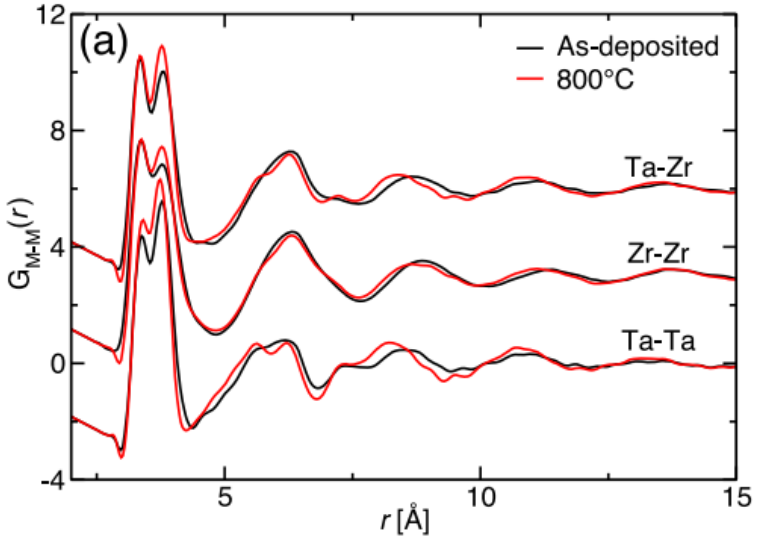

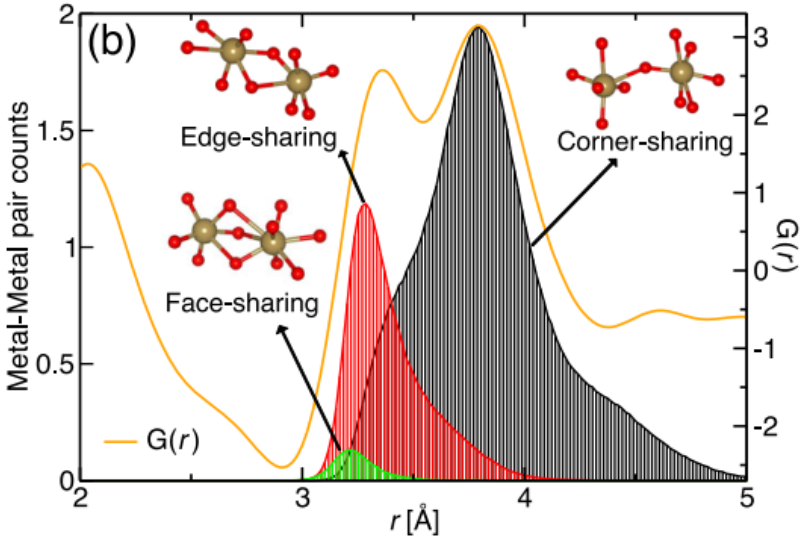

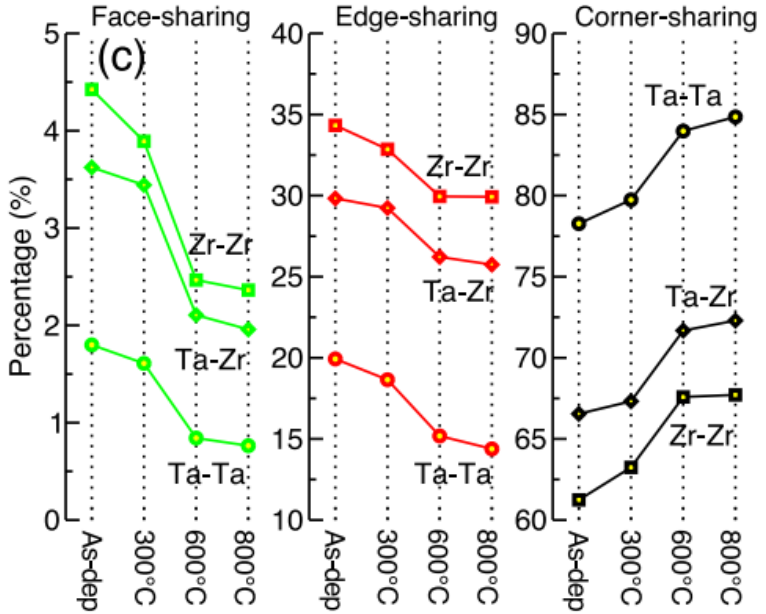

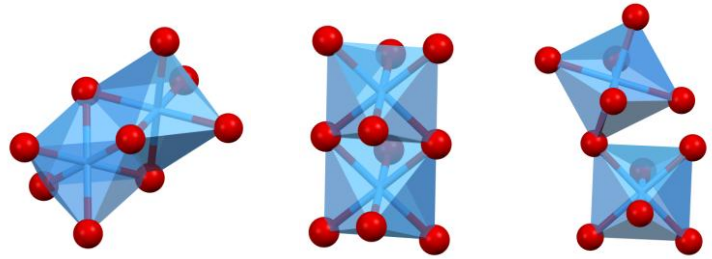

Magnozzi, unpublished results

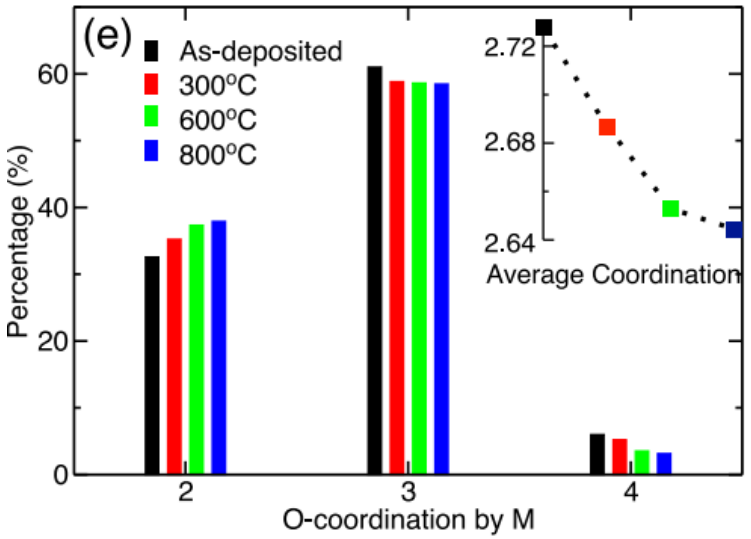

How annealing affects the structure:

- short-range order: *small changes*
- medium-range order: *sizable effects*

Optimizing annealing: ex situ approaches

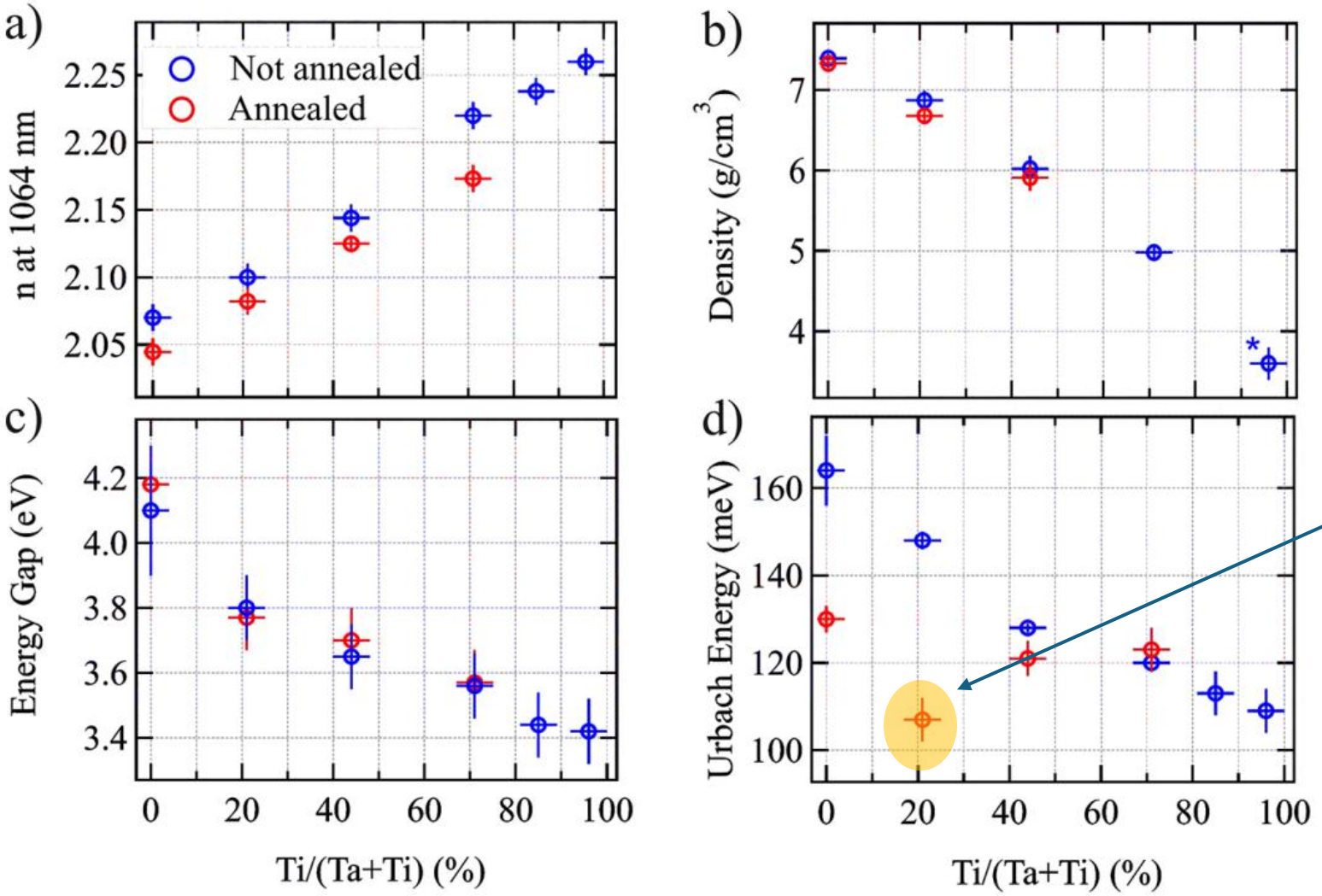

Samples: $Ti:Ta_2O_5$ coatings with Ti/Ta ratio variable from 0 to 100.

The effects of annealing on 4 key parameters are determined with ellipsometry.

Current GWD mirrors use this Ti/Ta composition

Lowest Urbach energy

Best-performing coatings

A. Amato, M. Magnozzi et al., *ACS Appl. Opt. Mater.* 1, 395, (2023)

A. Amato et al., *Sci. Rep.* 10:1670 (2020)

Optimizing annealing

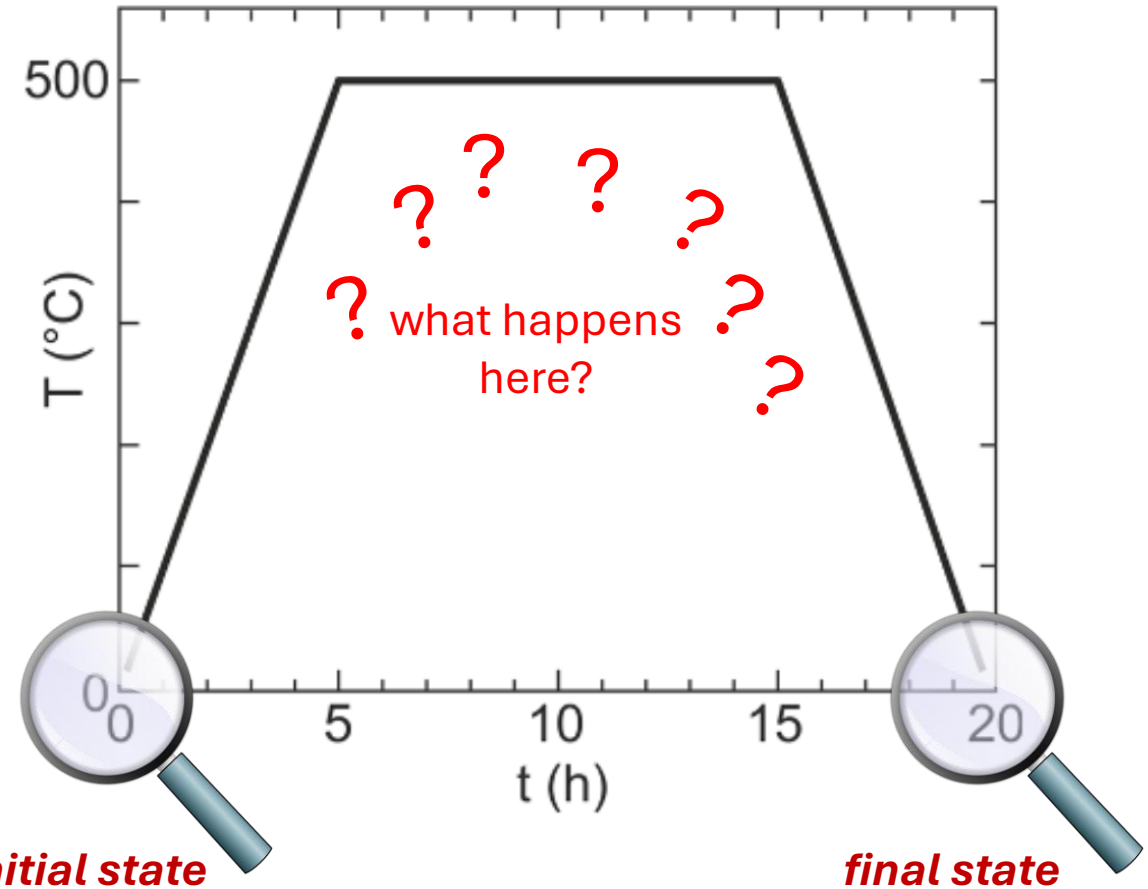

initial state
(as deposited)

final state
(after annealing)

The ex-situ analysis has several advantages, but it probes **only the initial and final state** of the coatings, while it leaves us blind about all the real-time evolution occurred during the annealing.

Disadvantages of ex-situ analysis:

- no information about the process
- optimization of annealing parameters is difficult (trial-and-error, but blind)
- if the final and initial state are similar: has anything happened at all during the annealing?

To optimize annealing, one should understand what happens during that process in the first place

Annealing TiO_2:GeO_2

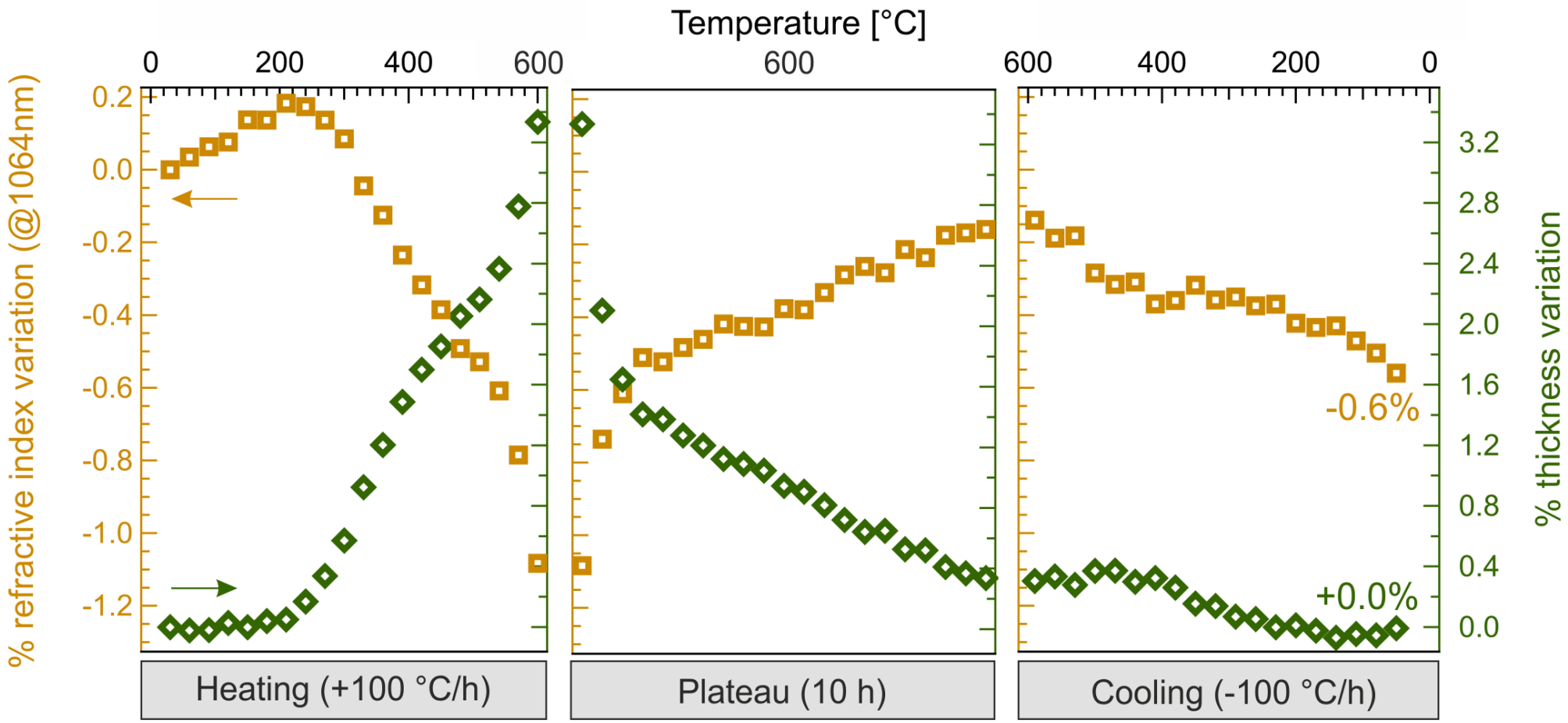

- Thickness increases
- Refractive index decreases

REVERSED TRENDS AT CONSTANT T

Reversible effects (T dependent)

M. Magnozzi et al., *J. Non-Cryst. Sol.* 667, 123886 (2026)

Annealing TiO_2:GeO_2

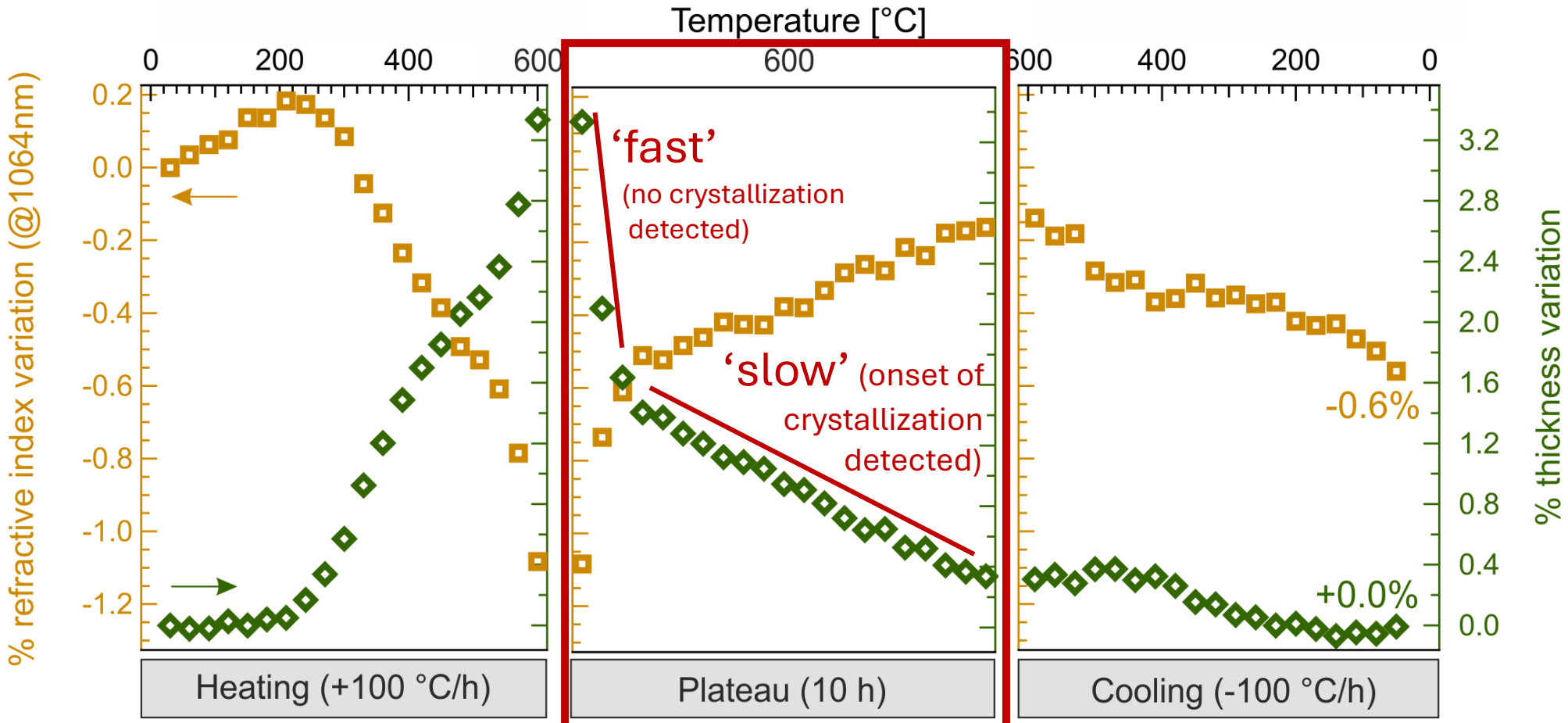

- Thickness increases
- Refractive index decreases

REVERSED TRENDS AT CONSTANT T

Reversible effects (T dependent)

'fast': Argon desorption (<0.7%) (E. Lalande et al., *Class. Quant. Grav.* 41, 115013 (2024))
'slow': onset of crystallization, as determined with Raman spectroscopy & XRD

M. Magnozzi et al., *J. Non-Cryst. Sol.* 667, 123886 (2026)

Annealing TiO_2:GeO_2

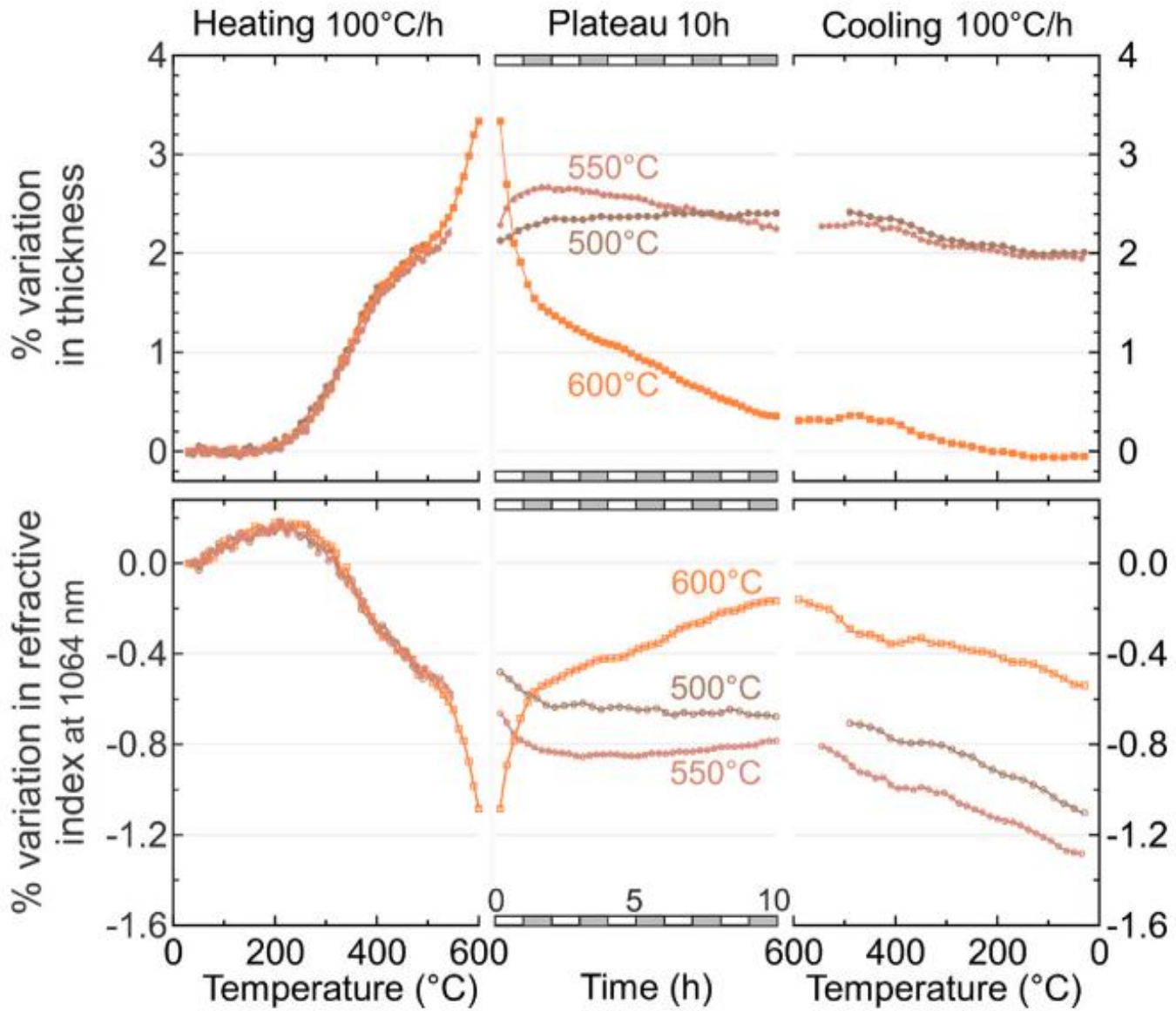

M. Magnozzi et al., *J. Non-Cryst. Sol.* 667, 123886 (2026)

Argon release during annealing

Argon is an almost unavoidable contaminant directly introduced by the Ion Beam Sputtering deposition technique.

It may or may not be released during annealing, and in doing so it might or may not cause catastrophic failures in the coatings (blistering)

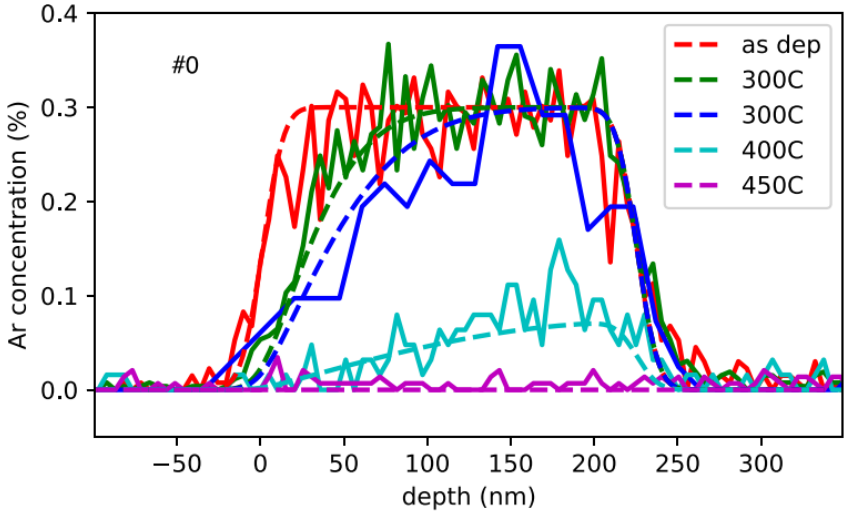

XPS spectrum of coating with 0.3% Ar:

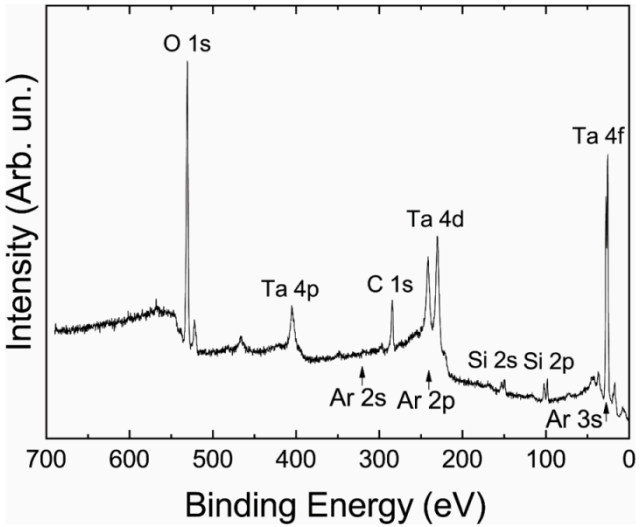

Paolone et al., J. Non-Cr. Sol. 557, 120651, 2021

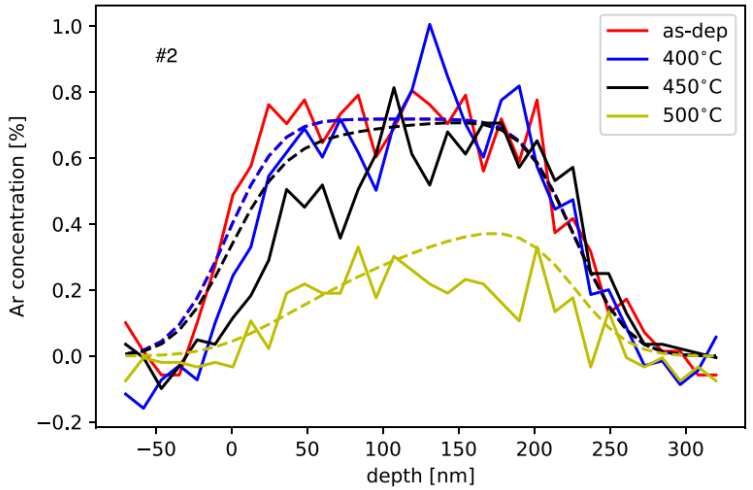

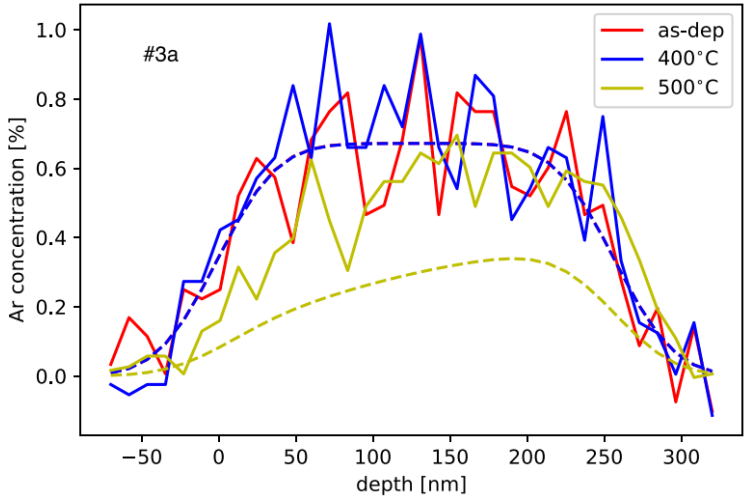

Lalande et al., *Class. Quantum Grav.* **41** (2024) 115013

Argon releasing during annealing

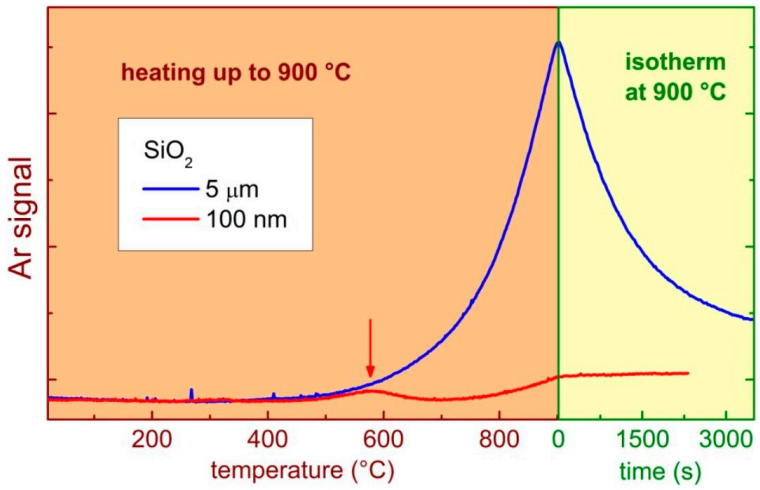

Paolone et al., Coatings 12, 1001, 2022

Multiple reports suggest that **the release of Argon is NOT linear with temperature.**

It is typically maximum around a given temperature, which changes from one material to the other.

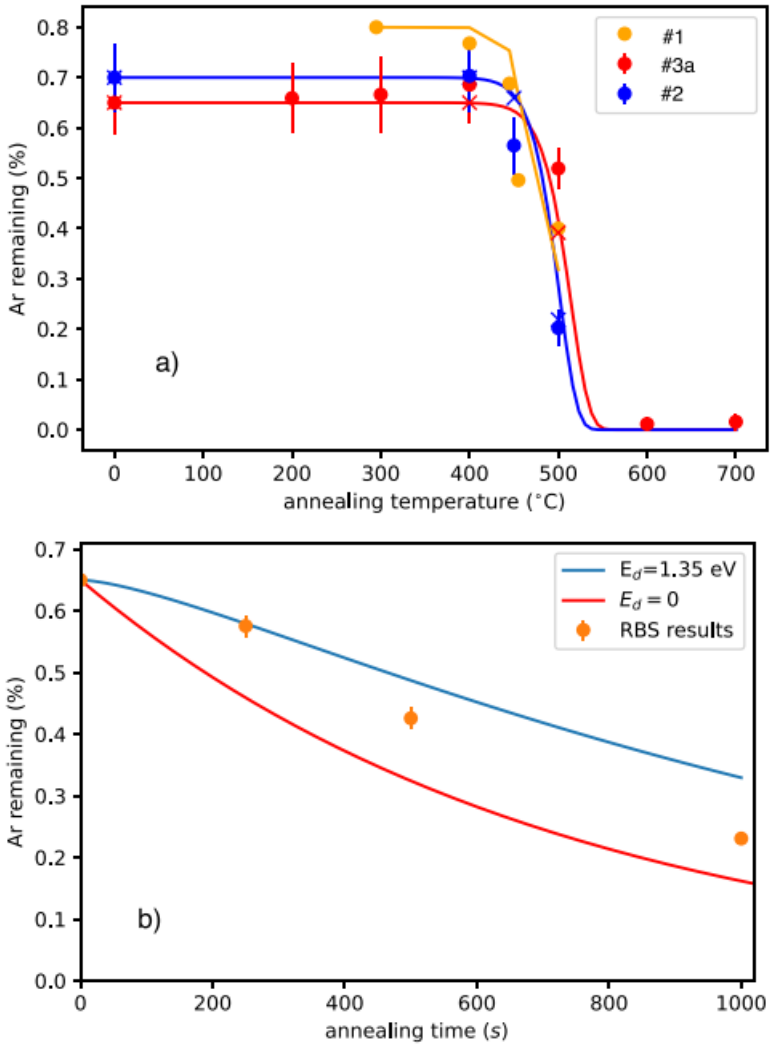

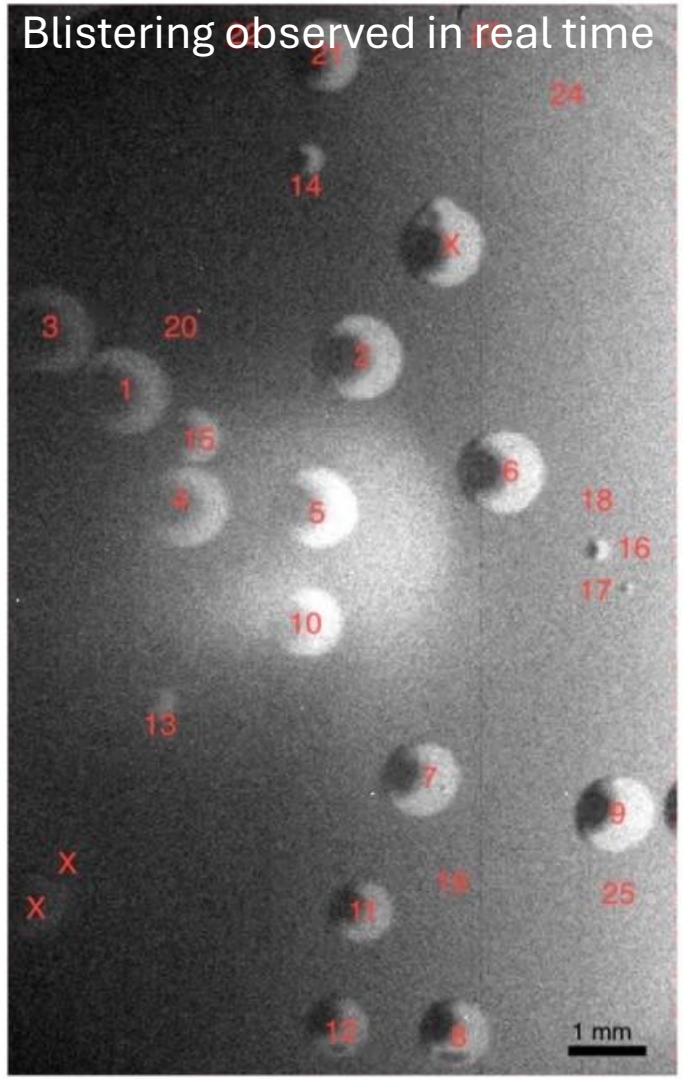

Lalande et al., *Class. Quantum Grav.* **41** (2024) 115013

Determining optical absorption

How do you measure ultralow (ppm-range) optical absorption?
Specialized, dedicated equipment is necessary.

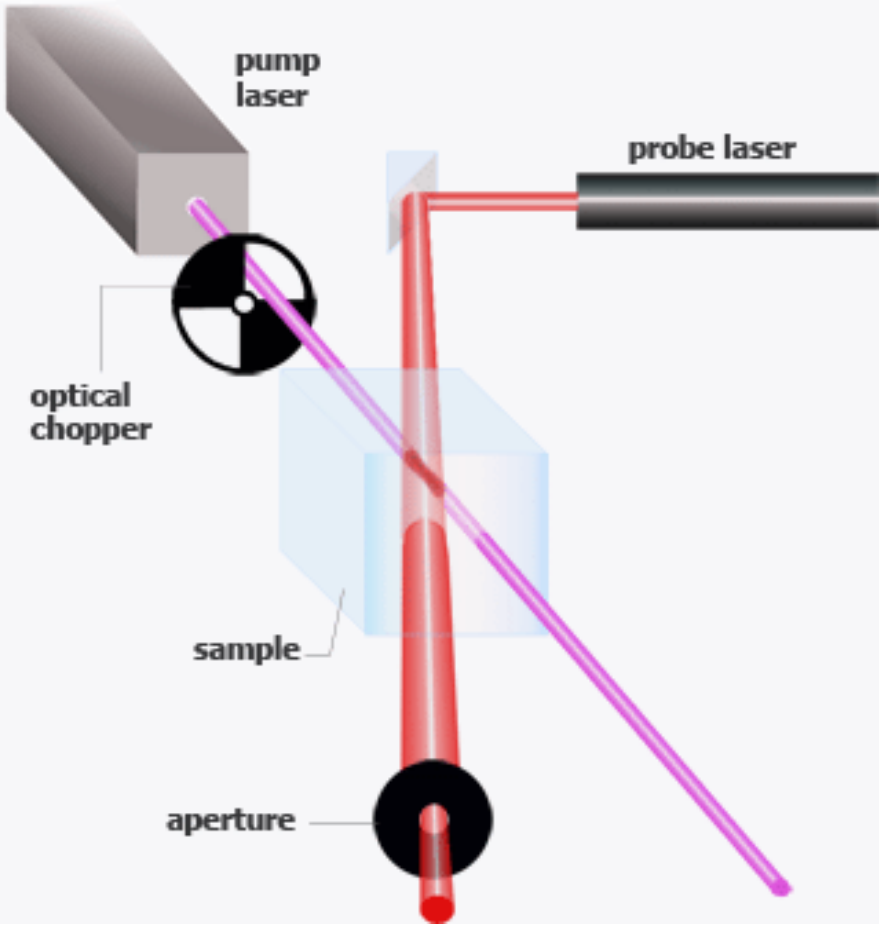

https://www.stan-pts.com/howitworks.html

Temperature Rise in Absorbing Medium

- Absorbed optical power inhomogeneously heats crystal
  - produces radially varying temperature
  - produces optical distortion due to photothermal effects

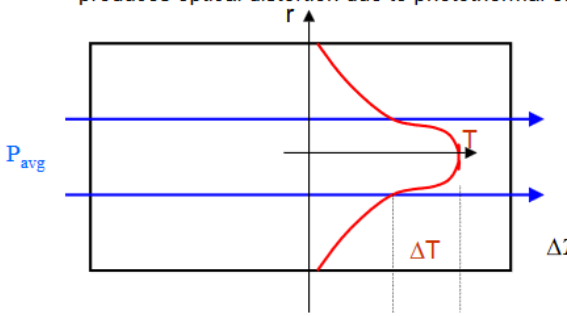

$$\Delta T = \alpha P_{avg} f(k_{th}, c_p, \omega)$$

Leads to radially varying index: $\Delta n = \frac{dn}{dT} \Delta T$

Leads to radially varying phase on optical beam:

$$\Delta\varphi = \frac{2\pi}{\lambda}\frac{dn}{dT}\Delta T\, L$$

$$= \frac{2\pi}{\lambda}\frac{dn}{dT}\alpha P_{avg} L\, f(k_{th}, c_p, \omega)$$

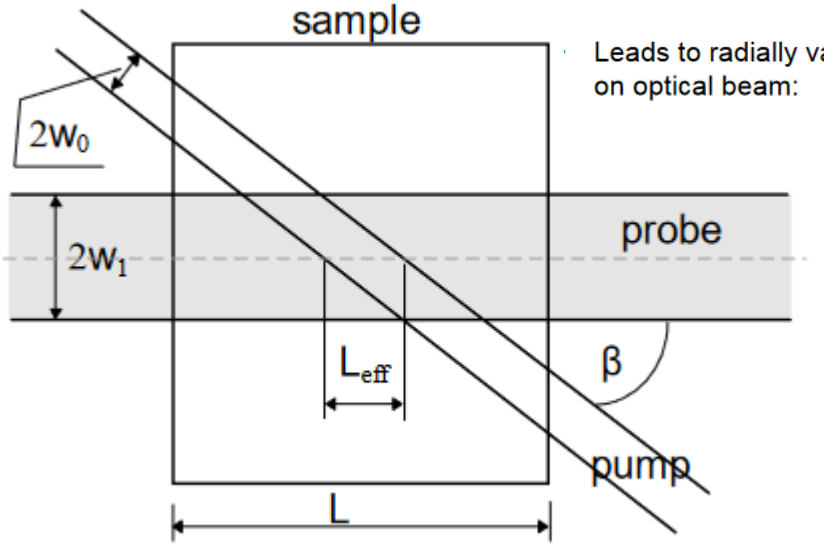

Determining optical absorption

$\alpha \leftrightarrow$ BULK [%/cm] Beer's Law Definition

$A \leftrightarrow$ SURFACE [%] $1 = R + T + A$

$$= \frac{AC}{DC} \cdot \frac{1}{P} \cdot \frac{C}{\mathcal{R}}$$

$\mathcal{R}$ = Responsivity from calib

AC = Demodulated Lock-in Signal

DC = Average Probe Signal at detector

P = Incident power - corrected using transmittance

C = correction factor to account for different $\frac{dn}{dT}$ of different materials, as compared to the reference sample (for fused silica = 1)

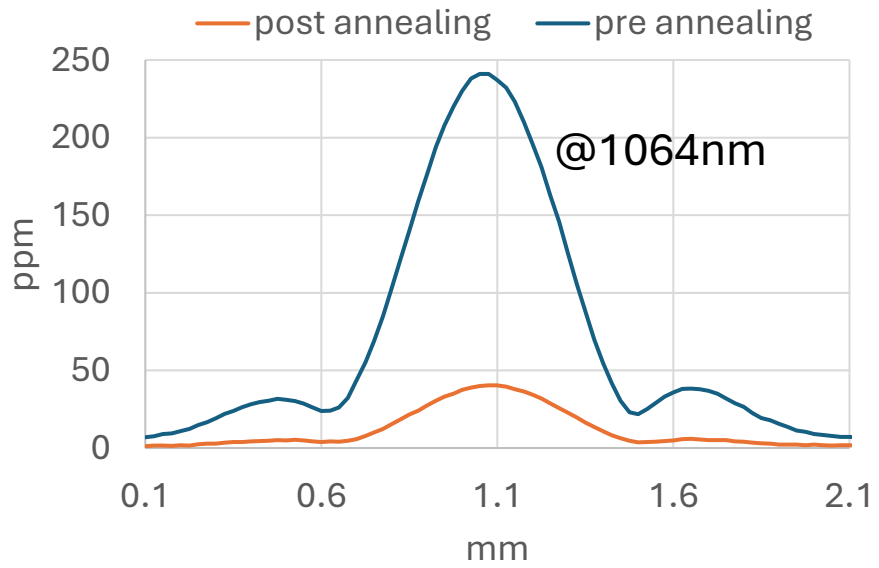

1550 nm

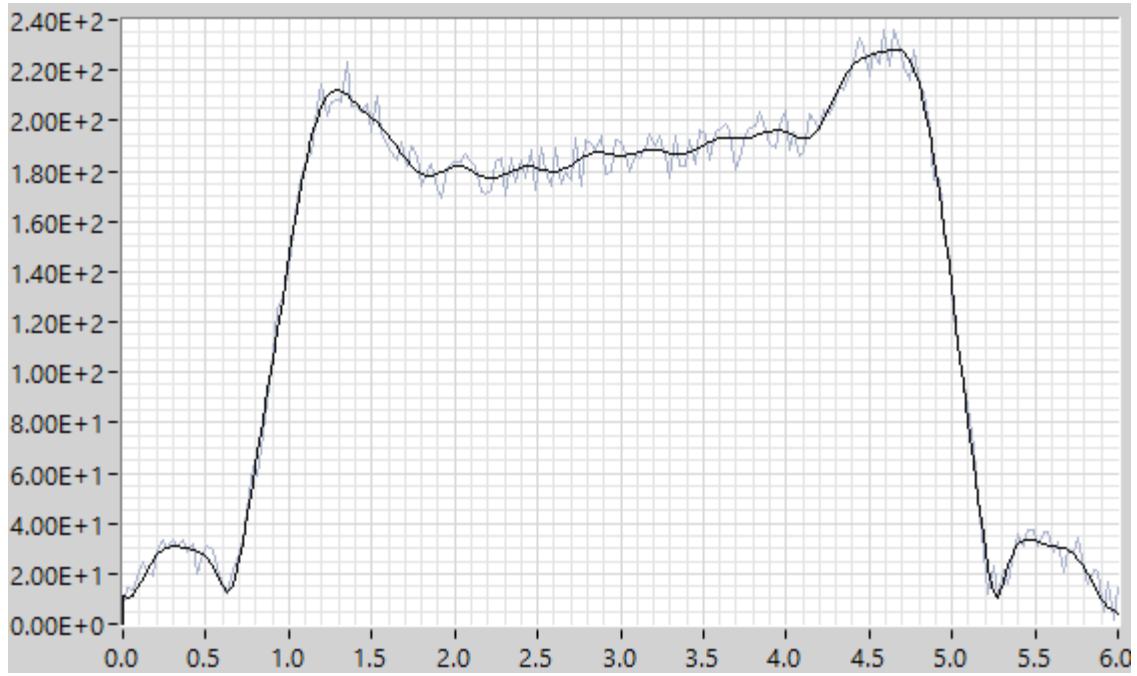

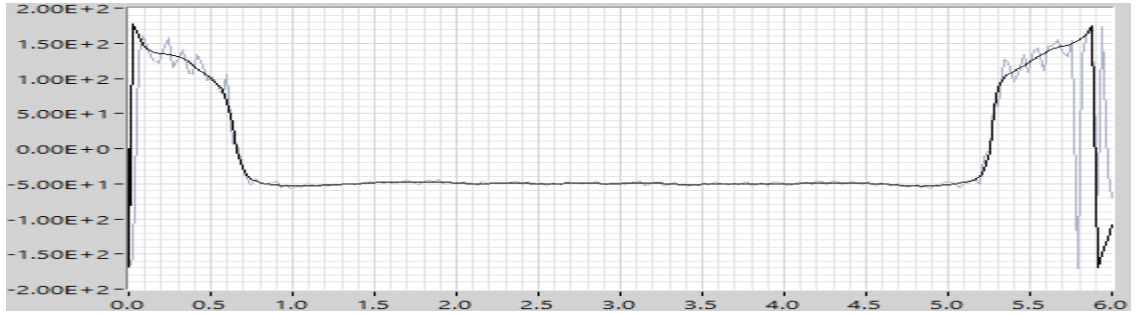

Determining optical absorption

Optical Interference Coatings (OIC) Conference 2025

Muhlig et al., *Appl. Opt.* 65, A147, 2026

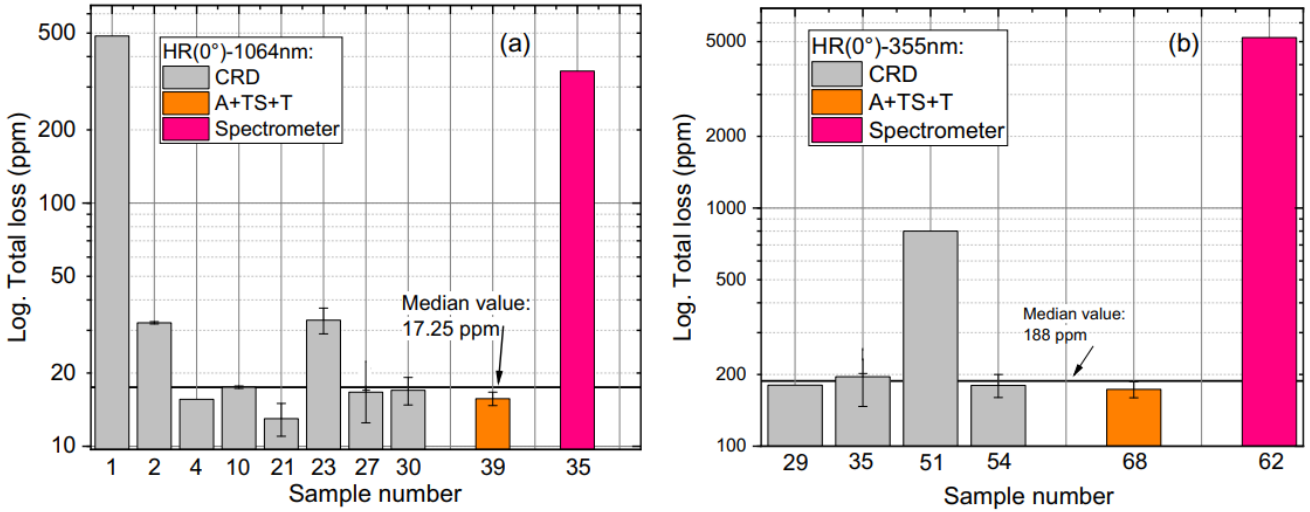

Measurement Challenge: Determining the optical absorption of a 1064-nm mirror
Several world-class laboratories working on optical coatings obtained results that are **mostly compatible, but clearly some dispersion among different reports is present.**

OptMatLab, Università di Genova, unpublished data

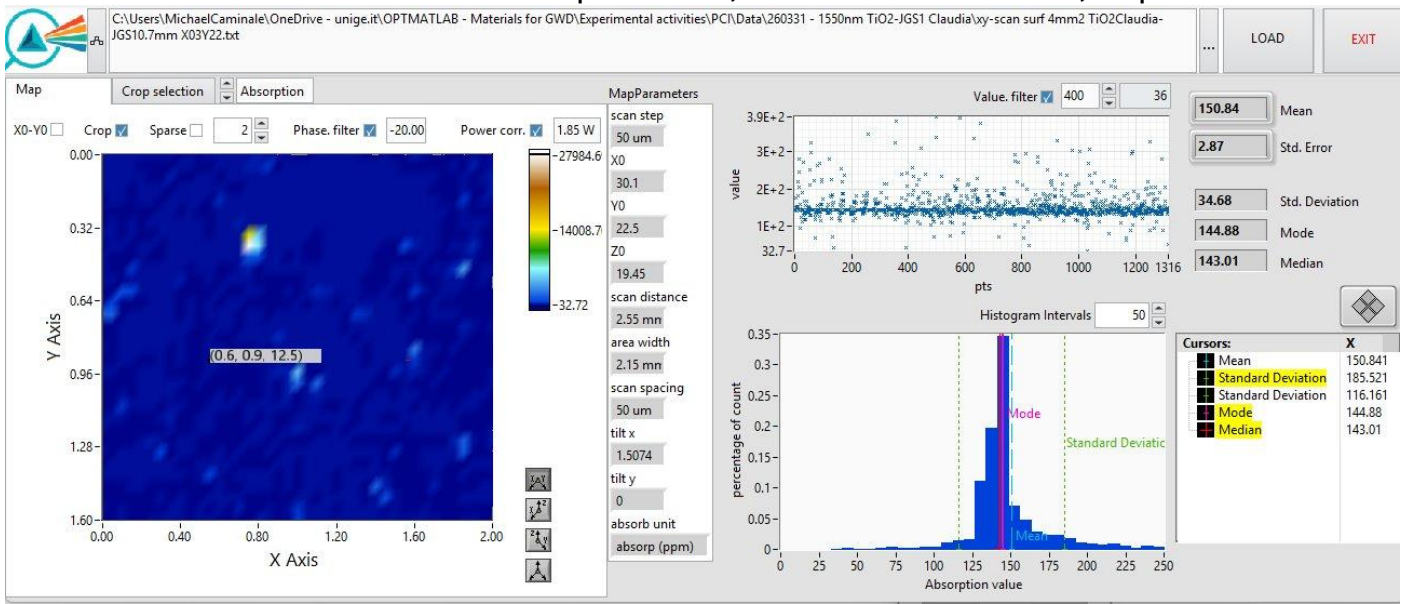

A special caution should be dedicated to **consider the optical absorption as a value with statistical error**, not simply as a number.

Generally speaking, (large) maps instead of single points should be preferred.

Determining mechanical loss

The ‘Gentle’ Nodal Suspension (GENS):

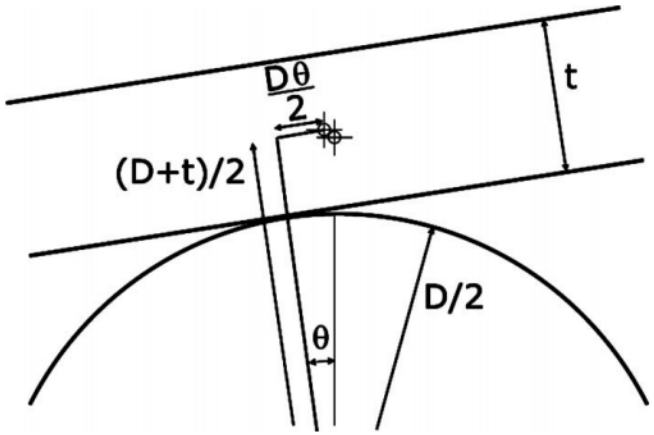

FIG. 1. Geometrical parameters useful to calculate the equilibrium condition. Only when $D>t$, at each small oscillation around the (horizontal) equilibrium position corresponds an increase in the vertical coordinate of the c.m.

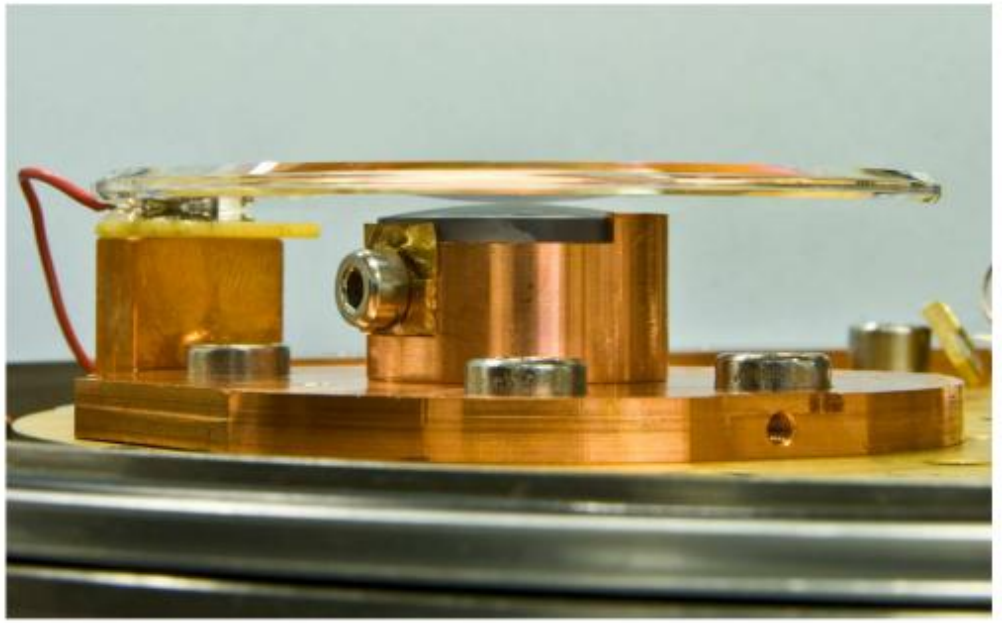

Working mechanism:
the suspended sample is excited, then its vibration amplitude decays exponentially as mechanical energy is lost.

Cesarini et al., *Rev. Sci. Instr*. 80, 053904 2009
Granata et al., *Phys. Rev*. D93, 012007 2016

Determining mechanical loss

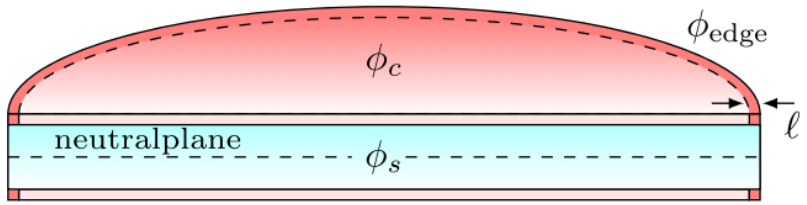

FIG. 3. Cross section of the disk, showing the substrate (blue), the bulk of the coating (light red), and the coating edge (deep red).

In general:

$$\begin{aligned}\phi_{\text{tot}} &= D_s\phi_s + D_c\phi_c \\ &= (1-D)\phi_s + D\phi_c\end{aligned}$$

This is how the loss angle of the coating is derived:

$$\phi_c = \frac{1}{D}[\phi_{\text{tot}} - (1-D)\phi_s]$$

Since *D* is at denominator, even small errors in *D* causes large errors in ϕ_c

The **dilution factor *D*** indicates **how strongly the coating participates in a measured vibration mode**.
When the disk vibrates, elastic energy is stored mostly in the **substrate**, because the substrate is thick.
Only a small amount is stored in the **coating**, because the coating is very thin.

"These results unambiguously support that **coating loss angle measurements are affected by an excess edge contribution** which, although small in value, dramatically affects the fitting procedure and **may lead to the attribution of erroneous values to the bulk and shear loss angles**, which are the key intrinsic material properties targeted by these measurements.

Amato et al., *Phys. Rev. D* 106, 082007 (2022)

Cryo-operated mirrors in ET-LF

Università di Genova

All current materials used in room-temperature-operated GWD are not suitable for low-temperature operations because of high mechanical losses.

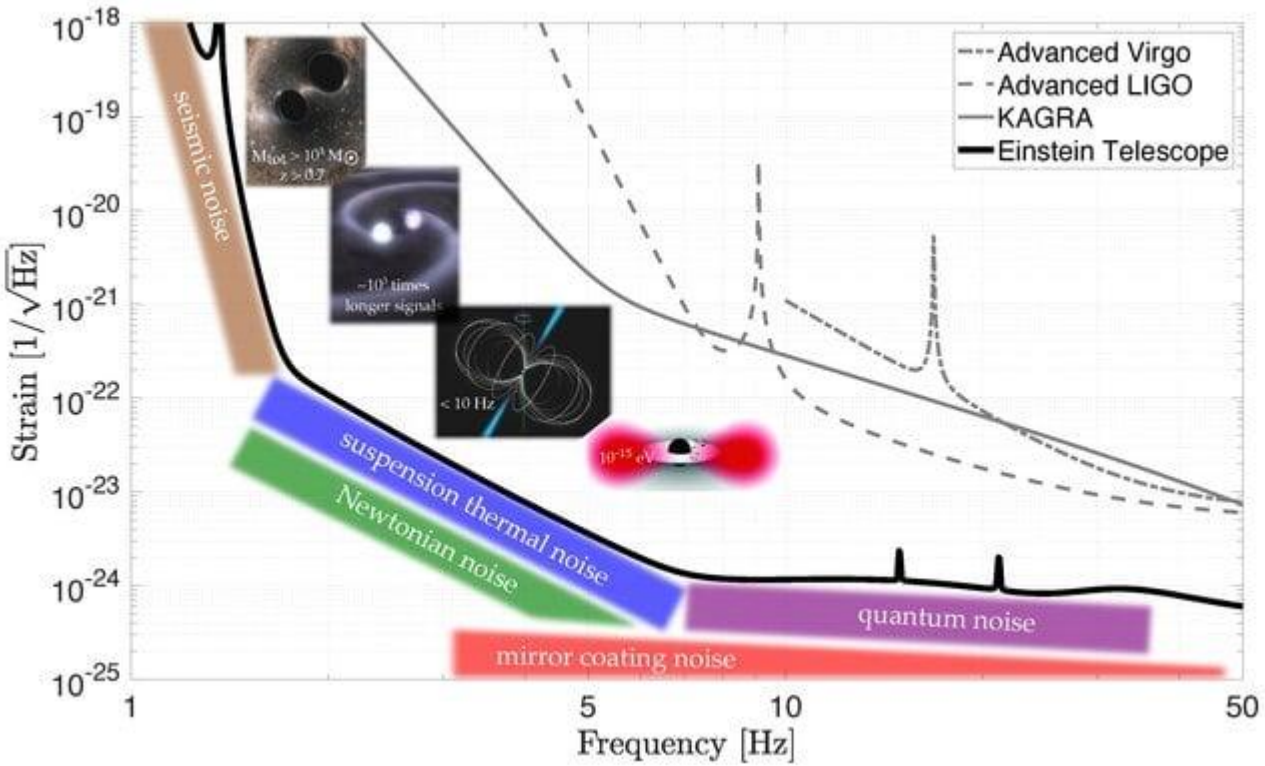

Di Pace et al., *Galaxies* 2022, 10, 65

Parameter	ET-HF	ET-LF
Arm length	10 km	10 km
Input power (after IMC)	500 W	3 W
Arm power	3 MW	18 kW
Temperature	290 K	10-20 K
Mirror material	fused silica	silicon
Mirror diameter / thickness	62 cm / 30 cm	45 cm/ 57 cm
Mirror masses	200 kg	211 kg
Laser wavelength	1064 nm	1550 nm
SR-phase (rad)	tuned (0.0)	detuned (0.6)
SR transmittance	10 %	20 %
Quantum noise suppression	freq. dep. squeez.	freq. dep. squeez.
Filter cavities	1×300 m	2×1.0 km
Squeezing level	10 dB (effective)	10 dB (effective)
Beam shape	TEM_{00}	TEM_{00}
Beam radius	12.0 cm	9 cm
Scatter loss per surface	37 ppm	37 ppm
Seismic isolation	SA, 8 m tall	mod SA, 17 m tall
Seismic (for $f > 1$ Hz)	$5 \cdot 10^{-10}$ m/ f^2	$5 \cdot 10^{-10}$ m/ f^2
Gravity gradient subtraction	none	factor of a few

ET-0007B-20

Sapphire mirror parameters
- TM size: 220 mm dia., 150 mm thick
- TM mass: 22.8 kg
- TM temperature: 22 K
- Beam radius at ITM: 3.5 cm
- Beam radius at ETM: 3.5 cm
- Q of mirror substrate: 1e8
- Coating: tantala/silica
- Coating loss angle: 3e-4 for silica, 5e-4 for tantala
- Number of layers: 22 for ITM, 40 for ETM
- Coating absorption: 0.5 ppm
- Substrate absorption: 50 ppm/cm

K. Komori et al., JGW-T1707038

Cryo-operated mirrors in ET-LF

Università di Genova

To meet the science goals, ET-LF requires **a reduction in coating displacement thermal noise by at least a factor of 10** with respect to current gravitational wave detectors. Some of this improvement can be obtained from operating at low temperature and through the use of larger laser beam spots on the mirrors. The remainder of the improvement will need to come form the coating materials themselves. **The most relevant material properties are the coating mechanical loss and the coating thickness** (which is determined by the combination of refractive indices of the materials used in the coating stack). However, the elastic modulus of the coating (and of the mirror substrate) also contributes to the magnitude of the coating thermal noise.

For operation at 10 K, after accounting for the effect of temperature and the use of larger beams in ET-LF, a reduction in the amplitude of coating thermal noise by a factor of 1.24 must be obtained from improved coating materials. When taking account of the substrate modulus effects, and assuming all coating properties except mechanical loss remain the same as in aLIGO, this translates to **a factor of 3.8 reduction in coating loss compared to the loss of SiO_2/TiO_2:Ta_2O_5 at 10 K.**

A look into the materials R&D

Other oxide coatings

Material	n_{1064}	n_{1550}	n_{2000}*	Y (GPa)	μ	φ (10^{-4} rad)
Ta_2O_5	2.12 ± 0.01	2.11 ± 0.01	2.10 ± 0.01	115 ± 2	0.26 ± 0.04	4.67 ± 0.61
Al_2O_3	1.61 ± 0.01	1.61 ± 0.01	1.60 ± 0.01	113 ± 4	0.42 ± 0.05	5.17 ± 0.38
Nb_2O_5	2.24 ± 0.01	2.23 ± 0.01	2.22 ± 0.01	89 ± 2	0.327 ± 0.002	5.2 ± 0.6
Y_2O_3	1.92 ± 0.01	1.92 ± 0.01	1.91 ± 0.01	151 ± 4	0.34 ± 0.4	3.04 ± 0.29
ZrO_2	2.19 ± 0.01	2.18 ± 0.01	2.17 ± 0.01	230 ± 10	0.41 ± 0.05	3.21 ± 0.54
HfO_2	2.09 ± 0.01	2.09 ± 0.01	2.08 ± 0.01	248 ± 6	0.32 ± 0.04	2.66 ± 0.40
SiO_2	1.46 ± 0.01	1.46 ± 0.01	1.46 ± 0.01	70 ± 2	0.264 ± 0.002	0.110 ± 0.055
GeO_2	1.60 ± 0.01	1.60 ± 0.01	1.59 ± 0.01	48.2 ± 0.6	0.29 ± 0.03	1.00 ± 0.14

Material	n_{1064}	n_{1550}	n_{2000}*	Y (GPa)	μ	φ (10^{-4} rad)
Al_2O_3:Ta_2O_5	2.01 ± 0.01	2.00 ± 0.01	1.99 ± 0.01	132 ± 6	0.37 ± 0.08	3.8 ± 1.0
SiO_2:Ta_2O_5	1.93 ± 0.01	1.92 ± 0.01	1.92 ± 0.01	121 ± 2	0.39 ± 0.02	3.16 ± 0.22
Sc_2O_3:Ta_2O_5	2.09 ± 0.01	2.07 ± 0.01	2.06 ± 0.01	133 ± 2	0.39 ± 0.03	3.17 ± 0.20
TiO_2:Ta_2O_5	2.19 ± 0.01	2.18 ± 0.01	2.16 ± 0.01	128 ± 4	0.35 ± 0.02	2.81 ± 0.10
ZnO:Ta_2O_5	2.05 ± 0.01	2.04 ± 0.01	2.04 ± 0.01	103 ± 2	0.49 ± 0.02	2.57 ± 0.22
Y_2O_3:Ta_2O_5	2.03 ± 0.01	2.02 ± 0.01	2.01 ± 0.01	123 ± 5	0.35 ± 0.07	3.74 ± 0.25
ZrO_2:Ta_2O_5	2.07 ± 0.01	2.06 ± 0.01	2.05 ± 0.01	143 ± 5	0.36 ± 0.05	3.12 ± 0.37
Nb_2O_5:Ta_2O_5	2.11 ± 0.01	2.09 ± 0.01	2.09 ± 0.01	118 ± 4	0.3 ± 0.1	4.14 ± 0.29
HfO_2:Ta_2O_5	2.05 ± 0.01	2.04 ± 0.01	2.04 ± 0.01	146 ± 5	0.32 ± 0.06	3.21 ± 0.18

"We concluded that the current high index material of **TiO_2-doped Ta2O5 is the optimal choice for reduced thermal noise** among Ta_2O_5-based mixed oxide coatings with low dopant concentrations"

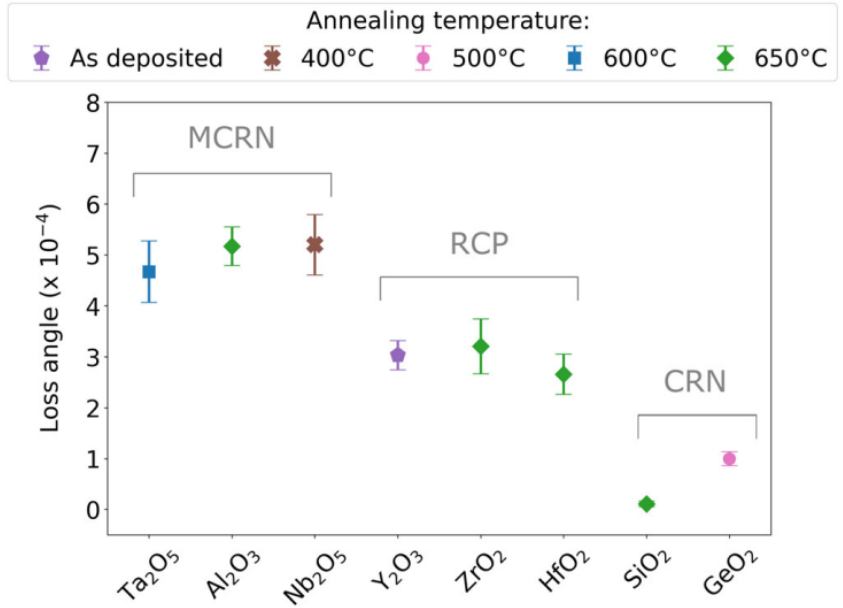

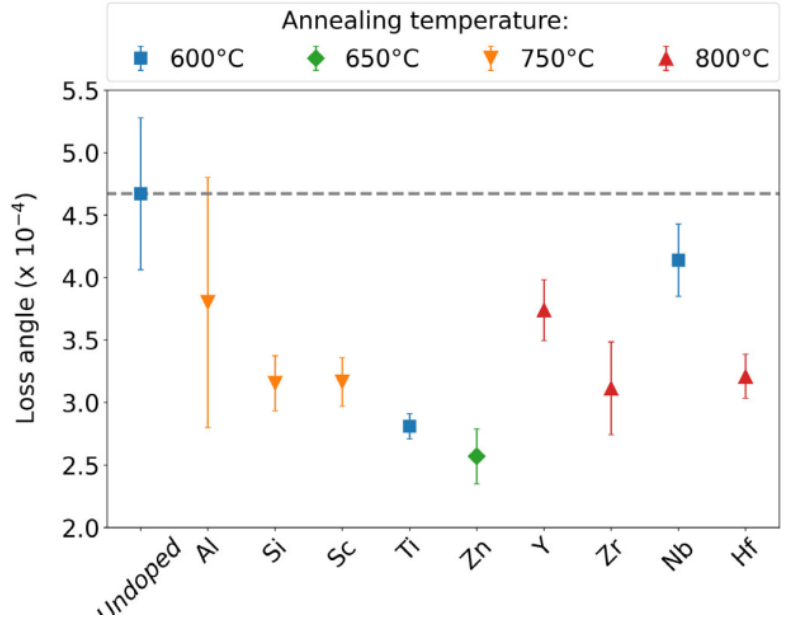

Fazio et al., *Phys. Rev. D* 105, 102008 (2022)

Germanium-oxide-based coatings

Università di Genova

If SiO_2 works so well at RT, **can we produce a high-index material that is as similar as possible to SiO_2?** GeO_2 has the same atomic structure of SiO_2, and like SiO_2, it is a strong glass former. But its refractive index is too low to build doublets. Then: **doping GeO_2 with TiO_2.**

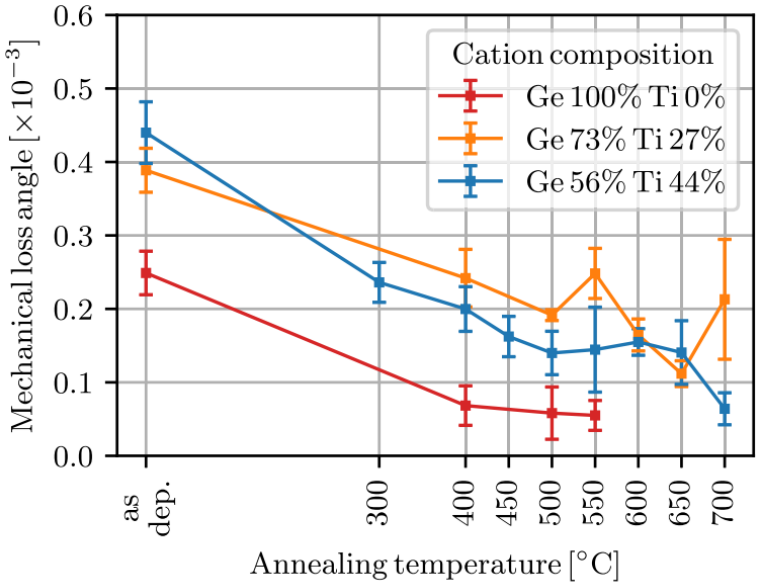

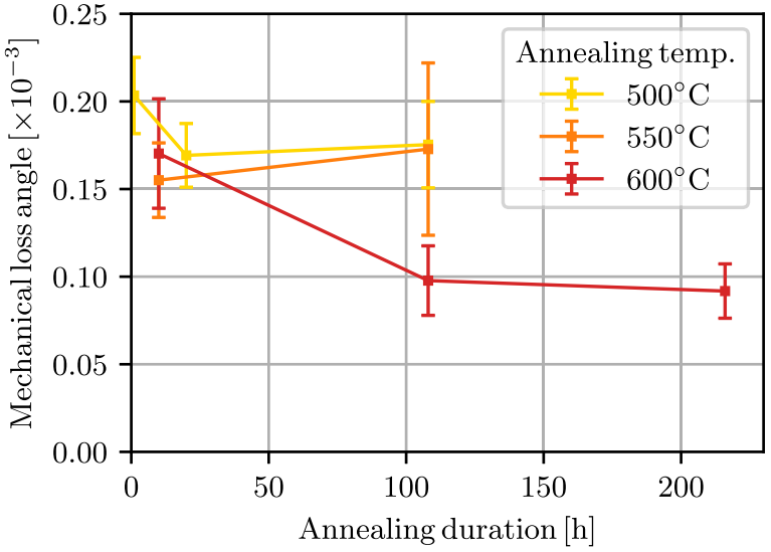

Vajente et al., *Phys. Rev. Lett.* 127, 071101, 2021

SiO_2 property	Value
Refractive index at 1064 nm	1.45 ± 0.01
Young's modulus	73.2 ± 0.6 GPa
Poisson ratio	0.11 ± 0.07
Loss angle	$\phi_K = \phi_\mu = (2.6^{+0.5}_{-0.6}) \times 10^{-5}$

TiO_2:GeO_2 property	Value
Cation concentration $Ti/(Ti + Ge)$	$44.6 \pm 0.3\%$
Refractive index at 1064 nm	1.88 ± 0.01
Optical absorption for a QWL	2.3 ± 0.1 ppm
Density	3690 ± 100 kg/m^3
Young's modulus	91.5 ± 1.8 GPa
Poisson ratio	0.25 ± 0.07
Bulk loss angle	$a_K = (22.0^{+10.6}_{-12.5}) \times 10^{-5}$ $m_K = 1.04^{+0.40}_{-0.36}$
Shear loss angle	$a_\mu = (8.4^{+2.9}_{-4.0}) \times 10^{-5}$ $m_\mu = -0.06^{+0.15}_{-0.30}$

Mixing GeO_2 and TiO_2 results in a 'hybrid' material with peculiar structural and temperature-dependent properties

GeO_2

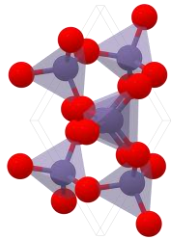

Tetrahedra

TiO_2

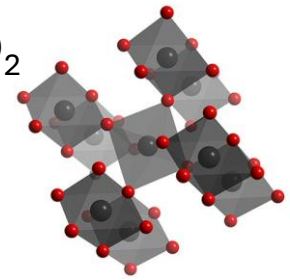

Octahedra

different atomic structures!

Silicon nitride

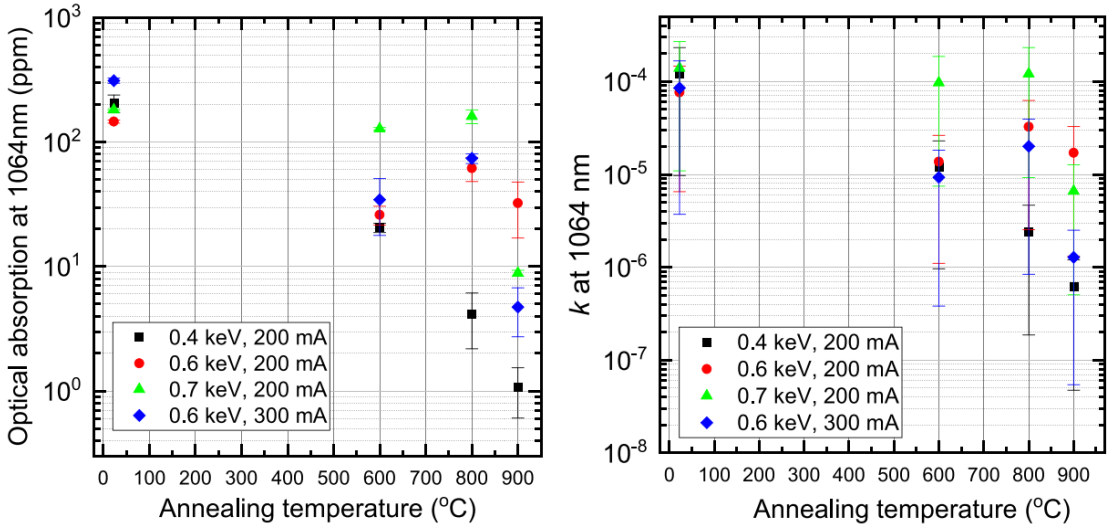

Structure of amorphous Si_3N_4

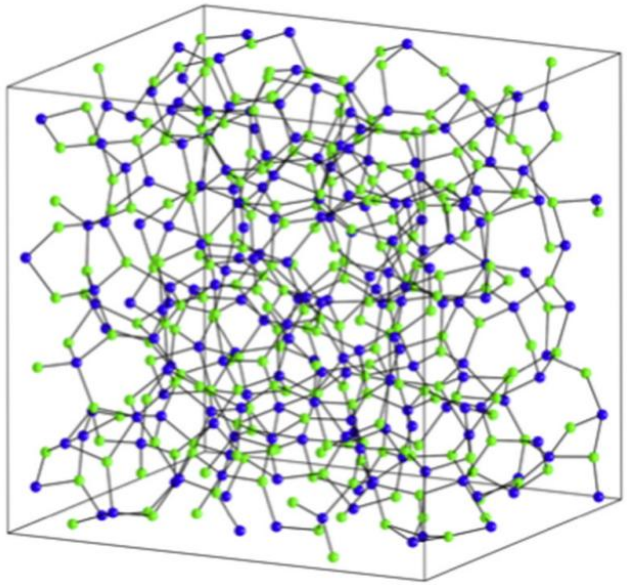

Non-stoichiometry is declared from the beginning.

Lowest optical absorption so far:
$k = 6.2(\pm 0.5) \times 10^{-7}$ at 1064 nm
for samples annealed at 900 °C

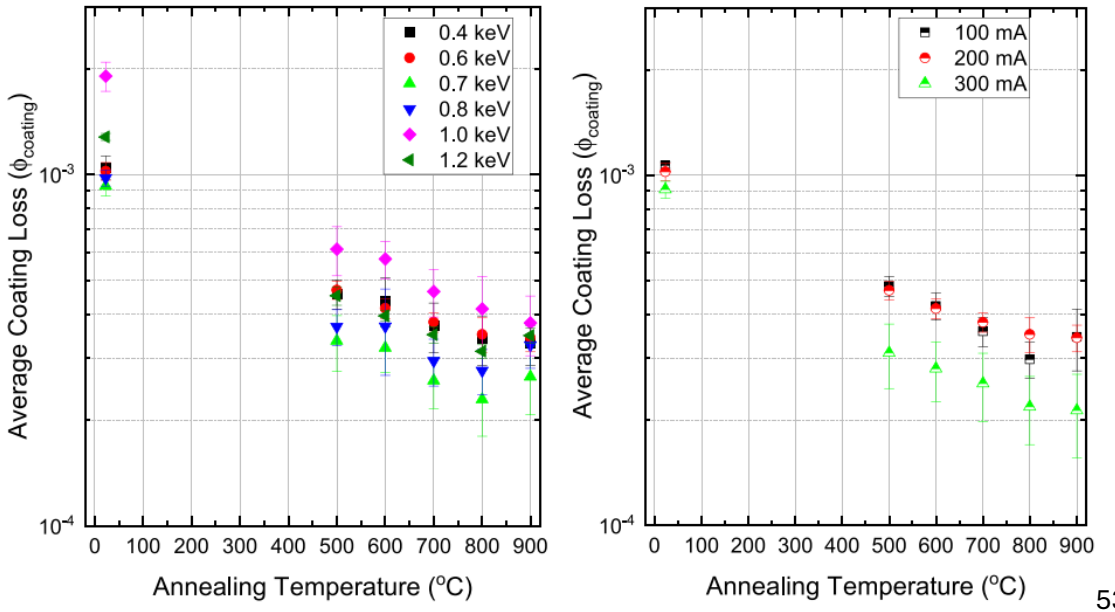

Wallace et al., *Class. Quantum Grav.* 41 095005 2024

Silicon nitride

TABLE VII. Loss angle φ of IBS SiN_x thin films, as measured at ~2.8 kHz, as a function of ion beam voltage V and current I, Ar and N_2 gas mass flows, and annealing. Values of tantala-titania layers in current mirror coatings of Advanced LIGO and Advanced Virgo are presented, for comparison [10].

Sample	V (V)	I (mA)	Ar (sccm)	N_2 (sccm)	Annealing		φ (10^{-4} rad)
c21013	700	100	5	10			7.0 ± 0.3
c21013	700	100	5	10	900 °C	10 h	1.0 ± 0.1
c21015	1000	75	0	10			7.6 ± 0.3
c21015	1000	75	0	10	900 °C	10 h	1.2 ± 0.1
d2008	700	195	5	10			8.0 ± 0.4
d2008	700	195	5	10	900 °C	10 h	2.2 ± 0.2
d2008	700	195	5	10	900 °C	100 h	1.5 ± 0.2
LP-CVD					900 °C	10 h	1.8 ± 0.1
Ta_2O_5-TiO_2					500 °C	10 h	3.3 ± 0.1

Improved stoichiometry

Lowest loss angle so far:
$(1.0 \pm 0.1) \times 10^{-4}$ rad @ 2.8 kHz
for samples annealed at 900 °C

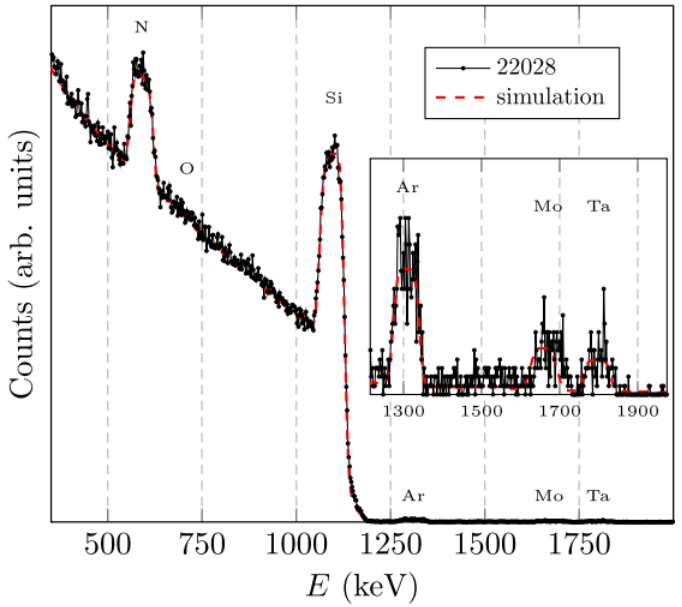

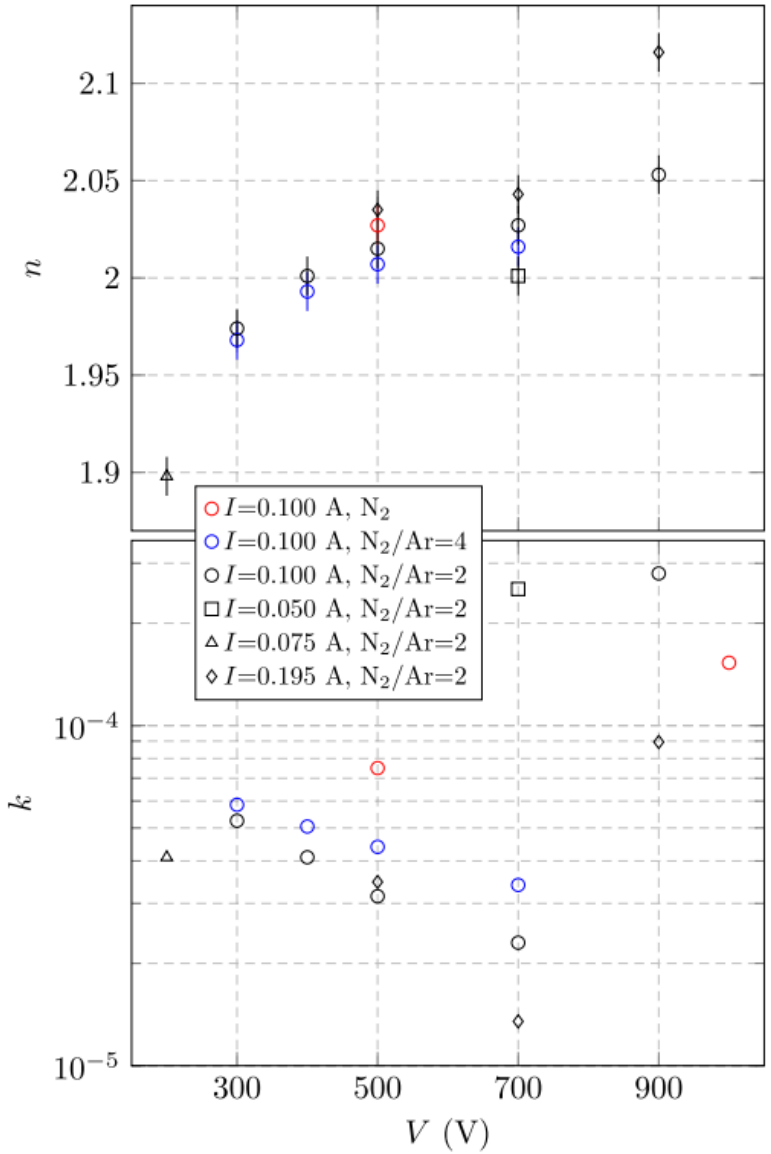

Amato et al., *Phys. Rev. D* 111, 042003 (2025)

Silicon nitride

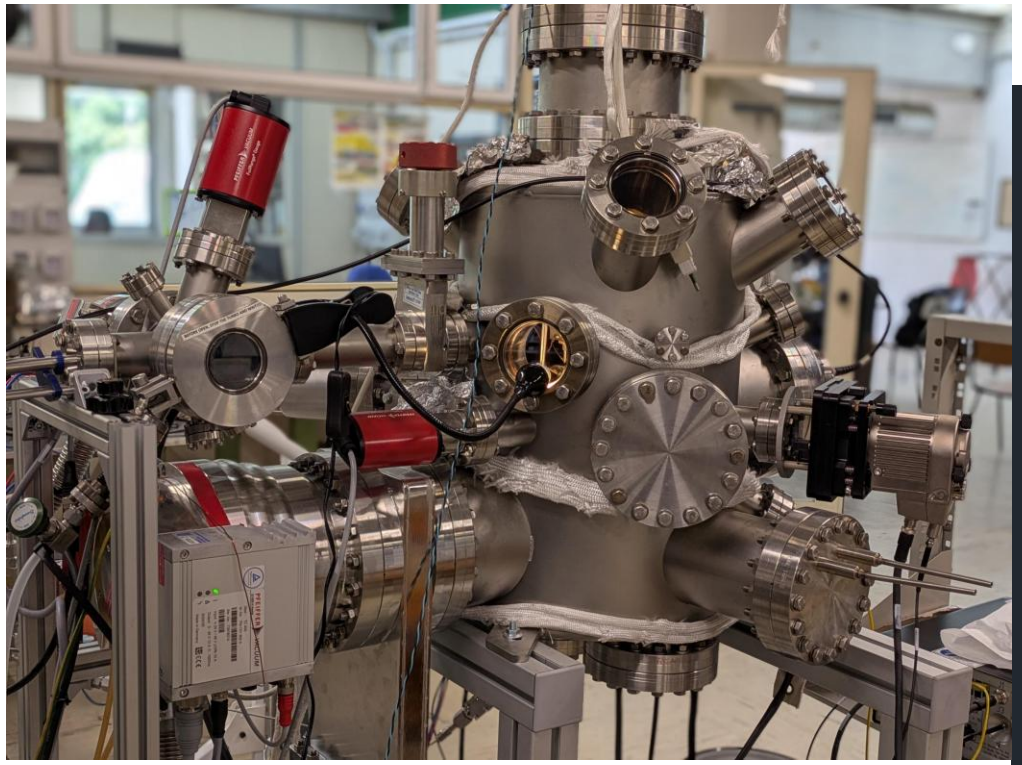

Einstein Telescope Infrastructure Consortium

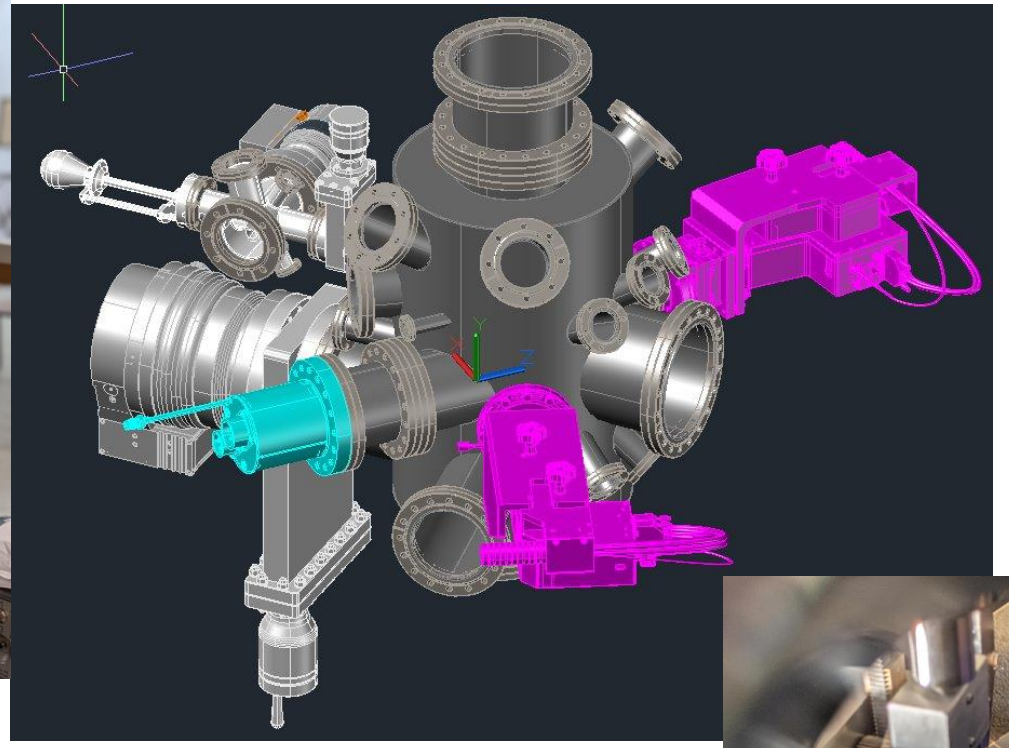

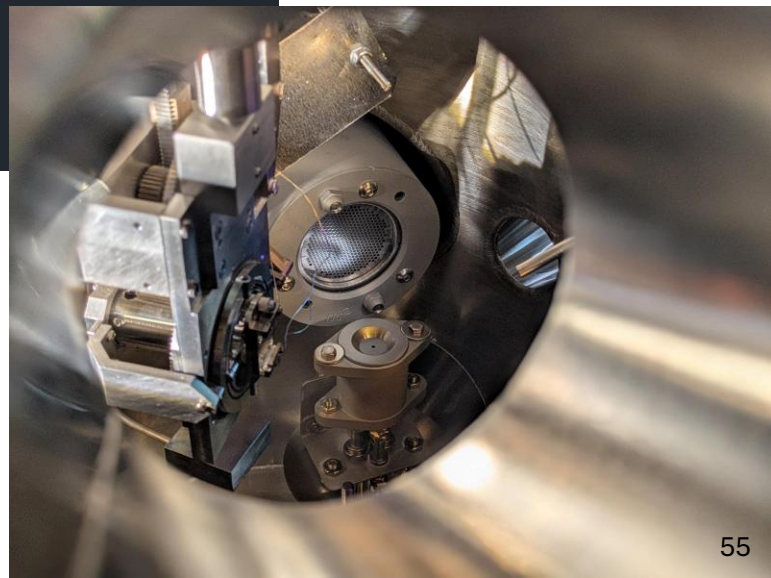

Key points for optimized deposition:

- Ultrapure deposition environment
- In-situ diagnostics

Ternary coatings

Pan et al., *Phys. Rev. D* 98, 102001 (2018)

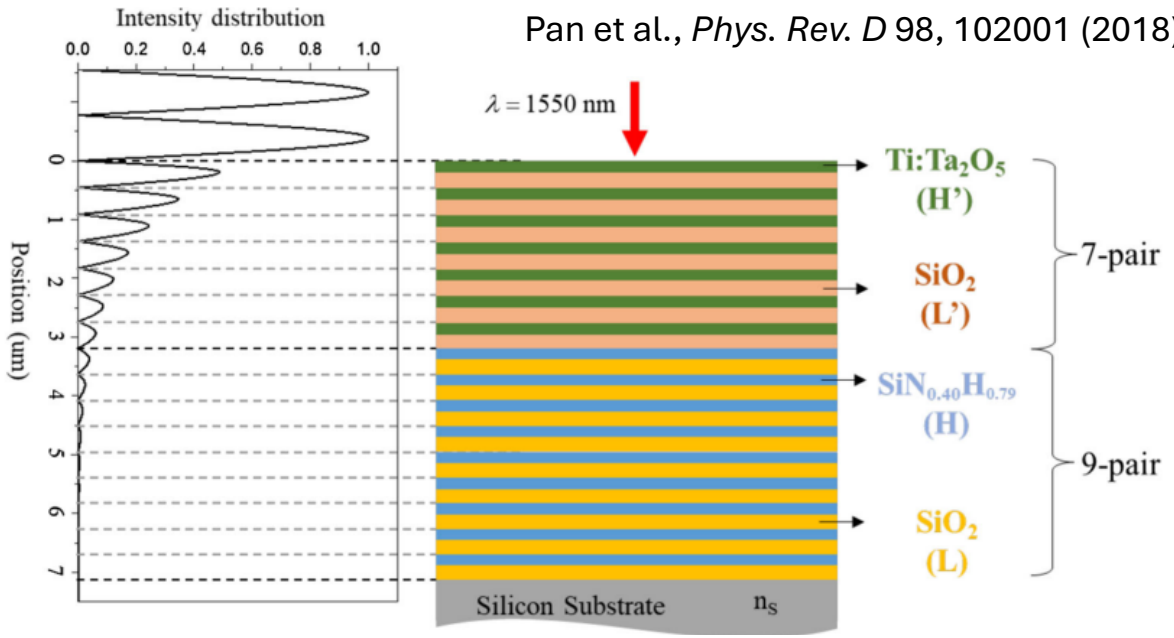

Multimaterial structure. Each layer has QW optical thickness at the wavelength 1550 nm and the total thickness d_c is 7.129 um.

Amato et al., *Phys. Rev. D* 111, 042003 (2025)

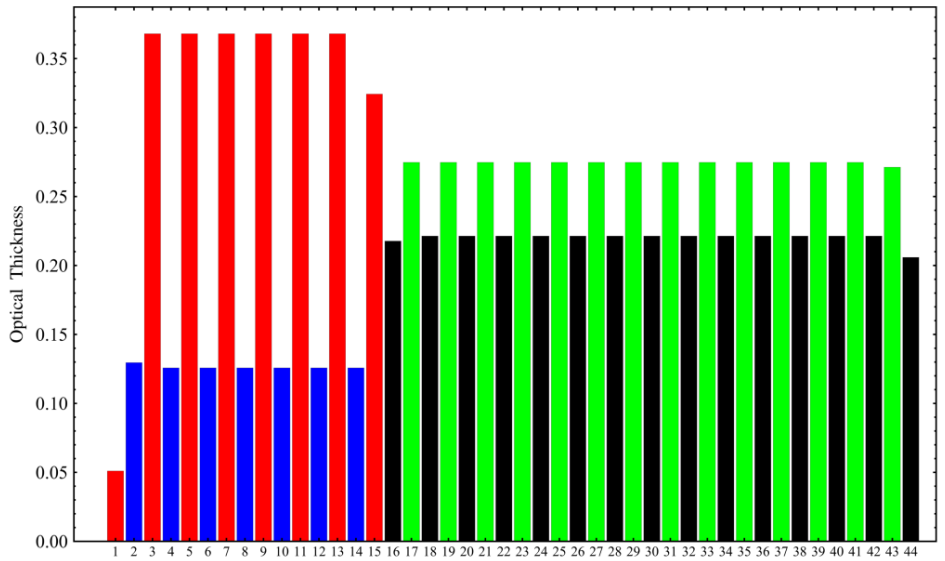

FIG. 14. Layout of a thickness-optimized ternary Bragg reflector for operation at $\lambda_0 = 1064$ nm, composed of IBS SiN_x (black), tantala-titania (blue) and silica (green and red) thin layers. The optical thickness of each layer, normalized to λ_0, is shown as a function of the layer number (the substrate is set to be on the right, by convention).

Generally speaking, the design idea of ternary coatings is based on the fact that **the incident electric field is maximum at the top of the coating**, and then it progressively decreases towards the substrate: therefore, not every doublet has the same 'weight' in terms of optical absorption and losses.

Ternary coatings

Università di Genova

TABLE IX. Comparison of the transmittance, absorption, and CTN between silicon nitride and silica QW HR, multimaterial QW HR, and the specifications of ET-LF and LIGO Voyager.

ETM properties	ET-LF			Voyager		
	Spec. [3]	$Si\|(LH)^{14}$	$Si\|(LH)^9(L'H')^7$	Spec. [4]	$Si\|(LH)^{14}$	$Si\|(LH)^9(L'H')^7$
T (ppm)	6	3.5	2.5	5	3.5	2.5
A (ppm)	<5	45.9	2.0	≤2	45.9	2.0
CTN[a]	0.45[b]	0.83	1.09	1.20[b]	2.20	2.81

[a]frequency at 100 Hz with the unit in 10^{-21} m/$\sqrt{\text{Hz}}$.
[b]lower limit of CTN of the ETM.

Pan et al., *Phys. Rev. D* 98, 102001 (2018)

TABLE IX. Measured properties of ternary mirror coating samples: coating noise CTN, optical absorption a_{CTN} as measured in the CTN setup, optical absorption a_{PTD} as measured via photothermal deflection. Sample 10039 was measured as deposited, sample 10036 was measured after annealing. Updated values of current ETM mirror coatings of Advanced LIGO and Advanced Virgo are presented, for comparison.

Sample	CTN (10^{-18} m $Hz^{-1/2}$)	a_{CTN} (ppm)	a_{PTD} (ppm)
10039	$(16.2 \pm 0.3) \times (\frac{100\ \text{Hz}}{f})^{0.48\pm0.02}$	9.1 ± 0.3	7.6 ± 0.4
10036	$(10.3 \pm 0.2) \times (\frac{100\ \text{Hz}}{f})^{0.50\pm0.03}$	1.3 ± 0.5	1.9 ± 0.2
ETM	$(13.7 \pm 0.3) \times (\frac{100\ \text{Hz}}{f})^{0.45\pm0.02}$	0.5 ± 0.2	0.27 ± 0.07

Amato et al., *Phys. Rev. D* 111, 042003 (2025)

Quaternary coatings

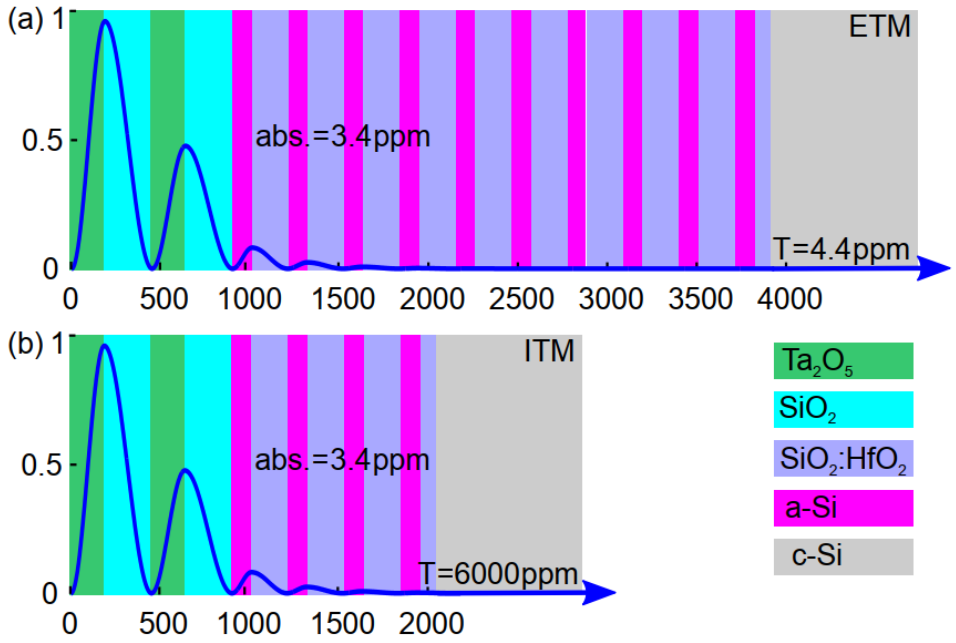

Craig et al., *Phys. Rev. Lett.* 122, 231102 (2019)

Material	$\phi(\times10^{-4})$ 10 K	n	k ($\times10^{-5}$)	Y (GPa)
SiO_2	8.5 (5) [45]	1.44 [46]	0.008[a]	72 [47]
HfO_2				220 [48]
$SiO_2:HfO_2$	3.8 ± 0.3	1.91 [49]	0.40 ± 0.09	180 [49]
Ta_2O_5	5 (7) [19]	2.05 [50]	0.008[a]	140 [47]
a-Si	≤ 0.17[b] [30]	3.48 [51]	1.22 ± 0.21 [30]	147 [48]

TABLE II. CTN of different coatings on c-Si substrates at a reference frequency of 10 Hz, a temperature of 10 K and a beam radius of 9 cm. The material parameters used are shown in Table I.

Case	Bilayers ETM (ITM)	Transmission ETM (ITM) (ppm)	Heat treatment (°C)	CTN ETM (ITM) ($\times10^{-21}$ m/$\sqrt{\text{Hz}}$)	CTN_D	α_{HR} (ppm)
(a)	18 (7) × SiO_2/Ta_2O_5	4 (8500)	600	4.0 (2.4)	6.6	0.6
(b)	10 (4) × $SiO_2:HfO_2/a$-Si	2 (9000)	400	1.4 (0.9)	2.4	11.9
(c)	2 × SiO_2/Ta_2O_5 + 10 (4) × $SiO_2:HfO_2/a$-Si	4.4 (6000)	400	1.9 (1.6)	3.5	3.4
ET-LF requirement [13]		5 (7000)			≈3.6	≤ 5

‘A coating meeting the thermal noise and optical requirements of ET-LF has not been tested to date’

“This coating design relies on a level of absorption in aSi films which has been observed, but has not yet been demonstrated reproducibly or on the scale required for ET.”

ET-0007B-20

Multi-nanolayers

Key idea: the high-index material is replaced by a **metamaterial based on multinanolayers**

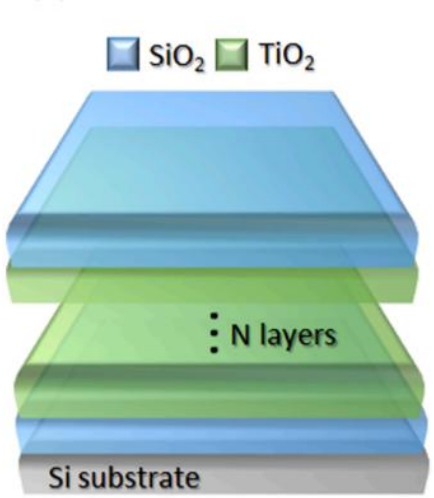

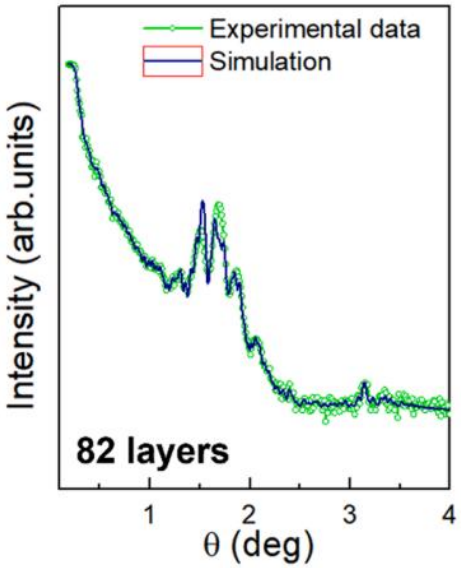

Layer number	Material	Thickness	Total Thickness (nm)	Equivalent Refractive index	Optical thickess (nm)
68	**Ta_2O_5**	1.39 ± 0.17(x34)	115 ± 13	2.32 ± 0.03	266 ± 30
78	**Al_2O_3**	1.08 ± 0.18(x39)	119 ± 15	2.25 ± 0.06	268 ± 30
62	**ZrO_2**	1.66 ± 0.35(x31)	113 ± 19	2.32 ± 0.03	262 ± 40
82	**SiO_2**	0.9 ± 0.2 (x41)	119 ± 20	2.09 ± 0.07	249 ± 40

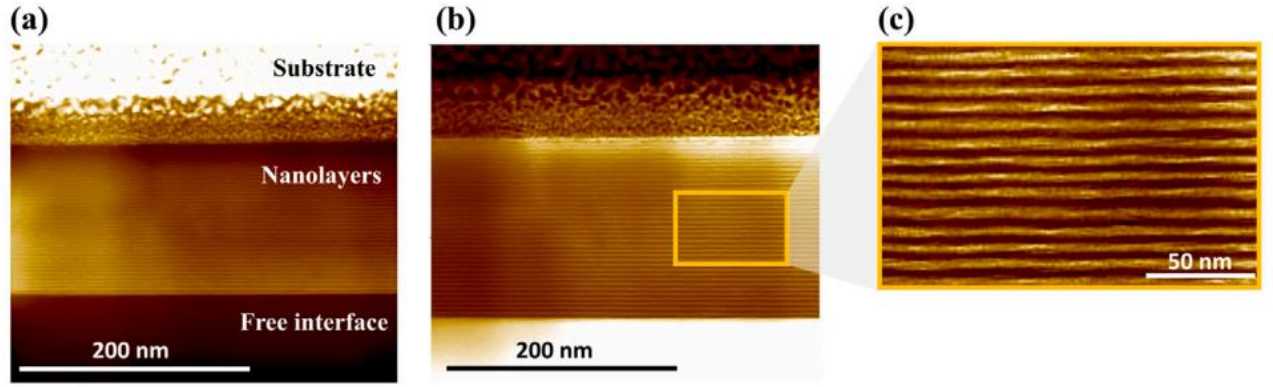

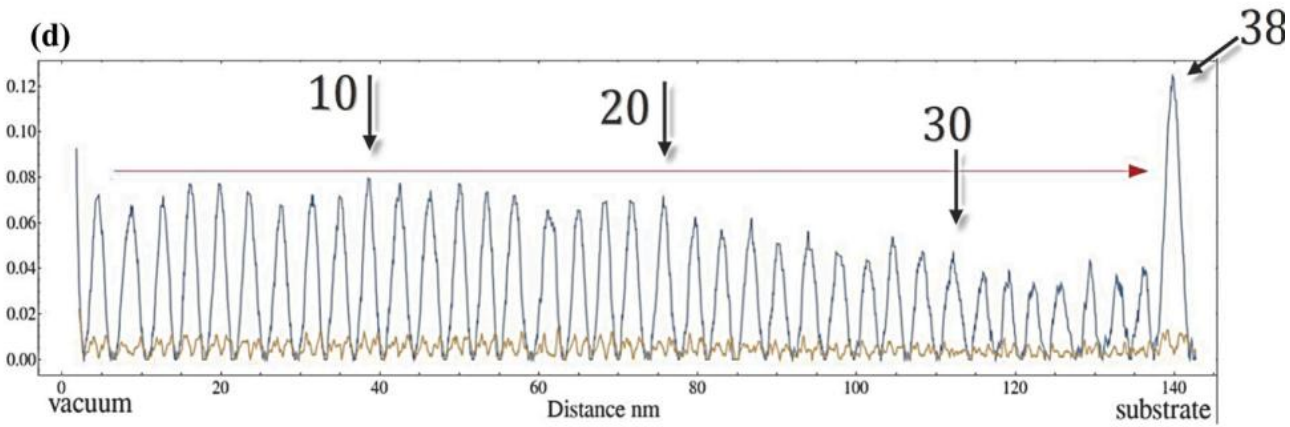

Durante et al., *Surfaces and Interfaces* 41 (2023) 103309

Durante et al., *Optical Materials* 157 (2024) 116038

It’s all about the atomic structure

Università di Genova

Amorphous structure

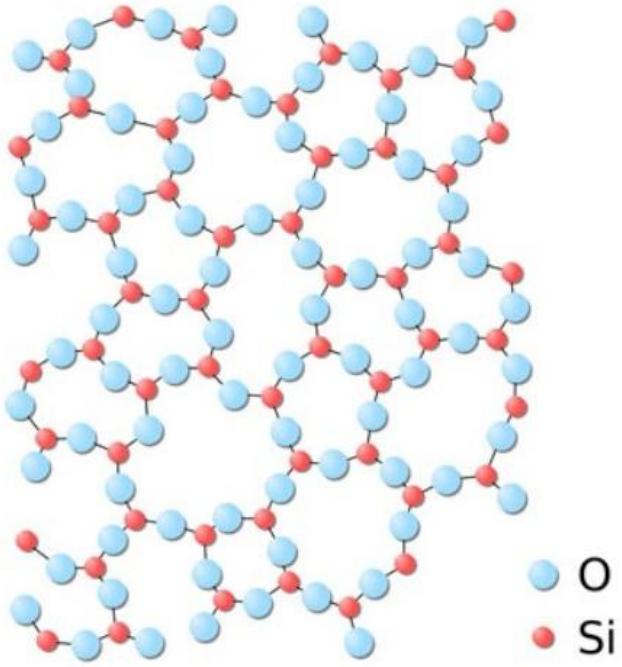

Current GWD mirror coatings have amorphous structure

Crystalline structure

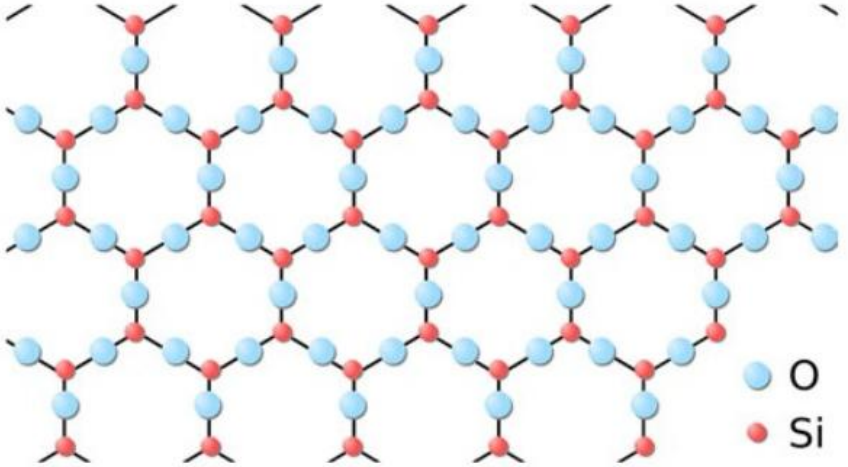

Crystalline coatings

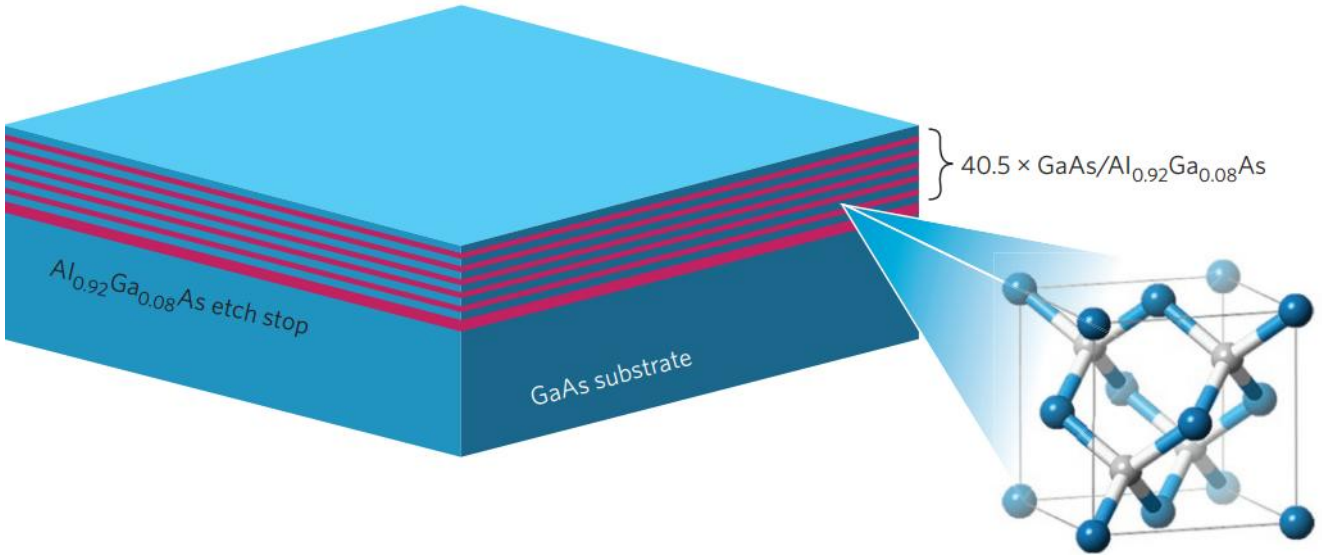

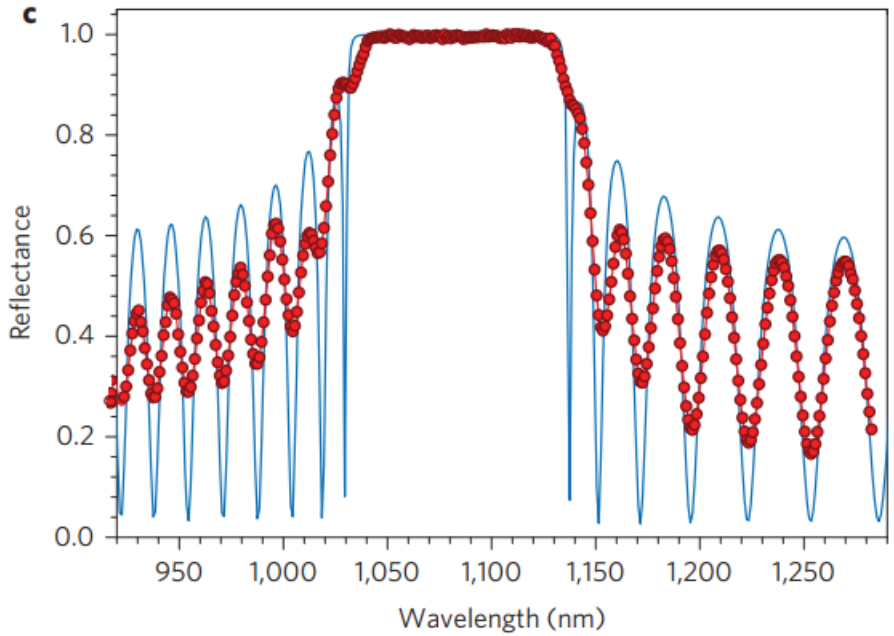

A change in paradigm: crystalline instead of amorphous coatings.

Crystalline coating can exhibit a **tenfold reduction** in the thermal noise with respect to amorphous coatings.

Makes it possible to go below 1 ppm optical absorption.

G. Cole et al., *Nat. Photon.* 7, 644, 2015

Crystalline coatings

Università di Genova

G. Cole et al., *Nat. Photon*. 7, 644, 2015

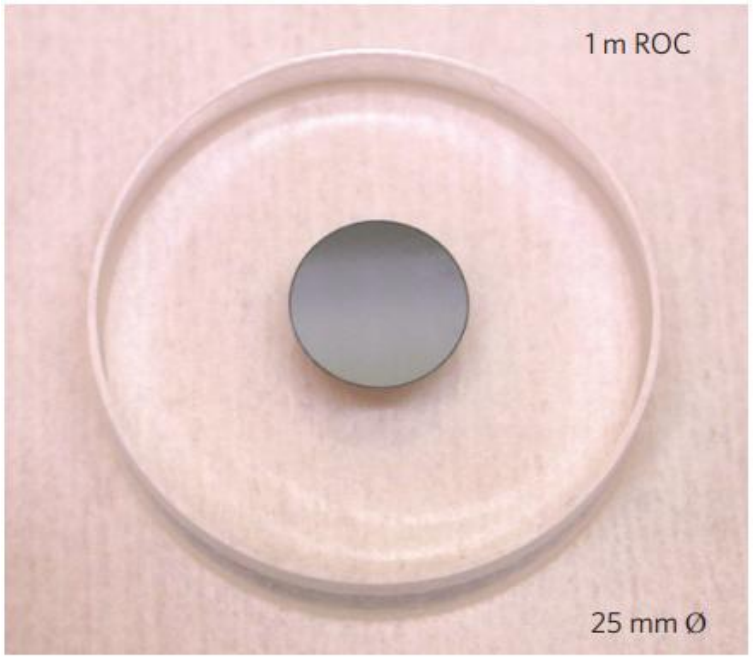

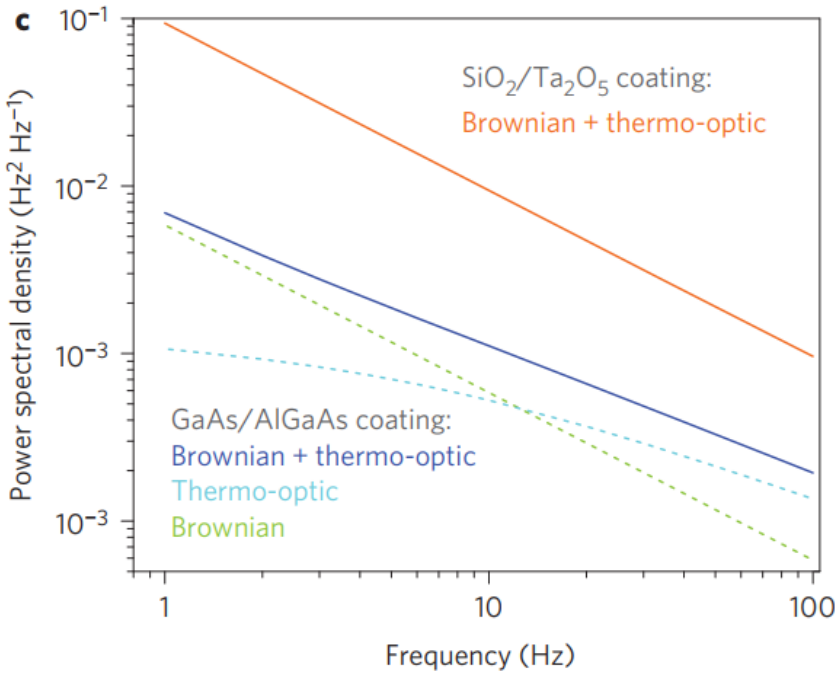

A change in paradigm: crystalline instead of amorphous coatings.

Crystalline coating can exhibit a **tenfold reduction** in the thermal noise with respect to amorphous coatings.

Bonding the coating to the substrate requires **highly specialized, very expensive equipment.**

https://www.thorlabs.com/supermirrors?tabName=Overview

A look at the reviews

Università di Genova

- S. Reid, I. Martin. Development of Mirror Coatings for Gravitational Wave Detectors.
  Coatings, 6, 61, 2016

- M. R. Abernathy *et al.*, An Overview of Research into Low Internal Friction Optical Coatings by the Gravitational Wave Detection Community.
  Materials Research, 2018; 21(suppl.2): e20170863

- J. Steinlechner, Development of mirror coatings for gravitational-wave detectors.
  Philosophical Transactions A 376, 20170282, 2018

- M. Granata *et al.*, Amorphous optical coatings of present gravitational-wave interferometers.
  Classical Quantum Gravity 37, 095004, 2020

- A. Amato, M. Magnozzi, J. Wöhler, Mirror Coating Research and Development for Current and Future Gravitational-Wave Detectors.
  Advanced Photonics Research 6, 2400117, 2025

Summary

Università di Genova

1.

- Mirror coatings of GWD are **multilayer structures, where each layer is transparent**. High reflectivity is given by multiple interference among the layers.
- GWD mirrors must satisfy simultaneously very stringent requirements in terms of thermal noise, optical absorption, light scattering and others. **These requirements push the limits of what's physically possible in optical coatings.**

2.

- Current GWD mirrors are the results of **20+ years of continuous R&D**.
- Improving the performance of GWD mirrors require deep, hard-to-gain **knowledge about the atomic structure of coatings**

3.

- **Metrology is of paramount importance** to develop better-performing GWD mirrors. It is not trivial!

4.

- New materials and designs have been proposed in the past few years. **A lot of work has been done, but much R&D lies still ahead before working solutions become available.**